Improvement Strategies for the Production of Renewable Chemicals by *Synechocystis* sp PCC 6803

by

Cesar Raul Gonzalez Esquer

A Dissertation Presented in Partial Fulfillment
of the Requirements for the Degree
Doctor of Philosophy

Approved July 2013 by the
Graduate Supervisory Committee:

Willem Vermaas, Chair
David Nielsen
Douglas Chandler
Scott Bingham

ARIZONA STATE UNIVERSITY

August 2013

ABSTRACT

Synechocystis sp PCC 6803 is a photosynthetic cyanobacterium that can be easily transformed to produce molecules of interest; this has increased *Synechocystis*' popularity as a clean energy platform. *Synechocystis* has been shown to produce and excrete molecules such as fatty acids, isoprene, etc. after appropriate genetic modification. Challenges faced for large-scale growth of modified *Synechocystis* include abiotic stress, microbial contamination and high processing costs of product and cell material. Research reported in this dissertation contributes to solutions to these challenges. First, abiotic stress was addressed by overexpression of the heat shock protein ClpB1. In contrast to the wild type, the ClpB1 overexpression mutant (Slr1641+) tolerated rapid temperature changes, but no difference was found between the strains when temperature shifts were slower. Combination of ClpB1 overexpression with DnaK2 overexpression (Slr1641+/Sll0170+) further increased thermotolerance. Next, we used a *Synechocystis* strain that carries an introduced isoprene synthase gene (IspS+) and that therefore produces isoprene. We attempted to increase isoprene yields by overexpression of key enzymes in the methyl erythritol phosphate (MEP) pathway that leads to synthesis of the isoprene precursor. Isoprene production was not increased greatly by MEP pathway induction, likely because of limitations in the affinity of the isoprene synthase for the substrate. Finally, two extraction principles, two-phase liquid extraction (e.g., with an organic and aqueous phase) and solid-liquid extraction (e.g., with a resin) were tested. Two-phase liquid extraction is suitable for separating isoprene but not fatty acids from the culture medium. Fatty acid removal required acidification or surfactant addition, which affected biocompatibility. Therefore, improvements of both the organism and product-harvesting methods can contribute to enhancing the potential of cyanobacteria as solar-powered biocatalysts for the production of petroleum substitutes.

DEDICATION

This dissertation is dedicated to my wife Nancy, who made great sacrifice leaving everything back home so she could be here with me. I dedicate this work to my son Mateo, who always has a smile from me when I get home from those long hours of lab work. I also dedicate this work to all my family and friends who supported me throughout this process.

ACKNOWLEDGMENTS

I thank my advisor Dr. Wim Vermaas and my Committee Members: Drs. Douglas Chandler, Scott Bingham and David Nielsen.

I thank David Lowry and Dr. Robert Roberson for their help with light and electron microscopy, Dr. Daniel Brune for his help with LC-MS, Dr. Hongliang Wang for his help with cloning work, and Waldemar Hauf for generating the isoprene synthase sequence.

I also thank my friends and colleagues: Adrian, Angela, Anna, Bing, Billi, Christoph, Danny, Heather, Ipsita, Jose, Julio, Lisa, Lucas, Luke, Nicole, Otilia, Ricardo, Sawsan, Shaw, Shuqin, Vicki, Wei and Yifei.

I am grateful to all the entities that provided funding at some point: ASU, British Petroleum, CONACYT, DOE-ARPA-E, LightWorks and ZuvaChem.

TABLE OF CONTENTS

Page

LIST OF TABLES vi

LIST OF FIGURES vii

LIST OF ABBREVIATIONS ix

CHAPTER

1 THE WHOLE-CELL CATALYST SYNECHOCYSTIS 1

Background 1

Clean Energy Research 2

Microalgae Technology 4

The Cyanobacterium *Synechocystis* sp PCC 6803 5

Synechocystis as a Production Platform 6

Biofuel Production Process 7

2 INCREASING STRESS TOLERANCE 10

Summary 10

Introduction 10

Materials and Methods 13

Results 19

Discussion 32

3 INCREASING PRODUCT YIELDS 36

I. "Induction of the MEP pathway in a *Synechocystis* sp. PCC 6803 mutant expressing a synthetic isoprene synthase"

Summary 36

Introduction 37

Materials and Methods 40

Results 46
Discussion 57
II. "Attempt at overexpression of *Synechocystis slr1471* to increase lipid content"
Summary 59
Introduction 59
Materials and Methods 61
Results and Discussion 63
4 INCREASING PRODUCT RECOVERY 67
Summary 67
Introduction 68
Materials and Methods 71
Results 74
Discussion 82
5 PERSPECTIVE 86

References 93

Appendix

A Sequence of the synthetic isoprene synthase gene 107

LIST OF TABLES

Table		Page
1	Daily Yield Comparison of Chemicals Produced by *Synechocystis*	7
2	Primers Used to Amplify ORFs by PCR During Vector Generation	13
3	Primers Used for Cloning of MEP Genes into the Overexpression Vectors	42
4	Overexpression Vectors Used for MEP Enzyme Overexpression	42
5	List of Generated IspS+ Strains	43
6	Primers Used for RT-PCR of IspS+ Strains	44
7	Expression Levels of Select Genes in Wild Type vs. IspS+	48
8	RT-PCR of IspS+ Variants Showing Overexpression of the Desired Genes	50
9	Phenotype Comparison of IspS+ Strains	52
10	Half-labeling Times of MEcPP from ^{13}C-Glucose in Different Strains.	56
11	Primers for Vector Generation, Cloning, Segregation Check and RT-PCR of *slr1471*	62
12	Phenotype Comparison of Wild-type and Slr1471+	64
13	*In Situ* Laurate Extraction from 10-ml Cultures of *Synechocystis* TE/Δ*slr1609*	78
14	Percentage of *Synechocystis*-secreted Myristate Extracted *In Situ* by Dodecane and PGE-C12	80
15	Harvesting of Cyanobacterial Isoprene in Sealed Vials	81
16	Comparison of the Biocompatibility of Alkanes for Different Microbes	83

LIST OF FIGURES

Figure		Page
1	Scheme of a cyanobacterial biofuel production process	8
2	Constitutive ClpB1 overproduction	20
3	Immunodetection of ClpB1 and ClpB2	20
4	Phenotype of wild-type and Slr1641+ strains	21
5	Comparison of lipid profiles.	22
6	Transmission electron micrographs of *Synechocystis*.	24
7	Size profile of total protein extracts from *Synechocystis* cells.	25
8	Localization of ClpB1.	26
9	ClpB1-rich areas in unstressed Slr1641+ cells.	27
10	Micrographs of the immunolocalization of ClpB1-His and ClpB2-His cells..	28
11	Survival of cells upon heat shock.	29
12	Effect of overexpressed heat shock proteins in a fatty-acid producing strain..	31
13	Loss of phycobilisome absorption in the TE/Δ*slr1609*/Slr1641+/Sll0170+ strain.	31
14	Simplified MEP pathway	39
15	Confirmation of the functionality of the synthesized isoprene synthase	47
16	Electron micrographs of wild-type and IspS+	48
17	Western blot of IspS+/MEP overexpression strains	51
18	Isoprene production by *Synechocystis* strains containing an isoprene synthase	53

Figure Page

19 Comparison of pigments in methanol extracts from various photoautotrophic cultures. 54

20 Comparison of the accumulation of the MEP metabolite MEcPP....55

21 Plasmid that uses the *ftsQ* promoter to overexpress the *Synechocystis slr1471 gene.*....62

22 DNA electrophoresis of PCR products showing segregation of *ftsQ-slr1471* overexpresssion in the Slr1471+ strain....63

23 Absorbance spectra and 77K fluorescence emission spectra of the wild-type and Slr1641+ strains 64

24 Micrographs of wild type and Slr1471+ 65

25 Micrographs of Slr1471+ cells showing abnormal thylakoids in cells....65

26 Comparison of wild-type and Slr1471+ lipid profiles 66

27 Effect of resin beads free-floating in *Synechocystis* cultures. 74

28 SEM of resin beads....75

29 Biocompatibility of *Synechocystis* with hydrophobic solvents 76

30 Cell-free extraction of laurate from BG-11 by dodecane....77

31 Laurate extraction from BG-11 medium by different percentages of PGE-C8 in dodecane 79

32 Acyl homoserine lactone effects in *Synechocystis* cultures 92

LIST OF ABBREVIATIONS

AP- Alkaline phosphatase

AHL- Acyl homoserine lactone

CCM- Carbon concentrating mechanism

CFU- Colony forming unit

Chl- Chlorophyll

DAD- Diode array detector

DCW- Dry cell weight

DGDG- Digalactosyl diacylglycerol

DMAPP- Dimethylallyl pyrophosphate

DXP- 1-deoxy-D-xylulose 5-phosphate

DXR- DXP reductase

DXS- DXP synthase

GHG- Greenhouse gases

GGPP- Geranylgeranyl pyrophosphate

HSP- Heat shock protein

HMBPP- Hydroxy-3-methyl-but-2-enyl pyrophosphate

IPI- Isopentenyl pyrophosphate isomerase

IPP- Isopentenyl pyrophosphate

MEcPP- Methyl-D-erythritol 2,4-cyclopyrophosphate

MEP- Methyl erythritol phosphate

MES- 2-(N-morpholino) ethanesulfonic acid

MGDG- Monogalactosyl diacylglycerol

OD- Optical density

ORF- Open reading frame

PAGE- Polyacrylamide gel electrophoresis

PB- Phosphate buffer

PBS- Phosphate-buffered saline

PG- Phosphatidylglycerol

PGE- Propylene glycol esters

PHB- Polyhydroxybutyrate

PMSF- Phenylmethylsulfonyl fluoride

PPP- Pentose phosphate pathway

PVDF- Polyvinylidene difluoride

ROS- Reactive oxygen species

SDS- Sodium dodecyl sulfate

SEM- Scanning electron microscopy

SQDG- Sulfoquinovosyl diacylglycerol

Chapter 1

THE WHOLE-CELL CATALYST SYNECHOCYSTIS

"Production of Petroleum Substitutes Using Sunlight and Carbon Dioxide"

Background

With the surge of the Industrial Revolution in the late 18th century, humans began to modify their environment in ways never seen before. Technological advances greatly improved the quality of human life and increased the use of previously untapped natural resources such as the fossil fuels petroleum, coal and natural gas. The population of Earth grew to 6.7 billion and continues growing. In order to provide the population with food, fuel, etc. it is necessary to burn large amounts of fossil fuels, which release greenhouse gases (GHG) to the atmosphere; carbon dioxide (CO_2) is the GHG that is released the most. The physicist Arrhenius was the first to suggest that CO_2 plays a role in the greenhouse effect (Arrhenius, 1896). Many years later, Keeling and his colleagues showed a man-provoked accumulation of CO_2 in the atmosphere by long-term measurements in the Mauna Loa observatory in Hawaii (Keeling et al., 1995). When CO_2 increase in the atmosphere is added to temperature and precipitation changes (among others) in the biosphere, there was finally scientific consensus that climate change was induced by human activities and in direct correlation with the occurrence of GHG in the atmosphere (IPCC, 2007).

At the Mauna Loa Observatory nearly 400 ppm CO_2 was measured in May 2013. This value is well above the 280 ppm CO_2 predicted for pre-industrial levels and already past the 350 ppm that scientists proposed as "safe" to avoid further climate deterioration and to maintain the status of our biosphere (Hansen et al., 2008). Further increase in CO_2 would generate a positive feedback due to release of the even more harmful GHG

methane from methane hydrates found in ice sheets (Hansen et al., 2008), which would result in rising seas, extreme climate, loss of plant and animal diversity, etc. Pacala and Socolow (2004) predict that using existing technologies a 500 ppm level of CO_2 can be maintained within the next 50 years. Nevertheless, 500 ppm CO_2 is too risky to set as goal for CO_2 levels, and alternatives with neutral or negative carbon balance must be developed.

Clean Energy Research

It is believed that we have enough petroleum reserves to meet the demand until 2030 (Kjarstad & Johnson, 2009). Other unconventional sources, such as shale gas are being used more frequently with the development of hydraulic fracturing ("fracking"). While petroleum is obtained from natural deposits by drilling, shale deposits require that a deep cortex layer of Earth is fractured (using high-pressure, water and sand) to release shale deposits. Fracking is one of the technologies suggested by Pacala and Socolow (2004) that could help reducing CO_2 from the atmosphere, by reducing the burning of coal and burning natural gas instead. Shale deposits may be able to supply energy for up to 125 more years (Kerr, 2010), while releasing large amounts of carbon into the atmosphere upon burning. It is even more worrisome that shale extraction could release large amounts of methane into the atmosphere (Howarth et al., 2011).

Many advances have been made to meet the needs of clean energy for the electricity market (efficient solar panels, better batteries for wind turbines, geothermal, etc.); however, there is still a lot of research to be done to fulfill the need for renewable transportation fuels. In order to be considered as a potential substitute for petroleum derivatives, there are several characteristics that the alternative biofuel must meet: a) have superior environmental benefits, b) be economically competitive and able to be

produced in large amounts and c) have favorable energy balance compared to the materials used to produce it (Hill et al., 2006).

Three stages of biofuel research are generally recognized: the first-generation biofuels are currently produced from edible feedstocks (sugarcane, corn), the second-generation biofuels use feedstocks which are usually not edible (cellulosic biofuels) and the third-generation biofuels are produced by microalgae and other microbes, often through biotechnological processes (Lee & Lavoie, 2013).

The most important biofuel being produced in the US is corn ethanol. The main issues with this first-generation fuel are the unavailability of agricultural land to produce enough feedstock and a highly criticized potential of using the same feedstock as food. In addition, the technology requires government subsidies and often the life cycle assessments are not better than for petroleum (Doornbosch & Steenblik, 2008). Nevertheless, it remains as an alternative for immediate action against climate change. Other biofuel feedstocks being used to a lesser extent are palm and sunflower, whose oil content (triglycerides) can be transesterified to biodiesel (Yee et al., 2009), but as conventional crops they face the same issues as corn ethanol.

Second-generation biofuels are being developed in order to avoid the use of food crops/agricultural land, and instead to use non-conventional biomass to make the biofuel production as carbon-neutral and water-efficient as possible. Examples of second-generation biofuels are ethanol from cellulose, syngas, etc. Cellulosic ethanol has become relevant in the US in part thanks to government support for crop biomass feedstock other than corn. Even though the biomass feedstock is varied and abundant (corn stovers, switchgrass, etc.), the development of commercially available cellulosic biofuel is impeded by high pre-treatment costs of the biomass and the high cost of the cellulase enzyme (Sticklen, 2008).

The fuel produced from microalgae feedstock is considered third-generation, and is reviewed in the following section.

Microalgae Technology

The generation of renewable fuels from microorganisms is an appealing option to achieve sustainable energy production worldwide. Of special interest are photosynthetic microorganisms, which convert sunlight and CO_2 into useful molecules (Chisti, 2007), making them in theory a carbon-neutral biofuel source. Because microalgae grow rapidly, their harvest cycle is rapid too; most will double within 24 h and for those that produce triglycerides (storage molecules used to make biodiesel) their oil yield per area is 20 times higher than traditional oil crops (e.g., palm); in other words, microalgae could produce the same biomass in less area (Chisti, 2007). Microalgae can grow in closed structures known as photobioreactors or in open-air pond systems and do not compete with agricultural lands nor are they used as food for humans.

Although microalgae have been grown industrially for some time, their application was limited to certain markets. The commercialized products from microalgae were naturally occurring compounds that did not require any genetic engineering of the microalgae. For example, the biomass of *Spirulina* has been used for a long time as a dietary and therapeutic supplement (Deng & Chow, 2010) and the carotenoid astaxanthin from *Haematococcu*s is used as antioxidant (Yuan et al., 2011). In the current applications of microalgae (Pulz & Gross, 2004), the available products are the biomass itself (cheaper to produce since biomass is not processed extensively after it is produced) and molecules such as pharmaceuticals and health supplements used in high-value markets (more expensive to produce since they need to be processed, but can be sold at a premium price).

The growth of microalgae for biofuel production faces several disadvantages: expensive bioreactors, inability of cells to produce for long periods of time, contamination by heterotrophic microorganisms, high extraction costs, etc. In the case of biodiesel production from algae, ventures can hardly produce their fuel at a competitive price vs. petroleum fuels. The disadvantages related to production, extraction and contamination may be overcome in some cases by genetic engineering. By optimizing cellular processes we can increase CO_2 capture (by modification of carbon concentrating mechanisms, CCM), increase lipid and fatty acid production/secretion (by metabolic engineering and identification of transcriptional regulators) and increase stress tolerance (by chaperone overexpression). We could also decrease energetic inputs for harvesting (by induced flocculation), cell suspension (by induced gas vesicles), etc. (Work et al., 2012; Chisti, 2007). Achieved improvements are the direct generation of drop-in fuels such as aliphatic alkanes, secretion of fatty acids, increased resistance to salt and high temperatures, etc. (Radakovits et al., 2010). A review on algal optimization for biofuel production can be found in Rosenberg et al. (2008). Such optimization features require a strain that is easily transformable, like *Synechocystis* sp PCC 6803.

The Cyanobacterium *Synechocystis* sp PCC 6803

Synechocystis sp PCC 6803 (hereafter *Synechocystis*) is a unicellular photosynthetic cyanobacterium of the order of the Chroococcales that was isolated from a freshwater lake back in 1968. *Synechocystis* possesses characteristics that have turned it into a widely used model to study oxygenic photosynthesis. *Synechocystis* does not fix nitrogen and has a short doubling time (about 12 h), especially at alkaline pH and temperatures from 25 to 35 °C. It may grow photoautotrophically, photomixotrophically, photoheterotrophically or by light-activated heterotrophic growth (Anderson &

McIntosh, 1991). It has a well-established genome manipulation system, a well-studied physiology (Vermaas, 1996; Yang, 2002) and its genome is entirely sequenced (Kaneko et al., 1996).

Synechocystis already possesses the enzymes needed to generate some renewable precursors of petroleum substitutes. Research in this area has focused on optimizing production of polyhydroxybutyrates (PHB), cyanophycin and membrane lipids. PHB is a polymer that bacteria produce as a carbon and energy reserve that can be extracted and processed to produce a biodegradable plastic with characteristics similar to polypropylene. A review of polyhydroxyalkanoate characteristics and production in other bacteria can be found elsewhere (Reddy et al., 2003). *Synechocystis* normally produces no more than 5% w/w PHB per dry cell weight (DCW) at stationary phase, but yields can be increased with varying nutrient and growth conditions, accumulating up to 29% w/w PHB per DCW (Panda et al., 2006). Another polymer of interest that is exclusive to cyanobacteria is cyanophycin (multi-L-argynol-poly-L-aspartic acid), which is a nitrogen storage compound that accumulates under nutrient limitation at yields of 18% w/w per DCW (Maheswaran et al., 2006), with the potential of replacing polyacrylate. Biomass contains lipids from membranes, which can be converted into biofuel. *Synechocystis* grown in photobioreactors reportedly produced only a maximum of 5% w/w lipids per DCW (Sheng et al., 2011) and up to 15% in lab conditions, so genetic engineered strains would be required to achieve commercial feasibility.

Synechocystis as a Production Platform

Research is being performed to develop green, sustainable technologies using cyanobacteria as base-organisms (Quintana et al., 2011); some of this research is on its way for commercial production (Algenol Biofuels, Joule Unlimited, etc.). A summary of

produced molecules and their yields in *Synechocystis* is found in Table 1. Low productivity yields of isoprene, degradation of fatty acids by scavengers and increased sensitivity of mutants to outdoor conditions leave room for improvement. The goal of this research was to evaluate aspects of improvement regarding temperature tolerance, carbon flux towards isoprene production and extraction methods from cultures of *Synechocystis*, in order to improve its potential for industrial applications.

Table 1

Daily Yield Comparison of Chemicals Produced by Synechocystis

Chemical	Daily yield	Reference
Ethanol	5.2 mmol/l/day	(Dexter & Fu, 2009)
Fatty acid	150-200 μmol/l/day	(Vermaas lab data)
Isoprene	700 nmol/l/day	(Bentley & Melis, 2011)
Hydrogen	150 μmol/l/day	(Antal & Lindblad, 2005)
Heptadecane	10 μmol/l/day	(Wang et al., 2013)

Biofuel Production Process

The production chain of cyanobacterial renewable chemicals for our purposes is envisioned to be similar to algal lipid-to-biofuel production in Chisti (2008) and is summarized in Figure 1.

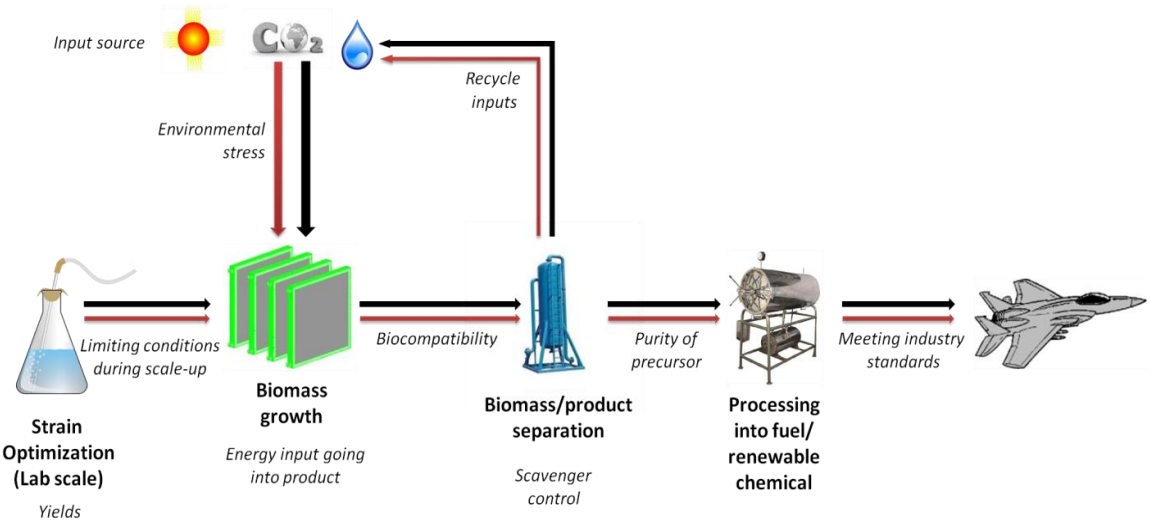

Figure 1. Scheme of a cyanobacterial biofuel production process. Unit operations appear in bold and issues appear in italics.

The starting point is the generation of a cyanobacterial strain that produces or secretes a molecule of interest. Secretion from cells (the "milking" concept (Hejazi & Wijffels, 2004)) overcomes many of the issues faced by conventional lipid extraction from algae, avoiding high economic and energetic costs of extraction and drying methods. Since cyanobacteria are the basis of the production process, the physiology of the strain affects the overall feasibility of growth and extraction processes. By collaborative work, engineers and molecular biologists can modify *Synechocystis* to show desired traits such as biocompatibility of organic solvents, tolerance to low pH and high temperatures, increased yields, etc. For example, modifications in thermotolerance could allow a simpler photobioreactor that does not require temperature regulation; modification of carbon fluxes can increase yields of the desired products and can make extraction easier, etc.

Strains need to be grown in a large-scale infrastructure, composed of photobioreactor "modules" that must be (1) efficient at light capture, mixing and energy use, etc., (2) economic so that multiple modules can add up to a viable commercial-scale production area and (3) hardy so that there needs to be only minimum maintenance for a long period of time (Borowitzka, 1999). The photobioreactor modules can be open ponds, closed tubes, flat panels and biofilm reactors. Besides the economic factor, selection of the type of photobioreactor will depend on water availability (e.g., open ponds have higher evaporation rates than closed systems), land availability (e.g., biofilm reactors can be arranged to occupy less area than an open pond), and relevance of keeping a culture free of contamination (e.g., open ponds have no barrier for other colonizing organisms) (Chisti, 2007). Appropriate product separation hardware must be in place and should allow recycling of spent media and nutrients, concentrate a high-purity product that will not affect chemical transformations downstream and be efficient in order to minimize losses due to scavengers (Scott et al., 2010). Once the product has been separated from the culture, an attempt must be made to limit the organic solvents used for purification and elution before going forward with the processing step.

Our objective for this research was to target issues during *Synechocystis* large-scale growth, and find solutions based on *Synechocystis* physiology. Specifically, our goal was to generate strains tolerant to heat stress, increase yields of isoprene and lipids, and develop liquid-liquid *in situ* extraction methods.

Chapter 2

INCREASING STRESS TOLERANCE

"ClpB1 Overproduction in *Synechocystis* sp PCC 6803 Increases Tolerance to Rapid Heat Shock"

Summary

ClpB1 is a heat shock protein known to disaggregate large protein complexes. Constitutive, 16-fold ClpB1 overproduction in the cyanobacterium *Synechocystis* sp. PCC 6803 increased cell survival by 20-fold when cultures were heated quickly (1 °C/s) to 50 °C and delayed cell death by an average of 3 min during incubation at high temperatures (>46 °C). Co-overexpression of ClpB1 and another heat shock protein, DnaK2, further increased cell survival. According to immunolocalization results, ClpB1 is dispersed throughout the cytoplasm but is concentrated in specific areas and is more prevalent near thylakoid membranes. However, ClpB1 overproduction does not lead to a change in the morphology, chlorophyll content, or photosystem ratio. Whereas electron microscopy demonstrated that apparent protein aggregation occurred after heat treatment in the control strain, protein aggregate size was maintained in the ClpB1 overexpresser. Constitutive ClpB1 overproduction allows an earlier response to heat shock and protects from damage due to rapid heating of cultures.

Introduction

Photosynthetic microbes are being modified to enable the production of eco-friendly alternatives to petroleum commodities by means of CO_2 conversion catalyzed by sunlight and photosynthesis (Machado & Atsumi, 2012). Such modifications are usually

analyzed under normal growth conditions; however, abiotic stress found outdoors may hinder the efficiency of large-scale production.

The mechanisms that cyanobacteria use to counter abiotic stress are mostly well-characterized (Los et al., 2008). One of the important abiotic stresses that cells may be exposed to in photobioreactor systems under natural conditions is temperature stress. *Synechocystis* growth typically occurs in the temperature range of 25 to 40 °C with an optimum of 30 °C; temperatures higher than 45 °C are inhibitory to growth (Inoue, 2001). The production of heat shock proteins (HSPs) is one of the most ubiquitous stress-defense mechanisms (Lindquist & Craig, 1988), mainly studied as a primary response to rapidly rising temperatures. One of the first genes to be induced after heat shock is *clpB*, with its gene product possibly serving a dual function (Clarke & Eriksson, 2000): disaggregation of large protein complexes (Eriksson et al., 2001), and aiding DnaK2 in resolubilization of damaged proteins (Lee et al., 2003). *Synechocystis* possesses three highly similar HSP70 homologs (DnaK1-3). Of these chaperones, DnaK2 is the most induced during heat shock. Interestingly, DnaK3 has been found to be tightly associated with thylakoid membranes (Rupprecht et al., 2007).

The active form of ClpB is a hexamer that is predicted to be soluble in the cytoplasm (Celerin et al., 1998). The ClpB hexamer requires ATP for stability and functionality and is required for thermotolerance in various bacteria (Eriksson & Clarke, 1996; Squires et al., 1991; Rowland et al., 2010). In addition, the ClpB homolog APG3 in *Arabidopsis* has been shown to be involved in thylakoid biogenesis (Myouga et al., 2006). The *Synechocystis* genome carries two genes, *slr1641* and *slr0156*, coding for ClpB homologs (proteins ClpB1 and ClpB2, respectively). ClpB1 is induced during heat shock (Suzuki et al., 2006), while at least in *Synechococcus* sp PCC 7942 ClpB2 is not induced under these conditions (Eriksson et al., 2001). A deletion of ClpB1 in this strain

led to an inability of cells to develop thermotolerance (Eriksson & Clarke, 1996). A *Synechocystis* ClpB1 deletion mutant showed no phenotype when grown at 30 °C, whereas a ClpB2 deletion could not be obtained (Giese & Vierling, 2002).

Overexpression of *clpB* in *E. coli* improves the cells' ability to survive exposure of cells to 50 °C temperatures for minutes or hours (Chow & Baneyx, 2005). However, to prevent or decrease protein aggregation or to boost solvent tolerance, previous studies have suggested that levels of ClpB and other chaperones such as DnaKJ, GrpE and GroESL need to be in balance (Kedzierska & Matuszewska, 2001; Zingaro & Papoutsakis, 2012). The effects of a constitutive increase of ClpB1 in *Synechocystis* are not known yet. As in photosynthetic systems ClpB may be involved in thylakoid biogenesis and as we are interested primarily in boosting temperature tolerance in this study, we will focus here on overexpression of *slr1641*, the gene coding for ClpB1 in *Synechocystis*. Although *slr0156* (ClpB2) is highly similar to ClpB1 and may also have some thermoprotective effects, it is not induced during heat and hence it was not looked into in this research.

Here, we analyze the effects of ClpB1 overproduction on temperature tolerance in *Synechocystis* on its own and when supplemented with DnaK2 overexpression, determine heat shock effects on protein aggregation in the cell, and monitor ClpB1 localization in the cell by electron microscopy. Finally, the ClpB1/DnaK2 chaperone combination was inserted into a fatty acid-producing strain and its effect was analyzed. ClpB1 overproduction in particular was shown to increase tolerance to rapid temperature swings.

Materials and Methods.

Cyanobacterial growth conditions and construction of a ClpB1 overexpression mutant. *Synechocystis* cells were grown at 30 °C in BG-11 medium (Rippka et al., 1979) in 125-ml flasks bubbled with air and illuminated at a light intensity of 45 μmol photons m^{-2} s^{-1} (defined as normal growth conditions for this study). Primers for amplification of the genes are found in Table 2. All sequences and location in the *Synechocystis* genome are stated according to Cyanobase.

Table 2

Primers Used to Amplify ORFs by PCR During Vector Generation

Primer	**Sequence**	**Strain generated**
slr1641-H fwd	GAA AAT CAT ATG CAA CCC ACA GAT CCT	Slr1641+ (ClpB1-His)
slr1641-H rv	GAG CGG CCG CTA ATG GTG GTG ATG GTG ATG ACC TCC CCC AAC GAT GAC TAA ATC C	
sll0170-H fwd	CGG GAG TTA ATT AAA CAT ATG GGA AAA GTT G	Sll0170+ (DnaK2-His)
sll0170-H rv	CTG CGG CCG CTA ATG GTG ATG ATG GTG ATG ACC TCC ACC TTT CTC CGG CTC AGA G	
slr0156-H fwd	CAA GCT AGT CCA TAT GCA ACC TAC	Slr0156+ (ClpB2-His)
slr0156-H rv	TAG CGG CCG CCT AAT GGT GAT GGT GAT GGT GGT GAT GAG ATG AAG AAA GAA CCT CG	
slr1641 fwd	GAC AAG GGC ATG CCG GCT TTG	psbA2KS-Slr1641 (ClpB1)
slr1641 rv	GAA AAT CAT ATG CAA CCC ACA GAT C	

To overexpress *clpB1*, we constructed a pUC19 backbone vector containing *slr1641* with a His-tag coding sequence at its 3' end under control of the *rbcL* promoter

(bases 2478137- 2478410) and with a chloramphenicol-resistance cassette from pBR325 at the 3' end of the *slr1641* gene with the T1/T2 terminator located in between. The p*rbcL*/*slr1641*-His/Cm^R DNA fragment had been inserted into the neutral, non-coding region between *slr1704* and *sll1575* between bases 729806 and 729807 to direct homologous recombination. The flanking region in the plasmid consisted of *Synechocystis* genome sequence between bases 729195 and 730287, a total of 1097 bp. The vector carrying p*rbcL*/*slr1641*-His/Cm^R in the neutral *Synechocystis* genomic site was used for transformation of wild type. Transformation was performed as described previously (Vermaas et al., 1987) and resulted in strain Slr1641+. Similarly, *slr0156*-His, coding for ClpB2 with a His tag at its C-terminal end, was inserted into the same vector in lieu of *slr1641*-His to generate the Slr0156+ strain. To rule out an effect of the ClpB1 His-tag, we alternatively inserted *slr1641*, without a His tag, into the overexpression vector pPSBA2KS: a pUC19 backbone with flanking regions from 6733-7227, which includes the strong *psbA2* promoter, and 8309-8801, with the kanamycin-resistance cassette from pUC4K (Lagarde et al., 2000). The *sll0170* gene, encoding DnaK2, was transformed into an overexpression vector containing the flanking regions around *slr0646* (bases 2676067 to 2676566) and *sll0601* (bases 2676567 to 2677047), the *psbA2* promoter (bases 6666 to 7227) and the kanamycin selection marker from pUC4K. Alternatively, the ClpB1-His gene was inserted in a vector containing the flanking regions from *sll1677* and *ssr2848* (729195-729806 and 729807-730288), the *rnpB* promoter (2478137-2478410) and zeocin resistance marker from plasmid pZErO-1 (Drocourt et al., 1990) and transformed together with the *dnaK2* overexpression vector into a fatty acid producing strain carrying a deletion of the acyl-ACP synthetase gene *slr1609* (by replacement of a 999 bp fragment with Cm^R marker between regions 487896-488898)

and expression of a codon-optimized thioesterase gene (TE) from *Umbellularia californica* under the control of the *rbcL* promoter (strain generated in the Vermaas lab).

Cell analysis. The growth rate, chlorophyll content and intact cell absorption spectra were determined using a Shimadzu UV-1800 UV-VIS dual beam spectrophotometer. Growth was observed over time as a change in optical density at 730 nm. Chlorophyll concentrations in cultures were measured by extracting cell pellets, obtained by centrifugation, with methanol and determining the chlorophyll concentration by monitoring absorbance at 663 nm (Lichtenthaler, 1987). Absorption spectra of cultures were determined in the 400-750 nm range using 0.5% buttermilk as a blank to correct for scattering. 77K fluorescence emission spectra in the 625-775 nm range were measured in a SPEX Fluorolog 2 instrument using an excitation wavelength of 435 nm and slith width set to 0.25 mm, which corresponds to a bandwidth of 1 nm.

Lipid and fatty acid analysis. The Folch method (Folch et al., 1957) was used to extract lipids from cells collected from 200 ml cultures in exponential phase (OD=0.5). Extracted lipids were dried under nitrogen gas and redissolved in a volume of methanol to bring the chlorophyll *a* concentration in the extract to 50 μM. A 5 μl aliquot was injected into a Dionex Ultimate 3000 HPLC system and separated using a gradient of increasing methanol in water (starting at 50%, then linearly up to 100% methanol in 26 min, then 100% methanol for 20 min) at a flow rate of 200 μL/min in a Zorbax Extend C-18 column. Both methanol and water contained 10 mM NH_4OH. Lipid mass and identification (by comparison to lipid standards) were determined using ESI-MS in a Bruker MicrOTOF-Q mass spectrometer in the negative ion mode with the capillary voltage set at +3,900 V and the collision energy set at 10 eV. A similar analysis has been performed by Sommer et al. (2006). Fatty acids were separated by HPLC using with the same setup and their concentrations were determined as a function of the relative

monoisotopic peaks compared to a heptadecanoic acid internal standard. *Synechocystis* does not produce heptadecanoic acid in significant amounts.

RT-PCR. RNA was extracted by Trizol reagent (Life Technologies), cleaned of DNA by Turbo DNA-free DNAse (Life Technologies), and cDNA was synthesized by using random primers from the iScript select cDNA synthesis kit (BioRad), each following the manufacturer's protocols. For RT-PCR, the iTaq SYBR Green supermix with ROX (BioRad) and the primers GCAGCGGAGTTACAGTATGGC (*slr1641* fwd), TTCCACTTGCCGCTGTAAATC (*slr1641* rv), AAAGCTTCCACCGTCGCTC (*sll1326* fwd) and GGCACCTTTTTCCGTCAGG (*sll1326* rv) were used; reactions were performed according to the manufacturer's instructions. Fluorescence was measured on an ABI Prism 7900 HT Sequence Detection System from Applied Biosystems and samples were analyzed by the $2^{-\Delta\Delta Ct}$ method (Livak & Schmittgen, 2001).

Western blotting and immunodetection. Polyclonal antibodies (rabbit) against ClpB1 were obtained from Agrisera (Sweden) and those against the His-tag from Genscript. Cell pellets from 200 ml cultures of pre-harvest OD_{730}=0.4-0.7 were resuspended in 50 mM MES-NaOH (pH 6.5), 10 mM $MgCl_2$, 5 mM $CaCl_2$, 25% glycerol, and "protease inhibitor cocktail" (1 mM each of phenylmethylsulfonyl fluoride (PMSF), benzamidine, and amino caproic acid). Cells were broken by 6 x 30 s of bead beating (0.1 mm glass beads) with 2 min of cooling on ice between all cycles. Cell debris, glass beads, and unbroken cells were spun down and the supernatant containing proteins was used for polyacrylamide gel electrophoresis (PAGE). Proteins were separated by 12% SDS-PAGE and transferred to a polyvinylidene difluoride membrane (PVDF; Immobilon®-P) overnight at 20 V and 4 °C. Western blotting was performed according to Millipore's Rapid Immunodetection without blocking protocol using 100 mM Phosphate-Buffered Saline (PBS; 0.1 M sodium phosphate, 0.15 M NaCl, pH 7.0) buffer, fat-free milk as

blocking agent, 1:5,000 dilution of the primary antibody and 1:3,000 dilution of an alkaline phosphatase (AP)-conjugate secondary antibody; the immunoblot was developed using an AP substrate kit (BioRad).

Electron microscopy. Chemical fixation of cells was carried out with 2% glutaraldehyde in 50 mM phosphate buffer (PB) pH 7.2 overnight at 4 °C. After a 10-20 volume wash with PB buffer, cells were pelleted and the pellet mixed with an equal volume of 2% agarose that had been cooled to a point close to solidification. The cell/agarose pellets were washed for 3 x 15 min with PB and incubated in 1% OsO_4 for 2 h, washed 3 x 15 min with PB and 3 x 15 min with H_2O prior to incubation in 0.5% uranyl acetate overnight at 4 °C. After dehydration in subsequent 20%, 40%, 60%, 80% and 100% acetone steps (10 min per step), the samples were embedded in Spurr's resin in 25% increments for a minimum of 3 h per step, up to 100% resin, which was then polymerized at 60 °C for 24 h in a conventional oven. For high-pressure freezing of samples (used for immunolocalization), 10 ml aliquots of cultures at OD_{730}=0.5 were spun down at 2,500 rpm in a clinical centrifuge, resuspended to 1 ml, pipetted on top of BG-11 agar plates, and allowed to dry to a paste. The paste was placed between B-type planchettes, frozen in a Bal-Tec HPM 010 high-pressure freezer, and freeze-substituted in 0.05% uranyl acetate in acetone for 72 h at -80 °C. After the samples were warmed up to 4 °C, they were embedded in LR-White resin. Samples embedded by both techniques where cut into 70-nm-thick sections using a Leica Ultracut R Microtome and placed on formvar-coated nickel slot grids (for immunolocalization) or copper mesh grids (regular electron microscopy).

Immunolabeling. Immunolabeling was carried out by incubating the nickel grids with cell sections for 1 h at 25 °C in the primary antibody solution (PBS, 1% non-fat dry milk and 1:50 primary antibody dilution), washed 2 x 15 min with PBS supplemented

with 0.1% Tween and 1 x 15 min with PBS, and incubated for 30 min at 25 °C in the secondary antibody solution (PBS, 1% non-fat dry milk and 1:100 15 nm gold-conjugated goat-anti rabbit antibody dilution (MP Biomedicals)). Afterwards, the washing procedure was repeated, followed by 3 x 10 min washes with H_2O, and the labeled sections were post-stained with 2% uranyl acetate in 50% (v/v) ethanol for five minutes followed by five minutes with Sato's lead citrate (Hanaichi et al., 1986). Grids were analyzed using a Philips CM12 transmission electron microscope with a Gatan Inc. charged-coupled device camera.

Heat-shock treatments. For experiments involving a rapid temperature ramp-up, cells in exponential growth phase (50-µl aliquots of OD_{730}=0.4-0.7) were removed from the culture, transferred to a BioRad thermocycler, warmed up at a controlled rate (ranging from 0.67 to 60 °C/min as indicated) from 30 °C to 50 °C, and then kept at 50 °C for 5 minutes at an illumination intensity of 40 µmol photons m^{-2} s^{-1}. When applying the heat shock more slowly, the temperature of 50-µl aliquots was increased linearly from 30 °C to 46-52 °C in a BioRad thermocycler in 15 minutes, and samples were taken as a function of time after reaching the final temperature. After heat treatment, aliquots were brought back to 30 °C and plated on BG-11 agar plates to determine colony forming units (CFUs) in comparison with CFUs of control aliquots that had not been heat-treated. Heat treatment of larger cultures (300 ml) that were growing exponentially (OD_{730}= 0.4-0.7) was performed in a water bath at 60 °C under illumination at 40 µmol photons m^{-2} s^{-1}. The temperature was monitored inside the culture and maintained by shaking every two minutes and submerging/removing from the water as necessary. In the case of experiments geared to protein analysis, the ramp-up rate from 30 to 48 °C was 1.8 °C/min followed by a 10-minute incubation. For experiments involving the determination of the ultrastructure of cells by electron

microscopy, a 1.07 °C/min ramp-up rate from 30 to 46 °C was used followed by a 1-h incubation at 46 °C prior to cell preparation for electron microscopy.

Size-exclusion chromatography. For protein extraction, 200 ml of culture (OD_{730}=0.5) were collected by centrifugation and resuspended to 1 ml in PBS buffer supplemented with protease inhibitor cocktail. The cell suspension was cooled on ice, mixed with an equal volume of glass beads (0.1 mm), and cells were disrupted by 6 cycles of 30 s in a Mini Bead-Beater (BioSpec Products, Bartlesville, OK) as described previously. Cell debris, glass beads and unbroken cells were removed by filtration through a 0.2-µm filter. Homogenate samples (0.5 ml) that had passed the 0.2-µm filter were injected into a self-packed Sephacryl S-300 HR matrix in a Kontes 1 mm I.D. x 50 cm length column and were eluted using PBS buffer and a HP1100 isocratic pump at a flow rate of 0.1 ml/min. Fractions (400 µl) were collected, diluted to 1 ml with H_2O, and absorbance at 280 nm was measured spectrophotometrically in a Shimadzu UV-1800 UV-VIS dual beam spectrophotometer.

Results

Initial Slr1641+ characterization. Constitutive overexpression of *slr1641* and increased accumulation of ClpB1 in the Slr1641+ strain relative to the wild-type control were confirmed by RT-PCR and immunodetection. Under normal growth conditions, the *slr1641* transcript level was 7.1±0.5-fold higher and the ClpB1 protein level was ~16-fold higher than in the wild-type control (Fig. 2). Interestingly, ClpB1 is detected on immunoblots as a doublet. This could be due to either detection of both ClpB1 and ClpB2 (Slr0156) by the antibody, or the genuine presence of two forms of ClpB1. As indicated in Fig. 3, probing with a His-tag antibody provided two bands for Slr1641+ and only a single band for Slr0156+ (the strain carrying an extra *clpB2*-His gene). Therefore, ClpB1

is represented by two separate bands on an immunoblot. This most likely is due to an internal translation start site in the *Synechocystis slr1641* open reading frame, as reported previously for *Synechococcus* (Clarke & Eriksson, 2000) and *E. coli*, where the two forms together have been shown to be most active (Chow & Baneyx, 2005).

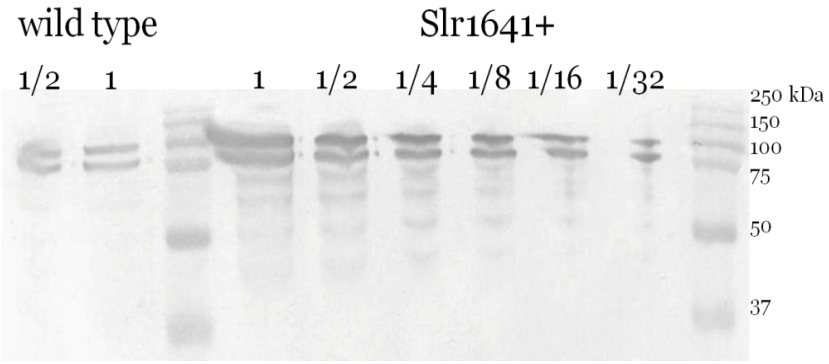

Figure 2. Constitutive ClpB1 overproduction. Immunoblot of protein extracts from wild type and the Slr1641+ strain, both grown under normal conditions, probed with ClpB1 antibodies. Maximal loading (1) corresponds to 10 µg chlorophyll *a* per well. Loadings in other lanes have been reduced as indicated in order to allow an estimation of the overexpression level of ClpB1 in the Slr1641+ strain. A marker lane separates the wild-type and Slr1641+ lanes, and another marker lane is to the right.

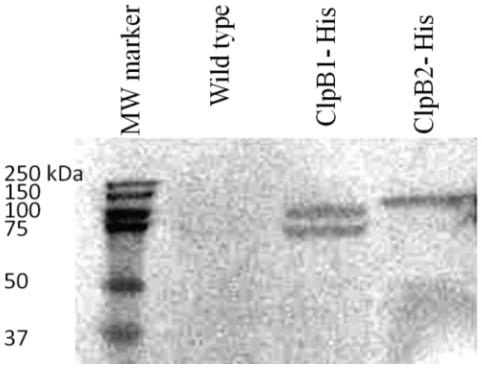

Figure 3. Immunodetection of ClpB1 and ClpB2. Immunoblot of total protein extracts from the wild type, the ClpB1-His and ClpB2-His strains probed with anti-His antibody.

The Slr1641+ strain is essentially normal in its growth phenotype, chlorophyll *a* concentration per cell, 77K fluorescence emission spectrum (indicative of the ratio of the two photosystems), and absorbance spectrum (Fig. 4). Attempts at co-isolation of ClpB1-His with other proteins (with special interest in association with VIPP1 protein (vesicle-inducing protein in plastids 1) (Hamad, 2008)) were not succesful. Distribution of chain lengths and degrees of unsaturation within the four lipid groups occurring in *Synechocystis*, phosphatidylglycerol (PG), sulfoquinovosyl diacylglycerol (SQDG), monogalactosyl diacylglycerol (MGDG) and digalactosyl diacylglycerol (DGDG) were similar between wild type and the Slr1641+ strain (Fig. 5) indicating that the lipid composition of the cell is not affected by constitutive overproduction of ClpB1. Large variability of wild type DGDG may be due to cells adjusting their membrane fluidity as needed.

	Doubling Time (h)	**chl *a* (µg/ml/OD)**
Wild type	9 ± 1	3.4 ± 0.2
Slr1641+	9 ± 1	3.2 ± 0.6

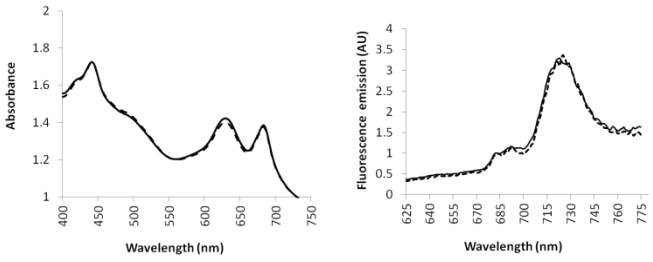

Figure 4. Phenotype of wild-type and Slr1641+ strains. Left: Doubling time and chlorophyll *a* concentration in the wild-type and Slr1641+ strains. Middle: absorbance spectra of both cell types. Right: 77K fluorescence emission spectra of the wild-type and Slr1641+ strains. For both middle and right panels: Wild type: solid line and Slr1641+: dashed line; for all measurements, OD_{730}=0.5; n=3.

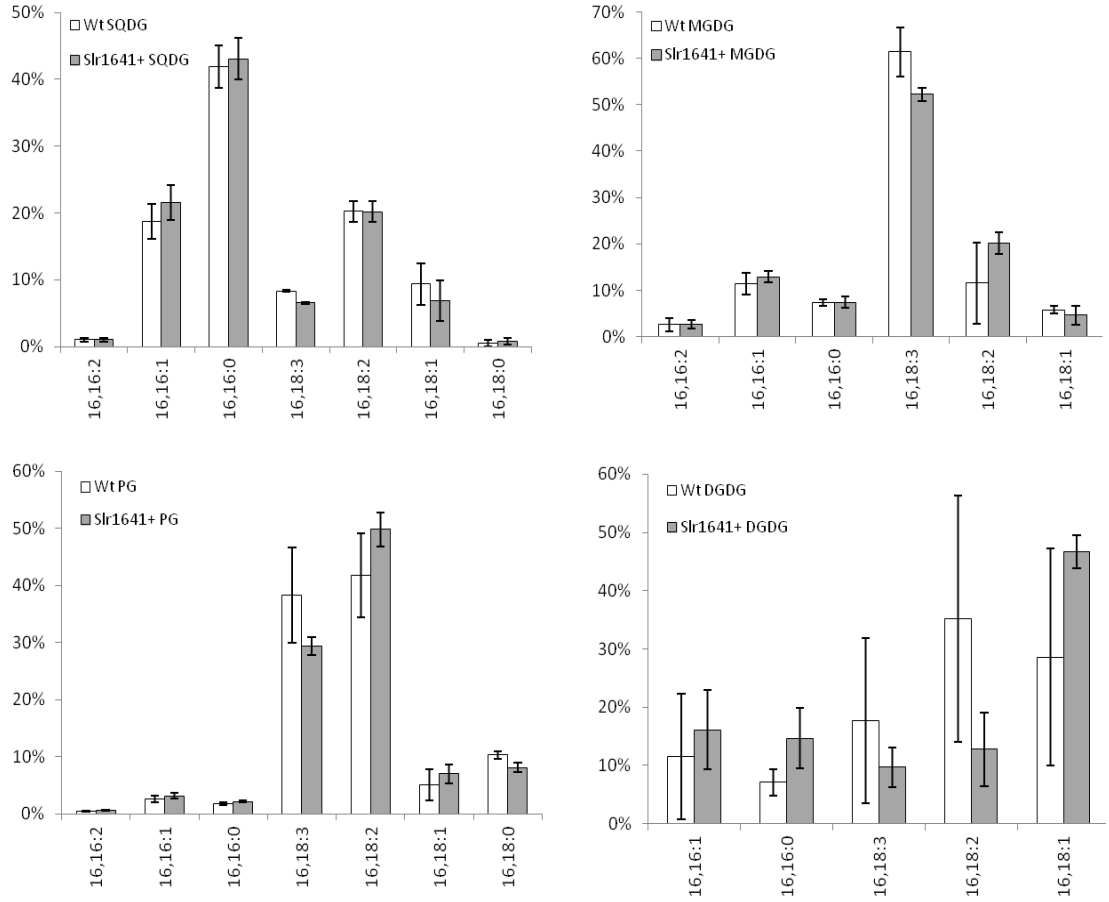

Figure 5. Comparison of lipid profiles. Composition of diglycerides (membrane lipids) with different chain lengths of the contributing fatty acids and total number of unsaturated bonds for each of the four different diglyceride classes (SQDG, top left; MGDG, top right; PG, bottom left; and DGDG, bottom right) extracted from wild type (transparent bars) and Slr1641+ (grey bars) (n=3).

Ultrastructure and ClpB1 localization in *Synechocystis* cells. In order to determine whether ClpB1 overproduction led to ultrastructural differences, transmission electron microscopy images of wild-type and Slr1641+ cells that had been growing exponentially under control conditions were compared (Fig. 6 A and B). The cells of the two strains were virtually indistinguishable. However, after cells were heat-shocked for 1 h at 46 °C in a waterbath, large differences in cytoplasmic homogeneity were found: in wild type, the ultrastructural changes in most cells are suggestive of protein aggregation, while the Slr1641+ cells have not changed their appearance as much (Fig. 6 C and D). Putative protein aggregation as seen in Fig. 6 is seen in 84% of the wild-type cells examined, whereas in 39% of the Slr1641+ cells some degree of aggregation is observed, and the remaining cells look normal. These observations suggest that overproduction of ClpB1 enables the cells to maintain a reasonably normal ultrastructure after heat shock.

In order to determine whether the ultrastructural changes upon heating that were much more pronounced in the wild type than in the Slr1641+ strain (Fig. 6) indeed are likely to be due to protein aggregation, we performed size-exclusion chromatography of total extracts from *Synechocystis* wild type and the Slr1641+ strain, before and after a non-lethal heat shock (a 10-min ramp-up from 30 to 48 °C and 10 min incubation at this temperature), and monitored elution of proteins by detection of absorbance at 280 nm (Fig. 7). Proteins eluted in four groups, labeled I through IV. Upon heat shock, the wild-type strain showed a loss in protein aggregates in group I, and a corresponding increase in aggregates in group III (Fig. 7 A). However, Slr1641+ did not change its protein aggregate profile (Fig. 7 B).

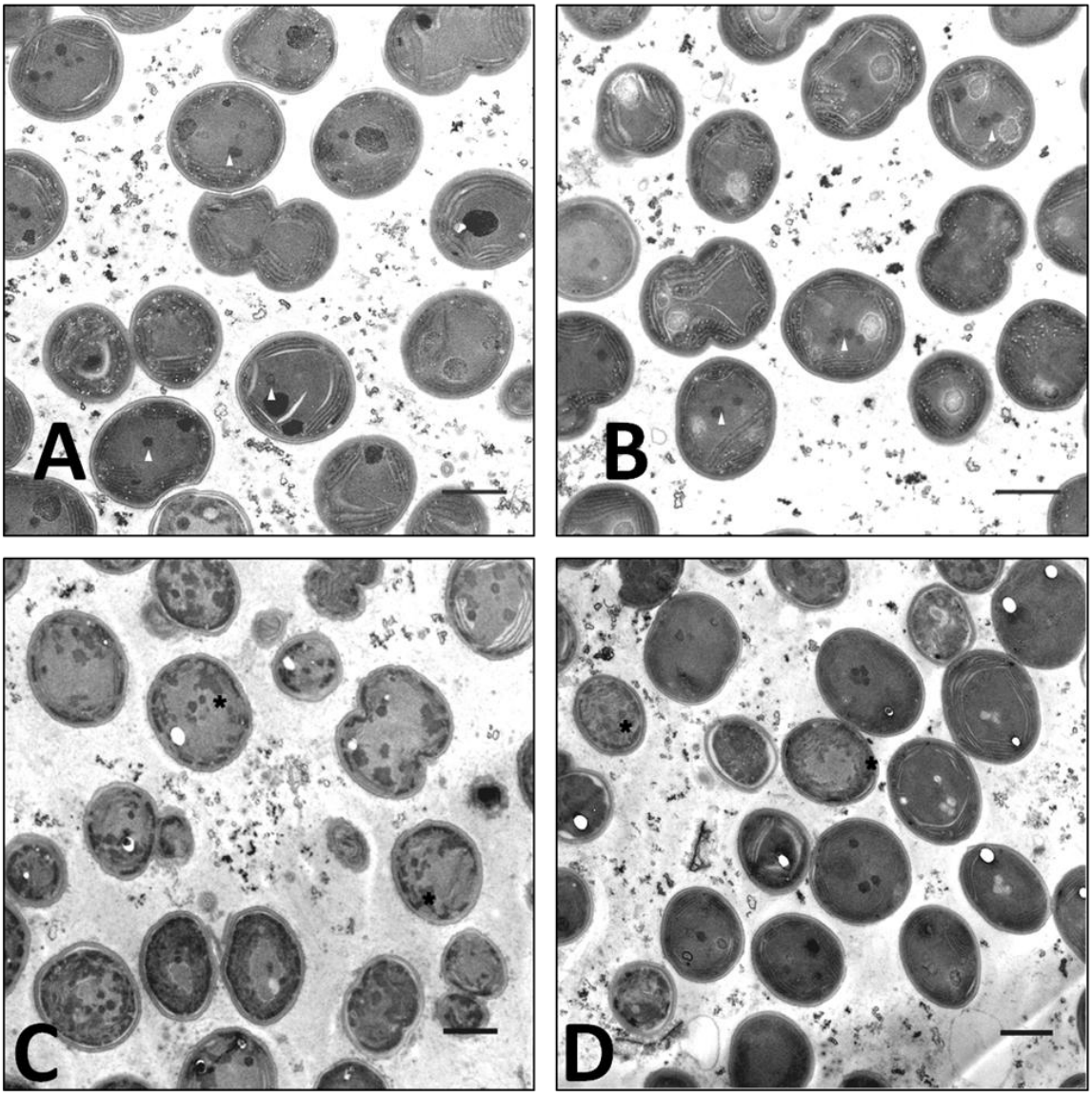

Figure 6. Transmission electron micrographs of *Synechocystis*. Wild-type (A, C) and Slr1641+ (B, D) cells from an exponential-phase culture that had not (A, B) or had (C, D) been exposed to heat stress (1 hour at 46 °C). White arrowheads: carboxysomes; black asterisks: electron dense areas formed after heat shock, primarily in wild type (scale bar=1 μm).

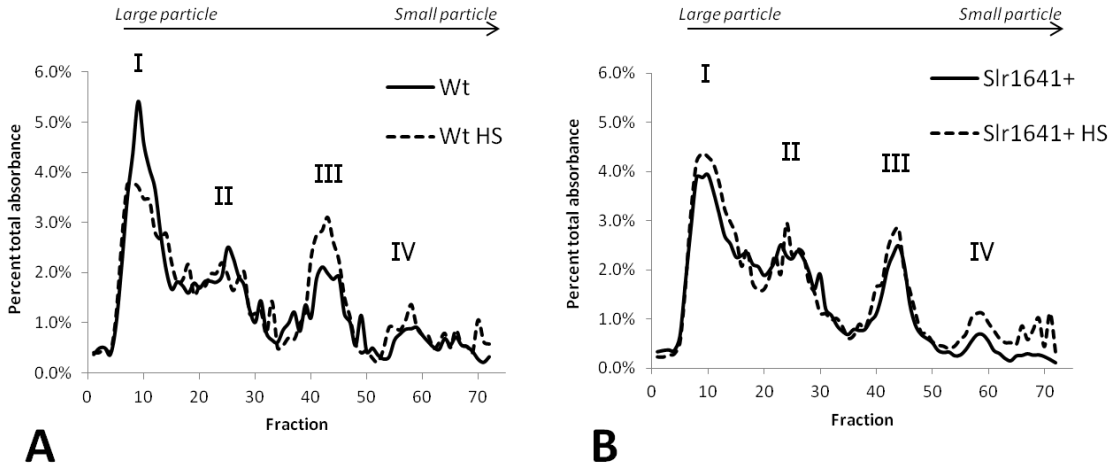

Figure 7. Size profile of total protein extracts from *Synechocystis* cells. Total proteins were separated by size-exclusion chromatography and eluted proteins were monitored by means of 280-nm absorbance. Protein extract from wild type (A) and Slr1641+ (B), from cultures with (dotted line) and without (solid line) heat shock (HS); heat shock consisted of a 10-min ramp-up from 30 to 48 °C, and a 10-min incubation at this temperature. The average of three measurements is shown.

In order to determine the location of ClpB1 in wild-type and Slr1641+ cells, cell sections prepared for electron microscopy were immunolabeled with anti-ClpB1 antibodies followed by immunogold. In control cells, ClpB1 is found throughout the cell, but particularly in the vicinity of thylakoid membranes in both wild type and Slr1641+ (Fig. 8 A and C). Gold-particle counts (3100 total counts over 14 samples) showed that 55 ± 12% of the particles are in the direct vicinity of thylakoids (often in between membranes). ClpB1-rich regions were observed in some locations near thylakoids in unstressed Slr1641+ cells; these are different from the ClpB1-rich regions throughout the cytoplasm after heat shock (Fig. 8; Fig. 9). However, after heat shock, a large part of ClpB1 maintained its proximity to thylakoids (Fig. 8 B and D).

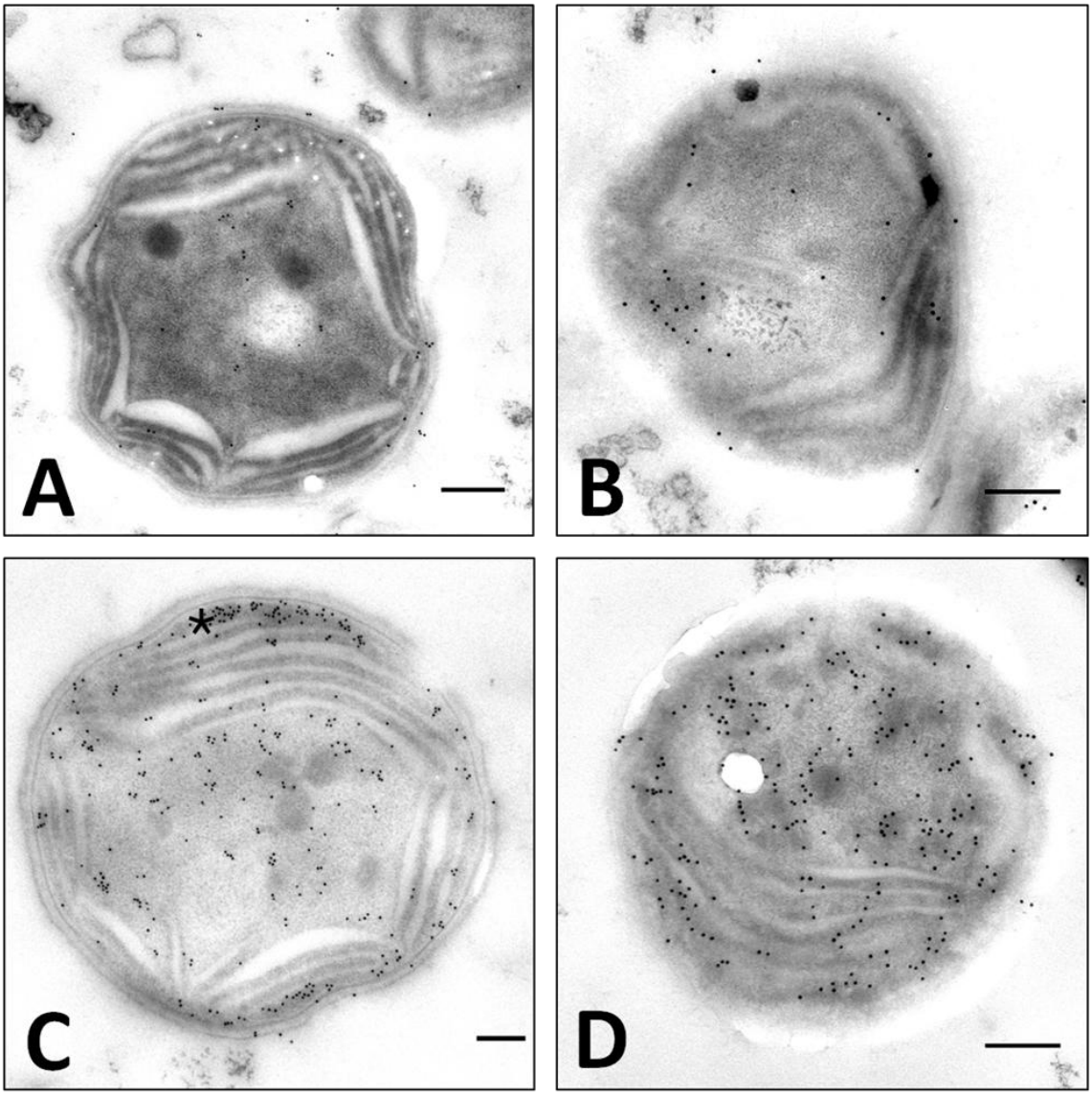

Figure 8. Localization of ClpB1. Anti-ClpB1 antibodies detected with secondary antibodies conjugated with 15 nm gold particles were monitored in 70-nm sections of wild type (A, B) and Slr1641+ (C, D) cells. Cells had been grown under standard conditions before fixation and labeling (A, C) or had been exposed to 46 °C for 1 h immediately before harvesting and fixation (B, D). Asterisk: Example of a ClpB1-rich area (scale bar = 0.2 μm).

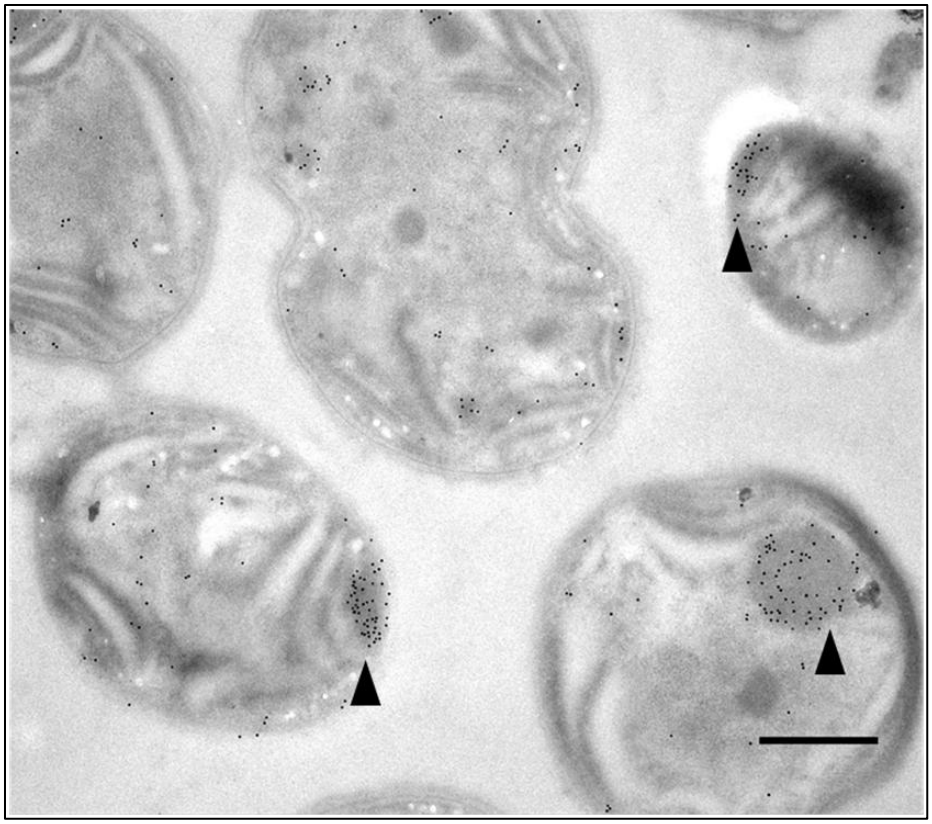

Figure 9. ClpB1-rich areas in unstressed Slr1641+ cells. Immunocytochemistry of sections of Slr1641+ cells that had been incubated with ClpB1 antibodies, with the antibodies subsequently labeled with secondary antibodies conjugated with gold particles. Somewhat electron-dense regions that are rich in ClpB1 have been indicated by black arrowheads (scale bar=0.5 μm).

In order to determine the location of ClpB2 in relationship to ClpB1, we performed immunolocalization of the His tag of these proteins in the ClpB2-His and ClpB1-His strains, respectively. As expected, the degree of labeling is less than for ClpB1 antibodies as just the His-epitope is recognized. However, colloidal gold particles were observed, and ClpB2 appears to be less frequently thylakoid-associated than was observed for ClpB1 (Fig. 10 A and B).

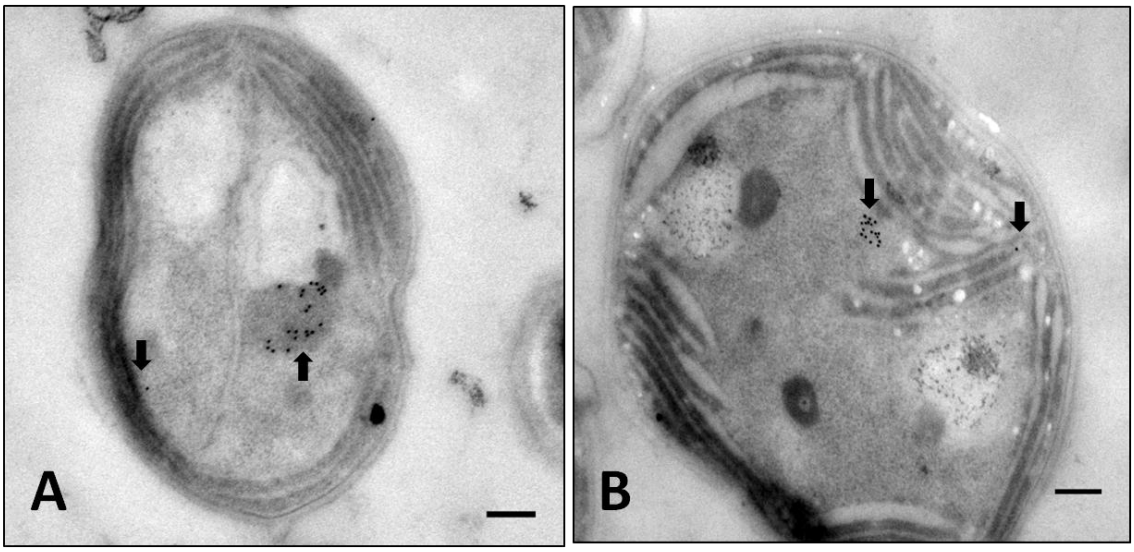

Figure 10. Micrographs of the immunolocalization of ClpB1-His (A) and ClpB2-His (B) cells. Anti-His-tag antibodies served as the primary antibody. Immunogold particles are indicated by black arrows. (scale bar=0.2 μm).

Survival upon heat shock. As ClpB1 is one of the heat-shock proteins that is most induced at early stages of heat shock (Suzuki et al., 2006), ClpB1 overproduction may protect against rapid heat shock relative to the control that first needs to synthesize ClpB1. To test this hypothesis, tolerance of wild-type and Slr1641+ cultures to heating at different rates ("ramp-up rates") to 50 °C, followed by a 5-min 50 °C incubation, was compared. At a ramp-up time of 20 s, the Slr1641+ strain, with a basal level of ClpB1 more than an order of magnitude higher than in the wild type (Fig. 2), had a >15-fold higher survival rate (Fig. 11 A). At a ramp-up rate of 1.3 °C/min (a 15-min linear ramp-up) the survival rate of the Slr1641+ cells was still about 5-fold higher than in the control (Figure 11 A). However, this difference in survival disappeared upon slower heating (at a ramp-up rate of 0.63 °C/min (30 min ramp-up time)) (Fig. 11 A) as the wild-type control is able to survive better upon slower ramp-up, possibly because of induction of heat-shock proteins during the heating process.

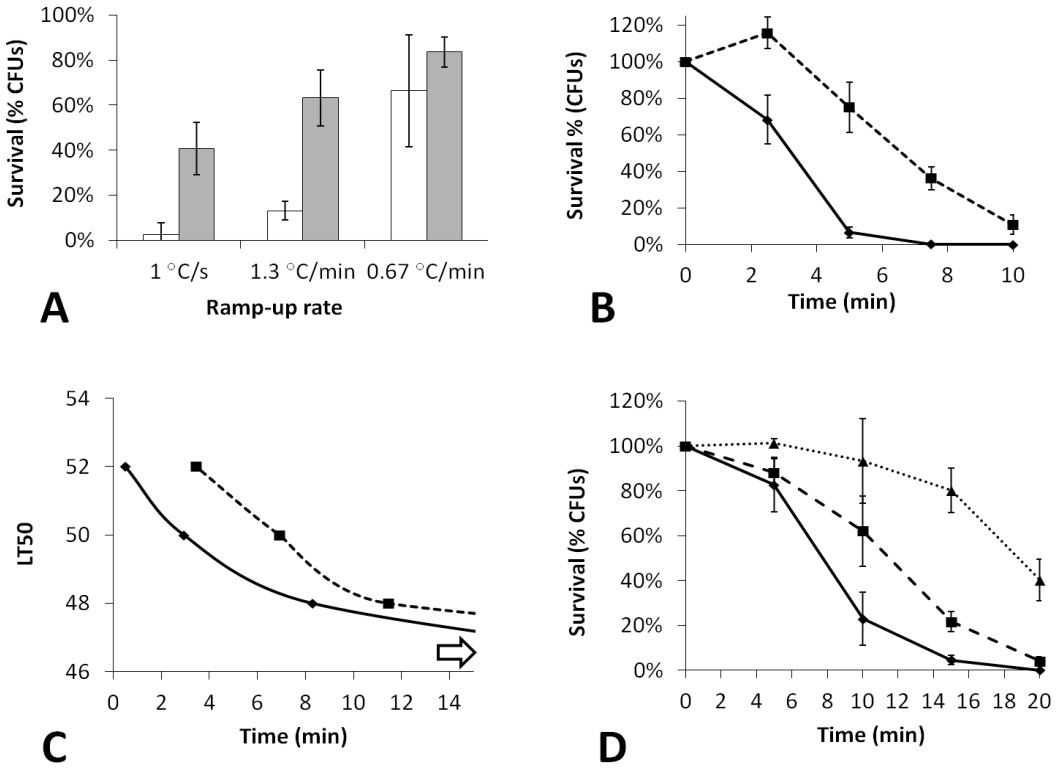

Figure 11. Survival of cells upon heat shock. A) Comparison of cell survival upon linearly heating up from 30 to 50 °C at the ramp rates indicated; wild type: white bars; Slr1641+: gray bars. B) Survival of wild type (diamonds; solid line) and Slr1641+ (squares, dashed line) upon exposure to 50 °C for the time indicated after having been heated up linearly from 30 to 50 °C (rate of 1.3 °C/min). C) Time of exposure at the temperature indicated (LT50) that resulted in 50% survival in wild type (diamonds, solid line) and the Slr1641+ strain (squares, dashed line) (Arrow: for 50% survival, an incubation of over 30 min was required for both strains at 46 °C). D) Survival of wild type (diamonds, solid line), Slr1641+ (squares, dashed line) and Slr1641+/Sll0170+ (triangles, dotted line) upon exposure to 48 °C for the time indicated after having been heated up linearly from 30 to 48 °C (rate of 1.2 °C/min) (all experiments n=3).

To compare survival upon exposure to non-permissive temperatures, cells were heated linearly to 50 °C over 15 min and were incubated at this temperature; again Slr1641+ showed increased survival upon exposure to 50 °C for several minutes (Fig. 11 B). However, exposure to 50 °C for more than 10 min led to few survivors, even in the Slr1641+ culture. Similar results indicating that Slr1641 overproduction led to only limited thermotolerance (used here as the ability to survive at high temperatures for long periods of time) were obtained when cells were incubated at other temperatures in the 48-52 °C range: the time of incubation at high temperature allowing for survival of 50% of the cells is plotted in Fig. 11 C and indicates that Slr1641+ cells are able to tolerate non-permissive temperatures for somewhat longer than the control. Both strains could tolerate 46 °C for at least 30 min after being brought to this temperature from 30 °C in 15 min. When Slr1641+ cells were modified further to introduce constitutive overexpression of DnaK2 (the Slr1641+/Sll0170+ strain), the time that cells could tolerate exposure to 48 °C was further increased (Figure 11 D) indicating that introduction of multiple heat shock proteins has cumulative effects.

To analyze if ClpB1 overexpression has the same positive effects on a *Synechocystis* mutant strain of biotechnological interest, the fatty acid-secreting strain TE/Δ*slr1609* was transformed to overexpress ClpB1 and DnaK2. The TE/Δ*slr1609*/Slr1641+/Sll0170+ strain grew slower than the control, but produced lauric acid proportional to the culture biomass growth (Figure 12, left). When submitted to heat shock treatment (a 15 minute ramp and incubation at 48 °C) the TE/Δ*slr1609* strain was more sensitive than wild type, and this effect was overcome in the chaperone overexpression strain (Figure 12, right). An unexpected effect of ClpB1 overexpression in the TE/Δ*slr1609*/Slr1641+ (not shown) as well as TE/Δ*slr1609*/Slr1641+/Sll0170+

strains was the virtual absence of phycobilisomes observed by a decreased absorbance peak at 630 nm (Figure 13).

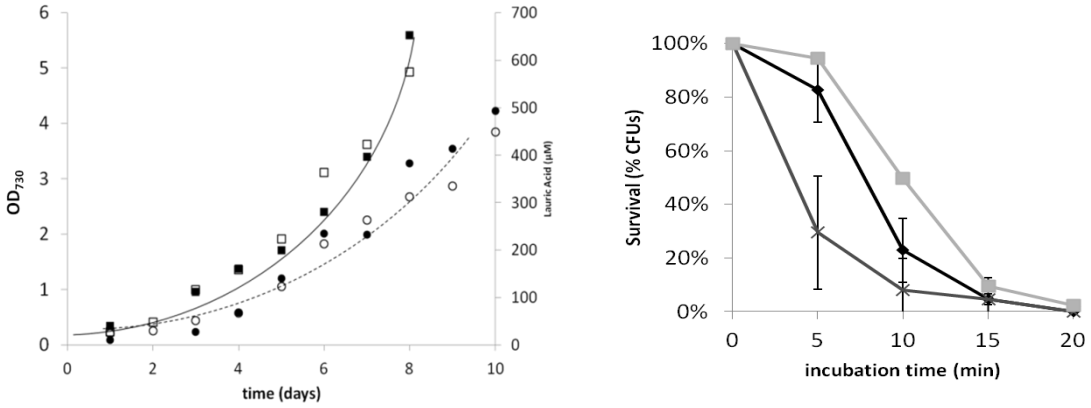

Figure 12. Effect of overexpressed heat shock proteins in a fatty-acid producing strain. Left: Comparison of growth and lauric acid production of TE/Δ*slr1609* and TE/Δ*slr1609*/Slr1641+/Sll0170+. Squares and straight line: TE/Δ*slr1609* OD_{730} (filled) and laurate concentration (empty), respectively; Circles and dashed line: TE/Δ*slr1609*/Slr1641+/Sll0170+ OD_{730} (filled) and laurate concentration (empty), respectively. Right: Survival of wild type (diamonds, solid line), TE/Δ*slr1609* (cross, gray line) and TE/Δ*slr1609*/Slr1641+/Sll0170+ (squares, light gray line) upon exposure to 48 °C for the time indicated after having been heated up linearly from 30 to 48 °C (rate of 1.2 °C/min).

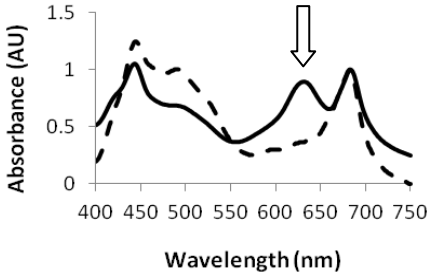

Figure 13. Loss of phycobilisome absorption in the TE/Δ*slr1609*/Slr1641+/Sll0170+ strain. TE/Δ*slr1609* (solid line) and TE/Δ*slr1609*/Slr1641+/Sll0170+ (dashed line); arrow indicates the maximum absorption peak of phycobilisomes.

Discussion

The ClpB protein is known to participate in heat shock response and adaptation to high temperatures, with a role conserved throughout phyla, of breaking down large protein aggregates (Schirmer et al., 1996). Furthermore, a role in thylakoid membrane formation has been reported (Myouga et al., 2006). Here we show the effects of a continuous overexpression of ClpB1 in *Synechocystis*, towards the goal of increasing tolerance to high temperatures.

During heat shock, transcript levels of *slr1641* have been found to spike but are rapidly degraded (Suzuki et al., 2006). However, in the Slr1641+ strain expression of the additional copy of *slr1641* is under a strong and rather constitutive promoter (the *psbA2* promoter), allowing to maintain 16-fold higher levels of ClpB1 than in wild type in the cell, in the absence of heat stress. Therefore, ClpB1 is present at high levels in the Slr1641+ strain even in the absence of heat stress. ClpB1 overproduction did not induce phenotypic changes in the cell under non-heat-stress conditions suggesting that cells tightly controlled ClpB1's activity, for example through competition with other proteins (Rosenzweig et al., 2013), storage as an inactive oligomer (Lee et al., 2003), etc.

The main ultrastructural difference between the Slr1641+ strain and wild type is observed upon exposure of cells to non-lethal heat stress. Micrographs of heat-shocked cells showed more electron-dense regions, which most likely are protein aggregates, in wild type than in the Slr1641+ strain (Fig. 6 B, D). A similar effect of heat shock on the appearance of the cytoplasm has been observed in *E. coli* cells (Laskowska, 2004), where the presence of an aggregate fraction after heat shock in ultracentrifuged samples correlated with the development of inclusions visualized by electron microscopy.

In our case, the protein aggregate size profile of Slr1641+ was unchanged in non-stressed vs. stressed conditions, suggesting a protective function of ClpB1 or a

preprocessing of heat-susceptible protein complexes. However, the wild-type pattern changed (Figure 7), in line with the electron microscopic evidence that protein aggregates are formed. Changes in protein size profile (protein aggregation) due to heat shock have been observed previously in *E. coli* (Laskowska, 2004).

ClpB1 immunolocalization showed that the protein was present throughout the cell but was concentrated in certain areas of the cytoplasm and around thylakoid membranes. The concentration of ClpB1 in specific cytoplasmic areas may suggest that there are areas where protein aggregates accumulate, as reported for *E. coli* (Rokney et al., 2009). In addition, Clp proteases have been found to be compartmentalized in some bacteria (McGrath et al., 2006; Simmons et al., 2008). It is unlikely that *Synechocystis* ClpB1 has protease activity (Clarke, 1996) but as ClpB1 as well as the ClpB1-rich clusters often are close to thylakoids (Fig. 8), ClpB1 may be stored to enable rapid mobilization upon heat shock. Moreover, the protein may be involved in, for example, protein assembly of thylakoid-related proteins as appears to be the case for *Arabidopsis* (Myouga et al., 2006). However, no change in thylakoid structure or abundance, or lipid composition was observed upon ClpB1 overexpression.

In support of a possible role of ClpB1 in thylakoid membrane biogenesis, ClpB1 has been reported to co-isolate with His-tagged VIPP1 (Hamad, 2008). However, we were unsuccessful in detecting VIPP1 associated with His-tagged ClpB1. Based on the large amount of ClpB1 that appears to be present in the cell (Fig. 8), it is possible that the fraction of ClpB1 that interacts with any specific protein is insufficient for reliable detection.

As expected, the main difference in phenotype observed between the Slr1641+ strain and the wild type is related to heat stress. However, the ~20-fold increase in the percentage of surviving Slr1641+ cells (relative to the wild-type control) upon rapid (1

°C/s) heating of cells to 50 °C was larger than we had expected. It is likely that this effect is due to ClpB1 protein being present at high levels in the Srl1641+ strain, rather than that it is *de novo* synthesized during heat shock. Slower rates of heating would allow wild type to respond with the native *clpB1* expression pattern, and therefore at increasingly slow heating rates survival percentages of wild type and Slr1641+ eventually become equivalent. These observations serve as a reminder that temperature ramp-up rates are relevant and must be considered when testing for heat tolerance of engineered strains.

Previous research has shown increased high-temperature tolerance due to increased levels of a group of HSPs controlled by Hik34 (Suzuki et al., 2005). Here we show that overproduction of ClpB1 also conferred a modest increase in the length of time that cells could be exposed to non-permissive temperature (48-52 °C) (Fig. 11). The relatively small effect reaffirms that other heat-shock proteins are also required to overcome the heat stress (Mogk et al., 2003). Indeed, upon *dnaK2* overexpression in the Slr1641+ strain increased survival upon incubation of cells at 48 °C was observed (Fig. 11 D). Not surprisingly, the TE/Δ*slr1609* strain was more sensitive to heat shock than wild type, likely due to similar effects of fatty acid production observed in *Synechococcus elongatus* PCC 7942 (Ruffing & Jones, 2012). As expected, the overexpression of the Slr1641+/Sll0170+ pair increased cell survival.

The loss of phycobilisomes after overexpression of ClpB1 in the TE/Δ*slr1609* strain is puzzling. It is known that phycobilisome degradation is triggered by depletion of the nutrients N, S and P in a process mediated by the peptide NblA (Collier & Grossman, 1994). NblA has been found to attach to HSP100 proteins (ClpC) (Karradt et al., 2008); however, ClpB1 does not possess the binding residues for NblA. A high abundance of ClpB1, or abundance of a ClpB1-associated HSP100 protein complex interacting with NblA is feasible. Another option could be that in a fatty acid-producing strain

phycobilisomes are not binding to the thylakoid membrane and accumulate somewhere in the cell, as seen previously in *Synechococcus elongatus* PCC 7942 (Ruffing & Jones, 2012). Free-floating phycobilisomes could be a target for degradation and ClpB1 would participate in this process, possibly facilitating the degradation by Clp proteases. Finally, Slr1641+/Sll0170+ overexpression does not affect laurate production rates based on cell biomass in the culture; this is an effect that could have been expected since the *U. californica* thioesterase is a protein that does not occur in *Synechocystis*.

Studying chaperone expression effects in cyanobacteria is relevant towards generating stress-tolerant strains that can be engineered to produce valuable petroleum substitutes in outdoor conditions. Overall, overproduction of the ClpB1 chaperone confers improved heat tolerance because cells carry a now-constitutive component of the stress response machinery. ClpB1 overexpression thereby aids in cell survival when cells are heated quickly and delays cell death when cells are incubated at high temperatures. ClpB1 serves an early-response role in the cell, and constitutive expression aids to ameliorate the effects of sudden heating. This ClpB1 overproduction may be combined with overexpression of genes for other heat-shock proteins to lead to even more robust cyanobacterial strains.

Chapter 3

INCREASING PRODUCT YIELDS

I. "Induction of the MEP pathway in a *Synechocystis* sp. PCC 6803 mutant expressing a synthetic isoprene synthase"

Summary

Isoprene is a molecule produced by nature in large amounts; however, commercially it is obtained from petroleum refining processes. Isoprene is used in the plastics industry (for synthetic rubber and tires) and it can also be used as biofuel precursor. Here we attempted to increase previously reported isoprene yields by transforming *Synechocystis* sp PCC 6803 with a codon optimized poplar isoprene synthase (IspS+ strain) and by overexpressing antioxidant enzymes and limiting enzymes in the methyl erythritol phosphate pathway (MEP pathway). It was found that the IspS+ strain produces more isoprene than the strain expressing a synthetic isoprene synthase from kudzu. Isoprene production does not provoke major changes in the cellular phenotype, and overexpression of the MEP pathway enzymes did not increase the levels of isoprene production significantly. The substrate for isoprene synthase, dimethylallyl pyrophosphate (DMAPP) could not be detected in any of the cell extracts, suggesting a concentration of less than 25 μM in the cell. The Km for the poplar and kudzu enzymes is 3.7 mM and 7.7 mM DMAPP, respectively, explaining why overexpression of MEP pathway enzymes did not lead to isoprene production enhancement. The only MEP metabolite detected in wild-type and IspS+ strains was methyl erythritol pyrophosphate (MEcPP).

Introduction

Isoprene (2-methyl-1,3-butadiene) is one of the most abundant hydrocarbons of biological origin in the atmosphere, produced naturally by species like poplar (*Populus alba*), aspen (*Populus tremuloides*) and kudzu (*Pueria montana*), especially at high temperatures where it stabilizes membranes: at high temperatures, membrane fluidity is increased, which leads to ion leakage and cell death (Loreto et al., 2001; Sharkey et al., 2008). Isoprene at an industrial scale is used (after polymerization) as a synthetic replacement for rubber. Even though it is abundantly released to the environment by some plants, air stripping is not commercially feasible. Nowadays, isoprene is mainly generated as a byproduct of petroleum processing; hence the interest in developing isoprene production by microbes.

Microbial native isoprene production has been reported previously by *Bacillus* (Kuzma et al., 1995). After insertion of an isoprene synthase, isoprene production has also been observed in yeast (Hong et al., 2012), cyanobacteria (Lindberg et al., 2010) and *E. coli* (Zhao et al., 2011). Efforts to increase isoprene yields in the heterotrophic hosts have focused on engineering of the two main precursor pathways: the mevalonate pathway and the non-mevalonate pathway, also known as the methyl 2-C-methyl-d-erythritol-4-phosphate (MEP) pathway (Xue & Ahring, 2011; Yang et al., 2012; Zurbriggen et al., 2012). Metabolic optimization of the MEP pathway in cyanobacteria to increase isoprene yields has not yet been reported.

Synechocystis possesses the genes for the MEP pathway (Kaneko et al., 1996). In this pathway, pyruvate (PYR) is condensed with glyceraldehyde-3-phosphate (G3P) by the Dxs enzyme (encoded by *sll1945*) to produce 1-deoxy-D-xylulose-5-phosphate (DXP). DXP is also a precursor to thiamine, and so the first committed step in isoprenoid precursor production is the synthesis of 2-C-methylerythritol 4-phosphate (MEP) from

DXP by the Dxr enzyme encoded by *sll0019*. After subsequent steps, catalyzed by enzymes encoded by *slr0951, sll0711* and *slr1542*, MEP is transformed to 2-C-methyl-D-erythritol 2,4-cyclopyrophosphate (MEcPP). MEcPP is transformed to 4-hydroxy-3-methyl-but-2-enyl pyrophosphate (HMBPP) by the enzyme GcpE (encoded by *slr2136*) and later to isopentenyl pyrophosphate (IPP) and dimethylallyl pyrophosphate (DMAPP) by the enzyme LytB (encoded by *slr0348*). Different organisms produce different proportions of DMAPP/IPP: in tobacco it has been reported to be 15/85 (Tritsch et al., 2010) whereas in *E. coli* they are obtained at an approximate ratio of 1/5 (Adam et al., 2002; Rohdich et al., 2002). An isopentenyl isomerase (Ipi) (encoded by *sll1556)* then converts IPP to DMAPP and vice versa, although the Keq favors the production of DMAPP (Berthelot et al., 2012). The isomerase activity in *Synechocystis* (possibly a type II Ipi) was previously debated, since some authors were able to identify an isomerase activity from Sll1556 (Barkley et al., 2004) and some authors were not (Poliquin et al., 2004). Even though it is likely that Sll1556 is an Ipi enzyme, deletion only affects *Synechocystis* physiology under high light intensity (Poliquin et al., 2008). As mentioned, *Synechocystis* contains the enzymes for the MEP pathway (Figure 14). However, it has been proposed that there might be an alternative metabolic route to isoprenoids, since the MEP pathway was not stimulated by pyruvate by itself or by DXP but rather by sugar phosphates (Ershov et al., 2002). Deletion of LytB results in a lethal phenotype (Cunningham et al., 2000), which proves that LytB is required for isoprenoid synthesis. The products of the LytB enzyme, DMAPP and IPP, are required for isoprenoid production (carotenoids, phytol tail of chlorophyll, etc.), usually at a ratio of 3 IPP per DMAPP, whereas only DMAPP can serve as substrate for the isoprene synthase (IspS) enzyme.

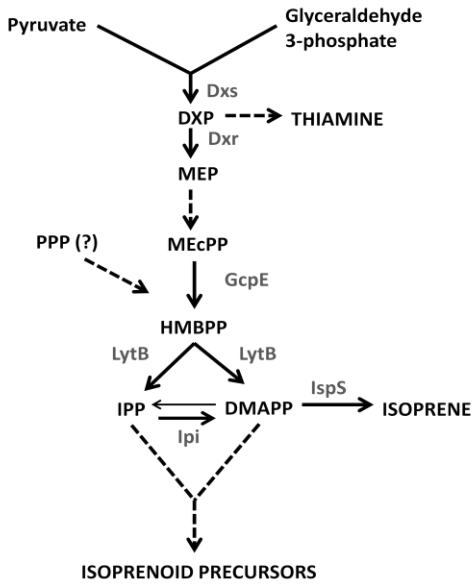

Figure 14. Simplified MEP pathway. Enzymes are shown in gray (Dxs: DXP synthase; Dxr: DXP reductase; GcpE: HMBPP synthase; LytB: HMBPP reductase; Ipi: IPP isomerase; IspS: isoprene synthase), metabolites in capital letters (DXP: 1-deoxy-D-xylulose-5-phosphate; MEP: 2-C-methylerythritol 4-phosphate, MEcPP:2-C-methyl-D-erythritol 2,4-cyclopyrophosphate; HMBPP: 4-hydroxy-3-methyl-but-2-enyl pyrophosphate; DMAPP: dimethylallyl pyrophosphate; IPP: isopentenyl pyrophosphate) and condensed pathways in dashed lines. PPP: pentose phosphate pathway.

Increased isoprene production in *Synechocystis* may result in a limiting concentration of DMAPP available for isoprenoids; however, this does not seem to be the case in the previously reported IspS mutant expressing a kudzu enzyme. While there is little carbon flux going towards isoprenoids (estimated 3-5% vs. 80-85% going to sugars) (Lindberg et al., 2010), only 0.08% carbon went to isoprene production in the kudzu IspS strain (Bentley & Melis, 2011). That would be less than 5% of the carbon for isoprenoids going into isoprene, which is not likely to cause adverse effects. In any case,

increasing the level of enzymes in the MEP pathway to increase carbon flux through the pathway is a direct attempt at increasing isoprene production.

A clue as to which enzymes should be overexpressed was shown by Li and Sharkey (2013) when they reported accumulation of MEP pathway metabolites (DXP, MEcPP and HMBPP) in aspen leaves. Such phenomena may be due to the requirement of reducing equivalents for their production or due to the insufficient turnover of the enzymes (Rivasseau et al., 2009). It is possible that having a larger pool of GcpE and LytB, which are prone to damage, allows to have more functional enzyme at any given time while the inactivated enzymes are repaired (Rivasseau et al., 2009). In *Arabidopsis*, overexpression of the first two and the last enzyme in the pathway (Dxs, Dxr and LytB, respectively) resulted in increased levels of isoprenoids in leaves (Botella-Pavía et al., 2004; Carretero-Paulet et al., 2006; Estévez et al., 2001), whereas GcpE overexpression did not (Flores-Pérez et al., 2008). Similarly, in *E. coli* it was shown that Dxs and LytB overexpression increased carotenoid levels, and even more so when combined. Expression of Ipi also increased carotenoids by itself and when combined with Dxs (Cunningham et al., 2000). Here we analyze the effects of overexpression of key enzymes in the MEP pathway on isoprene yields and carotenoid levels in a *Synechocystis* mutant expressing a synthetic isoprene synthase.

Materials and Methods

Design of a synthetic isoprene synthase gene. A synthetic *ispS* sequence was generated by Waldemar Hauf (Vermaas lab). The known amino acid sequences of isoprene synthases from *Populus tremuloides*, *Populus trichocarpa*, *Populus alba*, *Populus montana* and *Populus nigra* were aligned in order to determine conserved and variable regions of the enzyme. Variable regions of the isoprene synthase were the target

for amino acid changes, to produce a unique isoprene synthase that does not occur in nature. To avoid substitutions of amino acids that might disturb correct folding or change the active site of the isoprene synthase, the effects of amino acid changes were monitored *in silico*, using 5-epiaristolochene synthase from *Nicotiana tabacum* as template. Codons preferentially used in the rather highly expressed *psaA*, *psaB*, *psbA*, *psbB*, *psbC* and *apcE* genes in *Synechocystis* were used to optimize the codon usage in the newly designed isoprene synthase gene. Additionally, the T1T2-terminator sequence was added at the 3' end and the N-terminal plastid target sequence was removed from the enzyme. Having generated the desired DNA sequence (Appendix A), it was ordered from GeneArt (Invitrogen).

Mutant generation and growth conditions. A 125 ml culture of *E. coli* cells (BL21) containing the plasmid pET16-b and the inserted synthetic *ispS* under the control of the T7 promoter was grown at 37 °C on brain heart infusion (BHI) medium with 50 µg/ml ampicillin up to OD_{550}=0.5. Isoprene synthase production was induced by adding IPTG to a concentration of 400 µM IPTG and samples were prepared for SDS-PAGE or GC-MS.

Synechocystis was grown in BG-11 medium (Rippka et al., 1979) bubbled with air at 30 °C and illuminated at an intensity of 50 µmole photons/m^2/s. Transformation was performed as in Vermaas et al. (1987). The IspS+ mutant was generated by transforming wild-type cells with a fusion PCR product consisting of the neutral region between *slr0646* and *sll0601 (*2673415-2677109), with the *psbA2* promoter (6665-7227), synthetic *ispS* gene (Appendix A) and kanamycin-resistance marker inserted in between. Constructs to overexpress MEP pathway enzymes were generated by inserting the PCR-amplified ORFs (Table 3) into previously generated overexpression vectors with a pUC19 backbone and a T1/T2 terminator upstream of the resistance marker (separating the

inserted gene and the marker) (Table 4; vectors generated by Dr. Hongliang Wang) and were transformed into the IspS+ strain and combined when possible. The mutants obtained are summarized in Table 5.

Table 3

Primers Used for Cloning of MEP Genes into the Overexpression Vectors

Primer ID	**Sequence**
dxs fwd	AAT AGC ATA AGG AAT TAT AAC CAA ATG CAC ATC AGC GAA CTG ACC C
dxs rv	GCT CAT AGA TGT TTC CTC TTC TCA CTA ACT AAC TCC AGG AGC GAC AAC TGA TTC
ppa fwd	ATG GAT CTA AGC CGT ATT CC
ppa rv	TGC ATT TGG TTA TAA TTC CTT ATG CTA TTT GTA GTT CTT AAC GCA CTC
ppa fwd E coli	AGT TAG TGA GAA GAG GAA ACA TCT ATG AGC TTA CTC AAC GTC CCT G
ppa rv E coli	TTA TTT ATT CTT TGC GCG CTC GAA G
gcpE fwd	CTA AAC CTT CAT ATG GTA ACC GCT TC
gcpE rv	AGT ATG CGG CCG CTG GCG AG
lytB fwd	TCT CGT TTT CAT ATG GAT ACC AAA GC
lytB rv	GAA ATC GAA GCG GCC GCC CAA G
ipi fwd	TTG TAA TGT AAT TCA CAT ATG GAT AGC AC
ipi rv	TTG ATG CCC GCG GCC GCA GCT ATC

Table 4

Overexpression Vectors Used for MEP Enzyme Overexpression

ID	**Flanking regions (FR)**	**Location FR 1**	**Location FR 2**	**Promoter (location)**	**Antibiotic marker**
V 5	*slr1704/sll1575*	729195-729806	729807-730288	*rbcL* (2478137-2478413)	Cm
V 6	*ssr2848/ssl1577*	727061-727888	727913-728661	*rnpB* (152925-153165)	Zeo
V 7	*slr1285/sll1169*	1881887-1881237	1881221-1880814	*psbA2* (6666-7228)	Spec

Table 5

List of Generated IspS+ Strains

	Overexpression Strain	Gene(s)	Vector	Notes
1	IspS+	Synthetic poplar isoprene synthase	None; fusion PCR	
2	IspS+/GcpE+	*slr2136*	Vector 5	GcpE: MEcPP --> HMBPP
3	IspS+/LytB+	*slr0348*	Vector 6	LytB: HMBPP--> DMAPP + IPP
4	IspS+/Dxs+/Ppa+	*slr1622*, *sll1945*, *E. coli* Ppa	Vector 5	Dxs: G3P + PYR--> DXP
5	IspS+/Ipi+ *	*sll1556*	Vector 6	Ipi: DMAPP<-->IPP
6	IspS+/Ipi+ *	*sll1556*	Vector 7	
7	IspS+/SodB+/KatG+	*slr1516, sll1987*	Vector 6	SodB/KatG: O_2^- --> H_2O_2 --> $H_2O + O_2$
8	IspS+/GcpE+/LytB+	1 + 2 + 3	Vectors 5 and 6	
9	IspS+/LytB+/Ipi+	1 + 3 + 6	Vectors 6 and 7	
10	IspS+/Dxs+/Ppa+/Ipi+	1 + 4 + 5	Vectors 5 and 6	
11	IspS+/Dxs+/Ppa+/LytB+	1 +3 + 4	Vectors 5 and 6	

* IspS+/Ipi+ appears to be lethal on its own, but not lethal when combined with strains (3) and (4).

Cell analysis. Growth was observed over time as a change in optical density at 730 nm. Dry cell weight was determined by lyophilization overnight of cell pellets from 100 ml culture aliquots. 77K fluorescence emission spectra in the 625-775 nm range were measured in a SPEX Fluorolog 2 instrument using an excitation wavelength of 435 nm and a slit width of 0.25 mm, which corresponds to a bandwidth of 1 nm.

RT-PCR. RNA was extracted by Trizol reagent (Life Technologies), cleaned of DNA by Turbo DNA-free DNase (Life Technologies), and cDNA was synthesized by using random primers from the iScript select cDNA synthesis kit (BioRad), each following the manufacturer's protocols. For RT-PCR, the iTaq SYBR Green supermix with ROX (BioRad) and the specific primer pair for each gene (Table 6) were used; reactions were performed according to the manufacturer's instructions. Fluorescence of SYBR

green/double stranded DNA was measured on a ABI Prism 7900 HT Sequence Detection System from Applied Biosystems and samples were analyzed by the $2^{-\Delta\Delta Ct}$ method.

Table 6

Primers Used for RT-PCR of IspS+ Strains

Primer ID	**Sequence**
RT atpA fwd	AAA GCT TCC ACC GTC GCT C
RT atpA rv	GGC ACC TTT TTC CGT CAG G
RT ispS fwd	CCT ACC CCA TGC CGA ACT C
RT ispS rv	CAC TAC CAT CGG CGC TAC G
RT gcpE fwd	GTA ATG TTG GCC GCC TAT CG
RT gcpE rv	TGC CCA ACT CGT CCA TAC G
RT lytB fwd	GGT TTT GAC CCG GAC CAA G
RT lytB rv	ATG GTG GTT TGG TTG GCG
RT dxs fwd	TAA AGC TGA AAT TCT CCG GTC G
RT dxs rv	CCG TAG CCC AAC AGA AGC AC
RT ppa fwd	AAG ATC CCC GCT ACA CCT ACG
RT ppa rv	TTT CAT CCA AGC GGT GCC
RT ipi fwd	ACA GCC TGG AGT TTG CAA CAG
RT ipi rv	GGC GAA AAC CAG GAT CTG C
RT sodB fwd	ACC ATG CCG CCT ACG TTA AC
RT sodB rv	AAA TCA GTA CCC GCC ACT GC

Western blot. IspS (kudzu and poplar) polyclonal antibodies were a gift from Dr. Thomas D. Sharkey (Michigan State University). 200-ml culture aliquots from wild-type and all IspS+ strains (at OD_{730}=0.4-0.7) were pelleted and resuspended in 50 mM 2-(N-morpholino) ethanesulfonic acid-NaOH (pH 6.5) (MES buffer), 10 mM $MgCl_2$, 5 mM $CaCl_2$, 25% glycerol, and "protease inhibitor cocktail" (1 mM each of PMSF, benzamidine, and amino caproic acid). Cells were broken by 6x30 s of bead beating (0.1 mm glass beads) with 2 min of cooling on ice between all cycles. After centrifugation, the proteins contained in the supernatant were separated by 12% SDS-PAGE and transferred

to a PVDF membrane (Immobilon®-P) overnight at 20 V and 4 °C. Western blotting was performed according to Millipore's "Rapid Immunodetection without blocking" procedure using PBS buffer, fat-free milk as blocking agent, 1:5,000 dilution of the primary antibody and 1:3,000 dilution of an AP-conjugate secondary antibody; the immunoblot was developed using an AP substrate kit (BioRad).

Isoprene measurement by GC-MS. 1 ml culture aliquots (approx. OD_{730}= 0.5) were placed in 2 ml clear autosampler vials and supplemented with 10 mM bicarbonate or 5 mM glucose. Vials were incubated at a light intensity of 50 μmole photons/m^2/s for 12-16 h and 5 μl of headspace was injected into a HP 5890 GC connected to a MDN-5S column with He used as carrier gas. The injector temperature was set at 260 °C; the oven was started at 40 °C for the first 5 min, ramped to 250 °C (at a rate of 50 °C/min) and held for 2 min at 250 °C. The GC was interfaced to an HP 5972 Quadrupole MS Detector set at 200 °C and SIM acquisition mode (m/z 53, 67 and 68). Isoprene yields were obtained by comparison to a curve of known isoprene concentrations allowed to equilibrate in headspace.

Metabolite analysis by LC-MS. Cells at OD_{730}=0.5-0.7 were harvested by vacuum-filtering 50 ml of culture through a 0.2 μm pore nylon filter and cell paste was rapidly quenched by dipping the filter in 2 ml of -80 °C methanol. When appropriate, carbon isotope labeling was performed by adding 1 mM ^{13}C glucose prior to harvesting. Cells were scraped off the filters, transferred to a 2 ml microcentrifuge tube and pelleted. The supernatants were dried in a vacuum centrifuge and redissolved in 50 μl methanol. A 5 μl aliquot was injected into a Dionex Ultimate 3000 HPLC system and separated in a Synergi 4 um Hydro RP 250x1 mm ID column (Phenomenex) at a flow rate of 0.5 ml/min by the following linear gradients (A: 10 mM tributylamine adjusted to pH 4.95 with 15 mM acetic acid in H_2O, B: methanol): 0 to 5 min 100% A, 5 to 20 min gradient to

20% B, 20 to 35 min 20% B, 35 to 60 gradient to 65% B, 60 to 65 gradient to 95% B, 10 min at 95% B). Masses were determined using ESI-MS in a Bruker MicroTOF-Q mass spectrometer in the negative ion mode with the capillary voltage set at +4000V and the collision energy set at 10 eV. The methodology was based on that of Lu et al. (2010). Identification of compounds was confirmed by comparing with retention times of standards and peak areas were used to compare metabolite content (normalized by chlorophyll *a* content). Labeling speed was determined by comparing the peak intensities over time of the labeled metabolite against the unlabeled metabolite (corrected for natural isotope occurrence).

Pigment analysis by HPLC. A 1.5-ml aliquot from 50 ml cultures at OD_{730}=0.4-0.5 was spun down and the pellet was extracted with 1 ml methanol (2 x 500 µl). 150 µl were injected into a HP-1100 Chemstation system with a Spherisorb C18 ODS2 4.0 × 250 mm column (Waters). The following linear gradients of ethyl acetate (A) in methanol (B) and water (C) was used: 0 to 3 min a gradient of 10 to 0% C in B, 3 to 11 min a gradient of 0 to 70% A in B, 11 to 21 min a gradient from 70 to 100% A in B. The diode array detector (DAD) was set to detect elution at 452 nm and carotenoids were identified by their retention time.

Results

Expression of a synthetic poplar isoprene synthase. In order to confirm the functionality of the codon-optimized synthetic isoprene synthase gene (*ispS*), first we produced the protein in *E. coli* BL21 cells. IPTG-inducible expression of the synthetic *ispS* in the plasmid pET16-b/*ispS* resulted in isoprene accumulation in the headspace of autosampler vials. Isoprene increased with the incubation time (Figure 15). Isoprene production over time correlated with the synthesis of a protein of size between 75 and 50

kD, which corresponds to the predicted size of 64 kD for the synthetic IspS (Figure 15). Additionally, a N-terminal His-tag version of IspS cross-reacted with an Anti-His antibody (not shown).

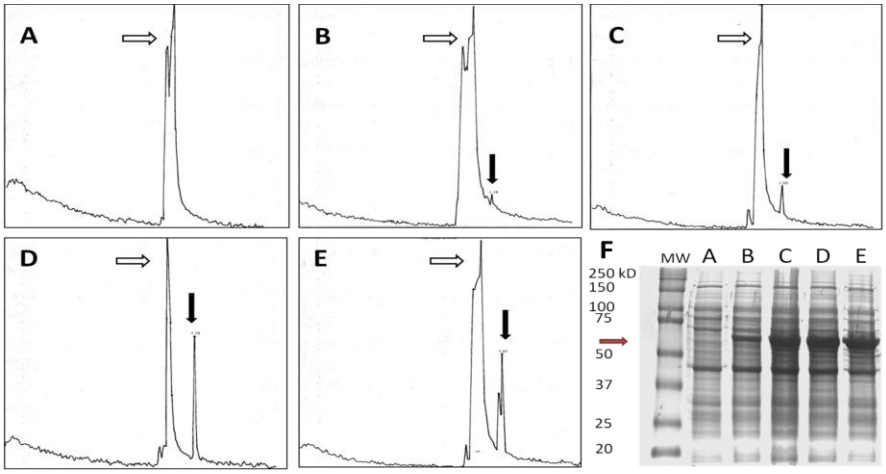

Figure 15. Confirmation of the functionality of the synthetic isoprene synthase. Chromatograms (A-E): Timecourse of isoprene production by *E. coli* cells expressing IspS after induction by IPTG. SDS-PAGE (F): IspS induction over time. A: 0 min; B: 30 min; C: 1 h; D: 2 h; E: 3 h after IPTG addition. White arrow: methanol from syringe washes; black arrow: isoprene; red arrow: isoprene synthase.

Once the synthetic IspS was confirmed to be functional in a heterotrophic host, the *ispS* fusion-PCR product was transformed into *Synechocystis* wild type, integrated into the genome by double-homologous recombination at the appropriate location, and complete segregation were obtained. RT-PCR was performed to determine the effects of synthetic *ispS* expression on select genes, especially those encoding enzymes in the MEP pathway (Table 7). The results suggest a moderate up-regulation of the transcript level for IPP isomerase (*ipi* gene), and down-regulation of pyrophosphatase (Ppa); which may be caused by an increased ratio of IPP to DMAPP.

Table 7

Expression Levels of Select Genes in Wild Type vs. IspS+. Cells were grown to an OD_{730} of about 0.5 at light intensities of 50 μmole photons/m^2/s and bubbled with air. Transcript abundance was normalized to the abundance of the *atpA* transcript.

	gcpE	***lytB***	***dxs***	***ppa***	***ipi***
Wild type	0.2 ± 0.1	0.12 ± 0.10	0.38 ± 0.39	0.48 ± 0.52	0.14 ± 0.09
IspS+	0.15 ± 0.08	0.04 ± 0.04	0.16 ± 0.15	0.24 ± 0.23	0.19 ± 0.13
Wild type vs. IspS+	0.6 ± 0.3	0.4 ± 0.1	0.4 ± 0.1	0.6 ± 0.1	1.8 ± 1.4

The phenotype of the generated *Synechocystis* strain IspS+ was then evaluated by transmission electron microscopy. Micrographs of the wild-type and the IspS+ strains were not clearly different (Figure 16). Small white inclusions in between thylakoid membranes were identified as glycogen bodies (frequently observed when glucose is used as carbon source); carboxysomes were present and unknown dark inclusions were observed. Further analysis of the IspS+ strain, together with strains overexpressing genes from the MEP pathway, is shown in the following sections.

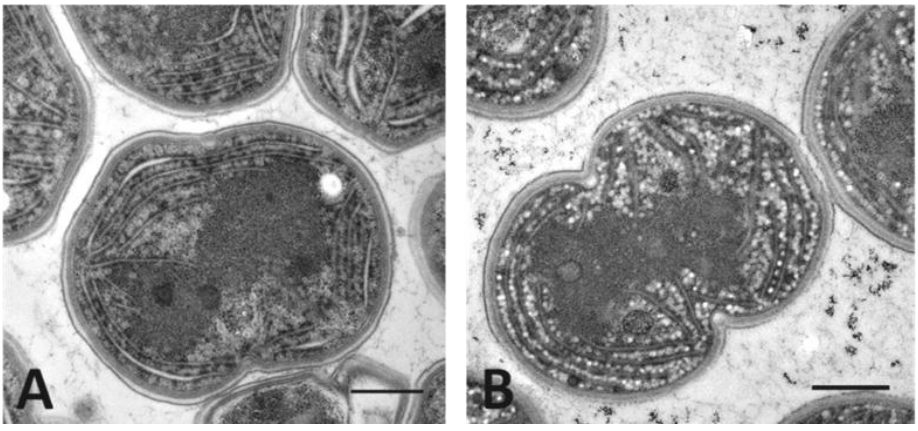

Figure 16. Electron micrographs of wild-type and IspS+. A) wild type and B) IspS+ grown under normal conditions to OD_{730}=0.5 in the presence of 5 mM glucose (scale bar: 0.5 μm).

Overexpression of enzymes from the MEP pathway enzymes in the IspS+ background. In order to increase the carbon flux through the MEP pathway, we overexpressed the open reading frames coding for the enzymes Dxs (the first step in the pathway), GcpE (since its substrate, MEcPP, accumulates the most (Li & Sharkey, 2013)), LytB (since it produces the isoprene precursors DMAPP and IPP) and Ipi (since it could drive the DMAPP/IPP equilibrium towards DMAPP). For this purpose, genes were cloned into three overexpression vectors and transformed into an IspS+ background. An artificial operon was generated with Dxs and two copies of pyrophosphatase genes (*ppa*, from *Synechocystis* and *E. coli*) to avoid phosphate limitation in case the MEP pathway flux was indeed increased: two pyrophosphates are produced per each isoprene produced by the MEP pathway. Similarly, the antioxidant enzymes SodB/KatG were overexpressed in an operon with the goal of increasing the antioxidant capacity of the cell, since 1) carotenoids are important antioxidants in the cell (Schäfer et al., 2005) and a decrease in carotenoid content due to DMAPP limitation was possible and 2) isoprene could react with reactive oxygen species, thus decreasing isoprene yields. Interestingly, we were not able to obtain an IspS+/Ipi+ strain; however, it was possible if IspS+/Ipi+ was combined with LytB or Dxs/Ppa. This observation could be explained if Ipi would lead to a limitation of DMAPP or IPP, which cells can overcome when the MEP pathway is stimulated. A summary of strains generated is presented in Table 5. To confirm that the genes of interest are indeed being overexpressed, we analyzed transcript levels by RT-PCR. All IspS+ variants were overexpressing the desired gene(s) (Table 8).

Table 8

RT-PCR of IspS+ Variants Showing Overexpression of the Desired Genes. Cells were grown to an OD_{730} of about 0.5 at light intensities of 50 μmole photons/m^2/s and bubbled with air. Transcript abundance was normalized to the abundance of the *atpA* transcript. A) Relative abundance of transcripts compared to *atpA* ($2^{-\Delta Ct}$) and B) relative expression of the transcripts of IspS+ strains vs. wild type ($2^{-\Delta\Delta Ct}$).

A	*gcpE*	*lytB*	*dxs*	*ppa*	*ipi*	*katG*
Wild type	0.2 ± 0.1	0.12 ± 0.10	0.38 ± 0.39	0.48 ± 0.52	0.14 ± 0.09	0.44 ± 0.48
IspS+	0.15 ± 0.08	0.04 ± 0.04	0.16 ± 0.15	0.24 ± 0.23	0.19 ± 0.13	0.18 ± 0.03
IspS+/GcpE+	2.90 ± 1.13	0.17 ± 0.23	0.17 ± 0.12	0.31 ± 0.29	0.27 ± 0.21	0.33 ± 0.18
IspS+/LytB+	0.20 ± 0.13	0.97 ± 0.47	0.21 ± 0.18	0.33 ± 0.25	0.39 ± 0.31	0.40 ± 0.06
IspS+/Dxs+/Ppa+	0.18 ± 0.06	0.07 ± 0.03	0.54 ± 0.36	1.67 ± 0.57	0.36 ± 0.35	0.30 ± 0.03
IspS+/SodB+/KatG+	0.29 ± 0.20	0.11 ± 0.06	0.38 ± 0.38	0.76 ± 1.06	0.31 ± 0.18	1.24 ± 0.44
IspS+/GcpE+/LytB+	5.99 ± 2.33	0.55 ± 0.01	0.12 ± 0.10	0.12 ± 0.05	0.21 ± 0.23	0.46 ± 0.33
IspS+/LytB+/Ipi+	0.18 ± 0.1	0.59 ± 0.56	0.15 ± 0.18	0.14 ± 0.13	0.11 ± 0.08	0.29 ± 0.07
IspS+/Dxs+/Ppa+/Ipi+	0.39 ± 0.32	0.08 ± 0.08	1.42 ± 1.92	2.93 ± 3.56	0.92 ± 0.03	0.5 ± 0.35
IspS+/Dxs+/Ppa+/LytB+	0.29 ± 0.35	0.16 ± 0.15	3.81 ± 5.83	6.19 ± 6.79	0.23 ± 0.04	0.40 ± 0.28

B	*gcpE*	*lytB*	*dxs*	*ppa*	*ipi*	*katG*
IspS+	0.6 ± 0.3	0.4 ± 0.1	0.4 ± 0.1	0.6 ± 0.1	1.8 ± 1.4	0.9 ± 0.9
IspS+/GcpE+	9.5 ± 0.3	2 ± 2.5	0.5 ± 0.3	0.7 ± 0.1	1.3 ± 1.5	2.5 ± 3.1
IspS+/LytB+	0.8 ± 0.5	7.5 ± 0.9	0.6 ± 0.2	0.8 ± 0.4	2.3± 1.8	2.1 ± 2.2
IspS+/Dxs+/Ppa+	0.6 ± 0.1	0.6 ± 0.4	1.6 ± 1.4	4 ± 2.8	2.1 ± 2.3	1.8 ± 2.1
IspS+/SodB+/KatG+	1.2 ± 0.7	1 ± 0.5	1.2 ± 0.3	1.2 ± 0.9	1.1 ± 0.2	8.5 ± 10.4
IspS+/GcpE+/LytB+	44.5 ± 42.7	15 ± 17.5	1.9 ± 2.3	0.9 ± 0.5	5.0 ± 6.7	3.7 ± 4.8
IspS+/LytB+/Ipi+	0.9 ± 0.2	7.2 ± 3.6	0.8 ± 0.7	0.7 ± 0.1	2.3 ± 2.9	1.9 ± 2.2
IspS+/Dxs+/Ppa+/Ipi+	1.9 ± 0.3	0.9 ± 0.4	4 ± 0.7	12.2 ± 8.3	14.9 ± 14.2	1.8 ± 1.1
IspS+/Dxs+/Ppa+/LytB+	1.4 ± 1.3	1.3 ± 0.3	8 ± 5.6	24.5 ± 21.8	2.7 ± 2.6	1.4 ± 0.9

To test the presence of the synthetic IspS resembling the poplar IspS in all IspS+ strains, a western blot was performed using anti-kudzu IspS and anti-poplar IspS antibodies. Extracts from all IspS+ strains tested cross-reacted with antibodies against the poplar isoprene synthase (Figure 17) but not with the antibodies against kudzu isoprene synthase (not shown). Such specificity has been shown previously (Sharkey et al., 2008). Some cross-reactivity was observed with a protein of ~130 kD, which is likely due to aggregates of the synthetic IspS.

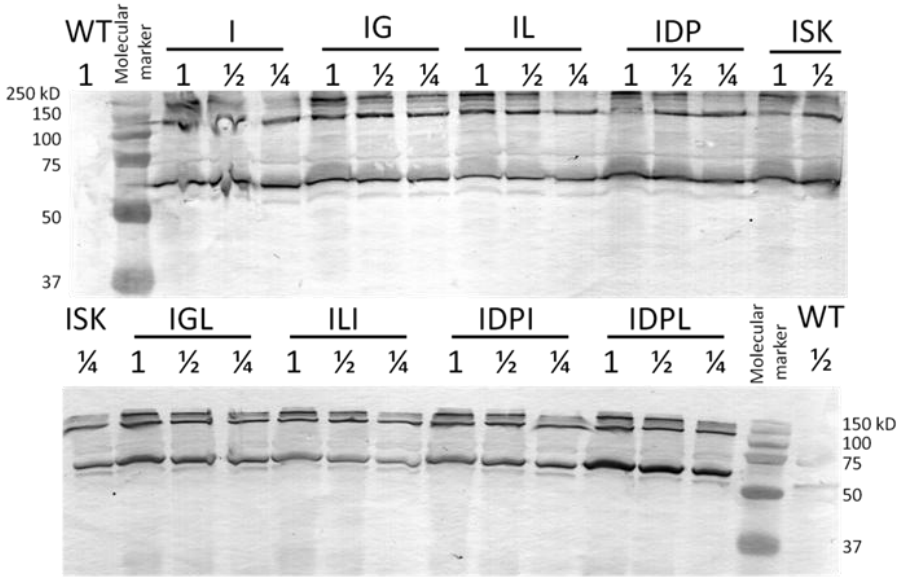

Figure 17. Western blot of IspS+/MEP overexpression strains. Protein extracts from strains grown under normal conditions, probed with rabbit anti-IspS (poplar) antibodies. Maximal loading (1) corresponds to 10 µg chlorophyll *a* per well. Loadings in other lanes have been reduced as indicated in order to allow an estimation of IspS levels between strains. Marker lanes separate the wild-type lanes from the IspS+ lanes (WT: wild-type; I: IspS+; IG: IspS+/GcpE+; IL: IspS+/LytB+; IDP: IspS+/Dxs+/Ppa+; ISK: IspS+/SodB+/KatG+; IGL: IspS+/GcpE+/LytB+; ILI: IspS+/LytB+/Ipi+; IDPI: IspS+/Dxs+/Ppa+/Ipi+; IDPL: IspS+/Dxs+/Ppa+/LytB+).

As indicated in Table 9, the doubling time, the number of cells per OD/ml, dry cell weight (DCW) per OD/ml and the ratio of fluorescence emission from the two photosystems of cultures in exponential phase (~OD_{730}=0.5) with CO_2 as carbon source were not greatly affected due to the expression of the synthetic IspS and/or the overexpression of the MEP enzymes.

Table 9

Phenotype Comparison of the IspS+ Strains. Cells were grown to an OD_{730} of about 0.5 at light intensities of 50 μmole photons/m^2/s and bubbled with air. Doubling times, cell numbers and dry cell weight (DCW) per OD/ml and the ratio of 77 K fluorescence emission from the two photosystems (723 nm/683 nm) are indicated.

Strain	**Doubling time (h)**	**Cells/OD_{730}/ml**	**DCW/OD_{730} /ml (μg)**	**77K Fluorescence (723 nm/ 683 nm)**
Wild type	13.6 ± 0.7	$1.6x10^8 \pm 2.4x10^7$	217 ± 42	4.2 ± 0.6
IspS+	14.9 ± 0.5	$1.7x10^8 \pm 2.8x10^7$	231 ± 67	3.8 ± 0.2
IspS+/GcpE+	15.2 ± 0.8	$1.4x10^8 \pm 3.6x10^7$	215 ± 61	4.2 ± 0.6
IspS+/LytB+	16 ± 0.5	$1.5x10^8 \pm 1.8x10^7$	254 ± 57	4.0 ± 0.2
IspS+/Dxs+/Ppa+	13.5 ± 0.1	$1.6x10^8 \pm 1.3x10^7$	268 ± 61	3.9 ± 0.3
IspS+/SodB+/KatG+	15.3 ± 0.2	$1.7x10^8 \pm 1.2x10^7$	200 ± 28	3.5 ± 0.4
IspS+/GcpE+/LytB+	15.2 ± 1.2	$2.2x10^8 \pm 2.7x10^7$	174 ± 39	3.8 ± 0.3
IspS+/LytB+/Ipi+	16.6 ± 2.1	$2x10^8 \pm 4.2x10^7$	191 ± 29	3.8 ± 0.01
IspS+/Dxs+/Ppa+/Ipi+	13.1 ± 0.4	$2.3x10^8 \pm 6.6x10^5$	240 ± 59	3.8 ± 0.01
IspS+/Dxs+/Ppa+/LytB+	13.6 ± 0.4	$1.1x10^8 \pm 1.2x10^7$	242 ± 48	3.6 ± 0.3

Isoprene production in MEP pathway overexpression strains. All mutants evolved isoprene, which accumulated in the headspace of autosampler vials (Figure 18). Most strains with a single additional overexpressed gene did not show significantly increased isoprene production when compared to the IspS+ control. The IspS+/Dxs+/Ppa+/Ipi+ strain produced the most isoprene of all strains with either glucose or bicarbonate as a carbon source. This agrees with the interpretation that DMAPP and IPP regulate the activity of Dxs (Banerjee et al., 2013). If we assume that there is accumulation of IPP (or decreased amounts of DMAPP), then Ipi overexpression becomes relevant. The second mutant with high average isoprene production is IspS+/SodB+/KatG+. Interestingly, this mutant produced significantly more isoprene under photoautotrophic conditions than photomixotrophic conditions, suggesting that photosynthetic production of isoprene can be affected by reactive oxygen species (ROS), and scavenging of ROS is a factor to consider when optimizing isoprene-producing strains for outdoor growth conditions (more stress would lead to more ROS).

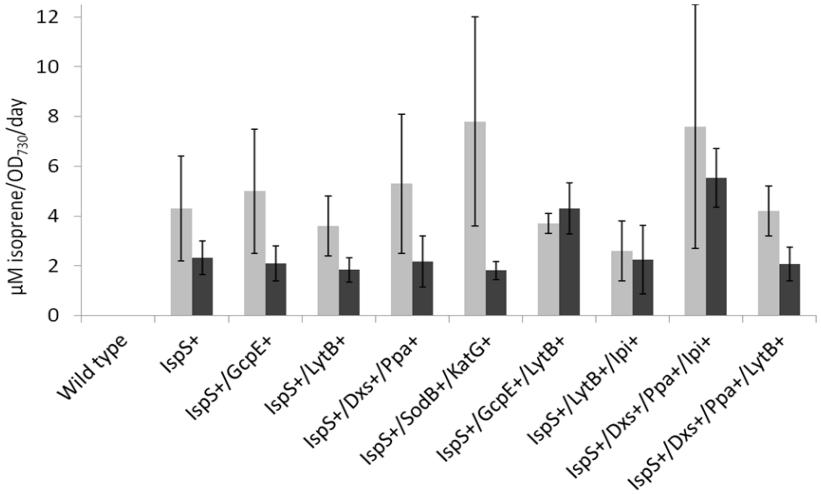

Figure 18. Isoprene production by *Synechocystis strains* containing an isoprene synthase. Light gray: photoautotrophic cultures (10 mM bicarbonate); Dark gray: photomixotrophic cultures (grown with 5 mM glucose) (n=3).

The major pigments from the *Synechocystis* cultures (myxoxanthophyll, zeaxanthin, chlorophyll, echinenone and ß-carotene) were analyzed since the MEP pathway is used for their synthesis. After running the extracts through the HPLC-DAD, the peak areas of each type of pigment were normalized to the corresponding pigment level in wild-type. The pigments in the IspS+ strain and its derivatives do not vary significantly from those in wild type (Figure 19).

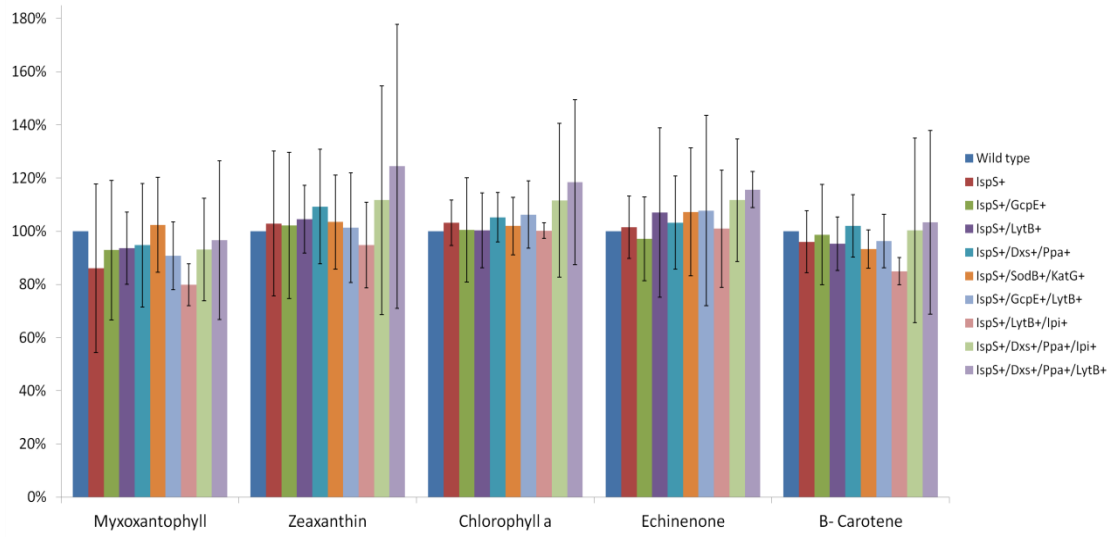

Figure 19. Comparison of pigments in methanol extracts from various photoautotrophic cultures. Extracts originate from wild type, IspS+ and its derivatives as indicated to the right. Peak areas for each pigment were normalized to the level of the corresponding pigment in wild type. ($n \geq 3$).

MEcPP accumulation in *Synechocystis*. It has been shown previously that hybrid aspen leaves accumulate DXP, HMBPP and especially MEcPP (Li & Sharkey, 2013). Similarly, *Synechocystis* accumulated MEcPP to detectable levels, whereas the rest of the MEP metabolites were below our limit of detection (~ 1 µM in the 50-µl extract) in all mutants even when larger (200 ml) culture volumes were extracted rather than the usual 50-ml cultures. The levels of MEcPP (normalized to chl *a)* were similar in

wild type and IspS+ strains bubbled with air, except in the strains that overexpress GcpE, which uses MEcPP as substrate. Wild type levels of MEcPP were ~21 μg/mg chl *a* in both photoautotrophic and photomixotrophic growth. Cells that grew on glucose as carbon source accumulated less MEcPP in the strains overexpressing LytB and Dxs/Ppa. Once more, the IspS+/GcpE+ strain accumulated a significantly lower level of MEcPP (Fig. 20).

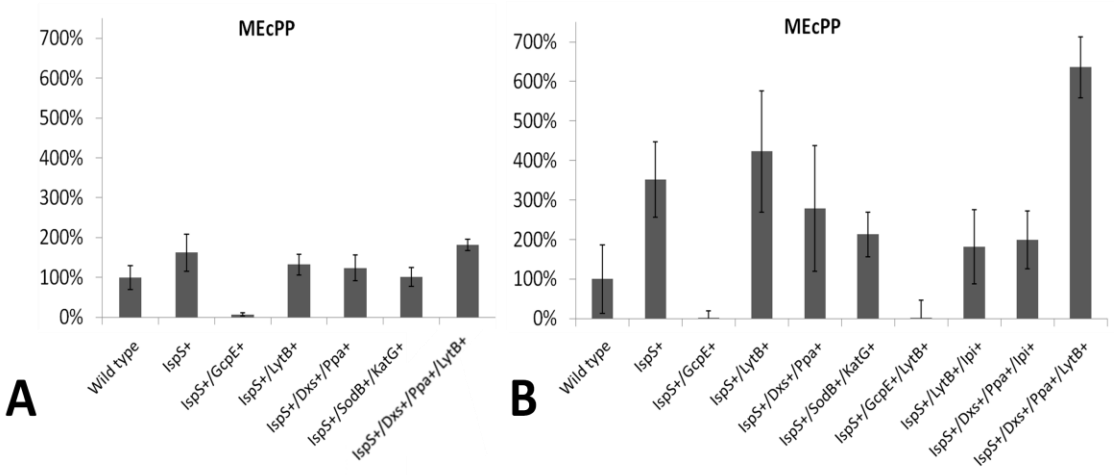

Figure 20. Comparison of the accumulation of the MEP metabolite MEcPP. MEcPP levels in strains grown photoautotrophically (A) and grown photomixotrophically (B) were normalized based on chl *a* in wild type. (100% is 20.9 μg/mg chl *a*) ($n \geq 3$).

As MEcPP was the only MEP metabolite we were able to observe, we isotopically labeled MEcPP by feeding the cultures ^{13}C glucose and in order to gain insight regarding the rate of carbon flux going through the MEP pathway (up to the point when MEcPP is synthesized) we observed the assimilation rate of the carbon isotopes into MEcPP by following the increase in the MEcPP molecular weight. As shown in Table 10, MEcPP was labeled faster in the IspS+/GcpE+ strain than in wild type, as expected from the small pool size (Fig. 20). Conversely, larger pool sizes tend to correspond to slower

labeling rates. However, overall there does not seem to be evidence for increased metabolic flux through the pathway. Several factors may contribute to the lack of increased metabolic flux. First, only some of the enzymes have been overexpressed, and other steps may now have become rate-limiting. Moreover, even though transcript levels of some of the MEP enzymes are higher, it does not necessarily mean that there is more active protein, as it has been observed that, at least in higher plants, enzymes in the MEP pathway can be regulated post-transcriptionally (Cordoba et al., 2009).

Table 10

Half-labeling Times of MEcPP from ^{13}C-Glucose in Different Strains

Strain	**Half-labeling time (min)**
Wild type	5.1 ± 0.6
IspS+	5 ± 1.5
IspS+/GcpE+	2.9 ± 0.6
IspS+/LytB+	5.3 ± 0.8
IspS+/Dxs+/Ppa+	6.2 ± 1.5
IspS+/SodB+/KatG+	5.7 ± 2.2
IspS+/GcpE+/LytB+	4.2 ± 1.9
IspS+/LytB+/Ipi+	3.9 ± 0.4
IspS+/Dxs+/Ppa+/Ipi+	4.6 ± 1
IspS+/Dxs+/Ppa+/LytB+	6.9 ± 1.3

Discussion

The IspS+ strain had no obvious phenotypic differences compared to wild type, except for a slight downregulation of the MEP pathway genes tested and an upregulation of the *ipi* gene. The upregulation of *ipi* is expected since LytB favors the production of IPP rather than DMAPP, and in an isoprene-producing strain the need for DMAPP is increased. Isoprene synthase competes with geranyl geranyl pyrophosphate synthase (GGPP synthase) for the DMAPP substrate. GGPP synthase catalyzes the formation of GGPP, an intermediate in isoprenoid production, from one DMAPP and three IPP molecules. Since the reported Km value for higher plant GPP synthase is in the μM range (Tholl et al., 2001) and the Km of IspS-poplar in the mM range (Schnitzler et al., 2005), IspS expression is not expected to induce changes in pigment levels unless the amount of IspS is so high that IspS competes effectively with GGPP synthase for available substrate.

Heterologous isoprene production had been shown previously in *Synechocystis* using a synthetic kudzu isoprene synthase gene (*ispS-kudzu*) (Lindberg et al., 2010). The synthetic *ispS* sequence reported in this work is 61% identical (analyzed by ClustalW2) to the *ispS-kudzu* sequence, and the synthetic IspS protein differs enough from IspS-kudzu (54% identity) that it is recognized by an antibody raised against poplar IspS but not by the antibody against kudzu IspS. Isoprene production rates differ between results published by Bentley and Melis (2011) (4 μg isoprene (l culture)$^{-1}$ h^{-1}) using IspS-kudzu and our data by about a factor of 2-3 (11.3 μg isoprene (l culture)$^{-1}$ h^{-1} using an average daily production of 4 μM isoprene). This factor of 2-3 difference is expected since the recombinant isoprene synthase enzyme from poplar expressed in *E. coli* showed a higher affinity for DMAPP than the kudzu enzyme (Kms are 3.7 mM for poplar (Schnitzler et al., 2005) vs. 7.7 mM for kudzu (Sharkey et al., 2005)). The difference may also be explained by a different approach to codon optimization. The *ispS-kudzu* was designed to avoid

rare codons in *Synechocystis* according to the Kazusa Codon Usage Database (Nakamura et al., 2000) and the *ispS-kudzu* sequence was adjusted taking into account the AT/GC ratio. In our study it was decided to use codons abundant in highly expressed genes encoding major photosystem proteins (*psaA, psaB, psbA, psbB, psbC, psbD* and *apcE*) and use one codon for each amino acid if possible. These two strategies in codon optimization may yield different translation efficiency or activity.

The improvement in isoprene yields resulting from MEP overexpression was lower than initially expected. It is unknown to what extent DMAPP production was increased, but it was insufficient to greatly boost the levels of isoprene evolved. The isoprene production rate of all strains is not significantly different from that in the IspS+ control. To boost isoprene production rates it will be important to increase DMAPP levels in the cell to levels near the Km of the isoprene synthase enzyme by increased flux through the entire MEP pathway and/or by downregulation of the GGPP synthase.

II. "Attempt at overexpression of *Synechocystis slr1471* to increase lipid content"

Summary

Lipids are the desired product when algal biomass is grown to produce diesel. In *Synechocystis*, lipids are mostly found as components of the thylakoid and cytoplasmic membranes. By genetic engineering, *Synechocystis* can be modified to accumulate a larger percentage of lipids. This section refers to an attempt at increasing lipids in *Synechocystis*, by overexpressing the *slr1471* gene. The Slr1471+ strain had little increase in *slr1471* transcript. The total lipids per dry cell weight were similar or even somewhat decreased in comparison to wild type. However, thylakoid membranes were irregularly organized in the cell. Overexpression levels of *slr1471* may need to be higher to detect a clear phenotype.

Introduction

Thylakoid membrane lipids from *Synechocystis* can serve as raw material for green diesel production (Griffiths & Harrison, 2009). As membranes are a very important component of the metabolic machinery of the cell (photosynthesis, respiration, regulation, molecule barrier, etc.), modification of certain regulators and membrane proteins are likely to result in altered membrane amounts in the cell. The complexity of membrane biogenesis and regulation represents thousands of possibilities for metabolic engineering. In this section of the dissertation, a genetic modification is presented that explores some of this complexity but that unfortunately did not result in a favorable phenotype.

The modification attempted was *slr1471* overexpression. In a fully functional cell, a variety of molecules are targeted towards the membrane space in order to be anchored to it, or even sent across the membrane to the extracellular space. When designing bacteria that produce metabolites at industrial scale, translocation pathways become even more important (e.g., secretion of lipases for biomass processing) (Jaeger & Eggert, 2002)). The Sec-dependent protein secretion pathway is a widely used complex protein channel that uses ATP to translocate nascent proteins across the cytoplasmic membrane (Mori & Ito, 2001). In contrast, the Sec-independent pathway is believed to use proteins such as Oxa1 in mitochondria, YidC in *E. coli* and Alb3 in chloroplasts to integrate proteins into membranes (Samuelson et al., 2000). It has been proposed that these proteins function in a manner similar to chaperones, interacting with hydrophobic regions and shielding hydrophilic regions of a protein from the hydrophobic lipid bilayer allowing the protein to cross the membrane (Serek et al., 2004). The proteins from the Sec-independent pathway may also play a role in folding and assembly of protein complexes in the membrane, by removing the preproteins being formed from the SecY translocase (Dalbey & Chen, 2004). Components of the Sec-independent pathway are also thought to be involved in thylakoid generation (Spence et al., 2004) and in PSII repair (Ossenbühl et al., 2006). Even though the *slr1471* sequence is not similar to other Oxa1/YidC/Alb3 proteins, Gathmann et al. (2008) found that Slr1471 was indeed part of the Oxa1/YidC/Alb3 family. Immunologic assays by Gathmann et al. (2008) using gold particles and immunoblotting by Fulgosi et al. (2002) located Slr1471 in the cytoplasmic membrane.

Creation of *slr1471* deletion mutants was attempted by both Fulgosi et al. (2002) and Spence et al. (2004); however, different phenotypes were observed. First of all, while one did not achieve segregation (Spence et al., 2004), the other obtained a fully

segregated, photosynthetic, viable strain (Fulgosi et al., 2002). The fully segregated strain was defective in cell division (YidC has been observed to interact with the protein FtsQ (Urbanus et al., 2001), a protein required for septum formation (Carson et al., 1991)), while the merodiploid non-segregated mutant was barely viable and had disorganized thylakoids. Here we aimed to determine if a *slr1471* overexpression strain would generate more thylakoid membranes. This could be expected since it has been observed that *Δslr1471* is altered in thylakoid generation (Spence et al., 2004) and that the Slr1471-homolog Alb3 has been found to associate with the vesicle-inducing protein in plastids (VIPP1; key enzyme for thylakoid biogenesis) in *Chlamydomonas* (Göhre et al., 2006), and because VIPP1 overexpression has been shown to increase lipids in *Synechocystis* (Hamad, 2008).

Materials and Methods

Creation of an overexpression vector and growth conditions. In order to facilitate insertion of genes into the *Synechocystis* genome an overexpression vector was created. All sequences and location in the *Synechocystis* genome are stated according to Cyanobase. The vector consisted of a shortened pUC19 backbone (the sequence between 289-785 was removed by PCR and EcoRI ligation) with the cloned neutral, non-coding regions between *sll1169* and *slr1285* divided in two fragments (1880815-1881221 and 1881237-1881887) and carrying the restriction sites BamHI and SphI near the contact point. Between those restriction sites, the *ftsQ* (*sll1632*) promoter (bases 1015775-1015397), the *slr1471* ORF, the T1/T2 terminator and a kanamycin resistance/sucrose sensitivity cassette from *psbA2*-KS (Lagarde et al., 2000) were cloned using the restriction enzymes SphI, NcoI, NdeI and BamHI as shown in Figure 21. Primers used for cloning are found in Table 11.

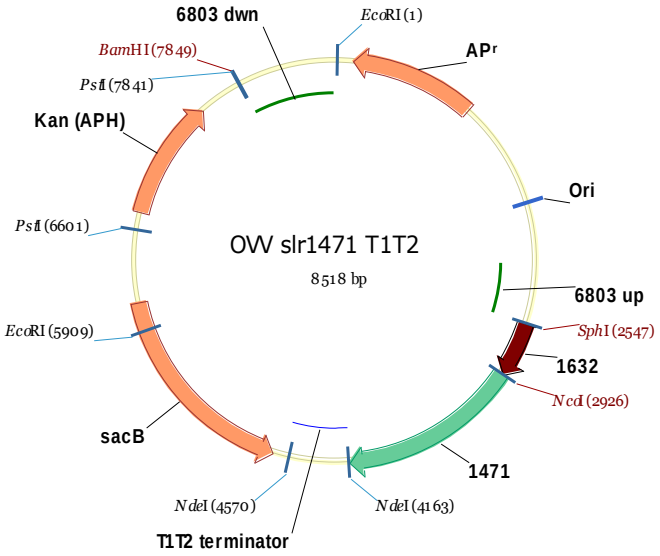

Figure 21. Plasmid that uses the *ftsQ* promoter to overexpress the *Synechocystis slr1471* gene.

Table 11

Primers for Vector Generation, Cloning, Segregation Check and RT-PCR of slr1471

Primer ID	**Sequence**
FR left fwd	AAT TCT CTG CAG TTG GGG AGA CTG
FR left rv	CAC AGT GAA ATG GAT CCC AAC GC
FR right fwd	TTT CTG CAT GCG TTG GGA TCC ATT TC
FR right rv	GAT GGG AAA GTT AAC AGC GGT AAC
cut pUC19 fwd	GAC GTT GTA AAA CGA CGG CC
cut pUC19 rv	GCG CGG AAT TCC TAT TTG TT
sll1632 fwd	CTT CTC CAG CAT GCC CCG AAT G
sll1632 rv	CAA CTA AAT CCG CCA TGG GAG
slr1471 fwd	GCT TGT TAG CCA TGG ATT TTG G
slr1471 rv	CAT CGT CCA TAT GCA GGT CTC
Segreg. screen fwd	CTT TTT GCC ACT GCA ATT TAA CAG AC
Segreg. Screen rv	GCC CAA ACC AAG AGT TTA TCT TC
RT slr1471 fwd	TCC CAT TGC TGT TTT CCT GC
RT slr1471 rv	TTT CTC CCC GAC TCC AAG C

E. coli DH10B cells were grown in LB medium at 37 °C and supplemented with 50 μg/ml kanamycin when appropriate. *Synechocystis* cells were grown at 30 °C in BG-11 medium (Rippka et al., 1979) in 500-ml flasks bubbled with air and illuminated at a light intensity of 40 μmole photons m^{-2} s^{-1}. Transformation was performed as described previously (Vermaas et al., 1987) and resulted in a fully segregated strain Slr1471+ (Fig. 22).

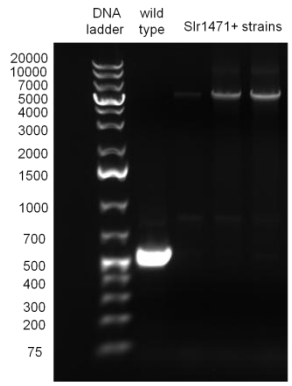

Figure 22. DNA electrophoresis of PCR products showing segregation of *ftsQ-slr1471* overexpresssion in the Slr1471+ strain.

- For cell analysis methods see previous section in this chapter.

Results and Discussion

Synechocystis wild-type was transformed with the vector containing *slr1471* under the control of the *ftsQ* promoter. The vector succesfully integrated into the genome and the tranformant segregated, thus obtaining the Slr1471+ mutant. However, RT-PCR results showed significant variation in *slr1471* transcript levels ranging from basal levels to ~4-fold overexpression. This effect is likely due to the use of the *ftsQ* promoter, which is not particularly strong. Furthermore, it has been reported that the

ftsQ promoter is controlled by transcriptional regulators, which could be a factor affecting *ftsQ*-based *slr1471* overexpression in the Slr1471+ mutant.

In any case, a comparison between wild type and Slr1471+ was performed (Table 12 and Figure 23). As expected, the strains were not very different from each other, except for a slightly higher dry cell weight (DCW) in the Slr1471+ strain, which results in a lower percentage of lipids per DCW. Electron micrographs did not show obvious differences between the strains (Figure 24), besides occasional stacking and disarrangement of thylakoid membranes (Figure 25).

Table 12

Phenotype Comparison of Wild Type and Slr1471+

	Doubling time (h)	**Cells/ml/OD_{730}**	**Chlorophyll *a* (µg/ml/OD_{730})**	**Dry cell weight (DCW; mg/L/OD_{730})**	**Lipids (% DCW)**
Wild type	12.2 ± 1.7	$1.7x10^8 \pm 3.3x10^7$	3.3 ± 0.2	216 ± 6	12 ± 1.3
Slr1471+	9.4 ± 0.9	$1.4x10^8 \pm 2.3x10^7$	3.1 ± 0.02	249 ± 24	9 ± 1.9

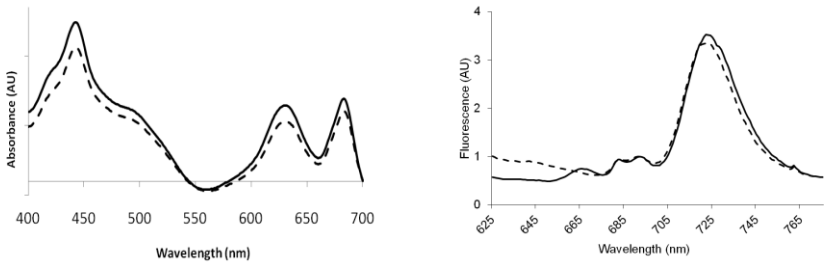

Figure 23. Absorbance spectra and 77K fluorescence emission spectra of the wild-type and Slr1471+ strains. Left: Absorbance spectra; right: fluorescence emission spectra. Wild type: solid line; Slr1471+: dashed line; for all measurements, OD_{730}=0.5.

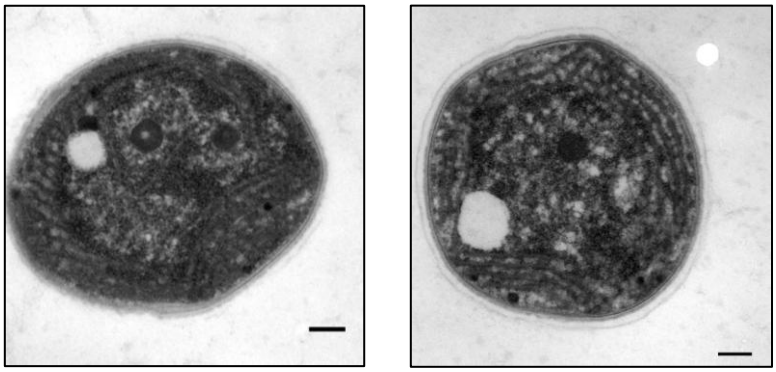

Figure 24. Micrographs of wild type (left) and Slr1471+ (right). (scale bar: 0.2 μm)

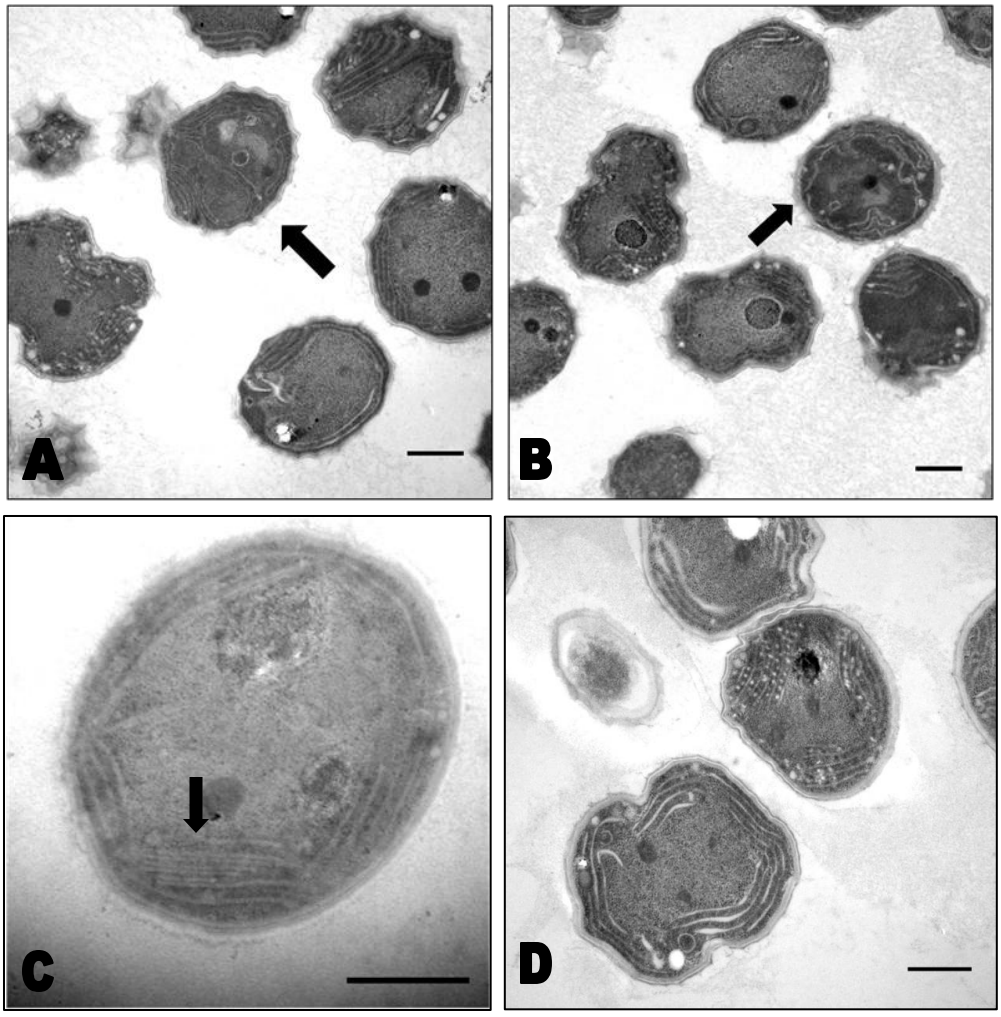

Figure 25. Micrographs of Slr1471+ cells showing abnormal thylakoids in cells. A,B and C: Slr1471+; D: wild type. Abnormal membranes: black arrow (scale bar: 0.5 μm).

Analysis of the lipid unsaturation profile by LC-MS showed that the diglycerides from wild type and Slr1471+ were similar; however, Slr1471+ accumulated more 16, 16:0 of SQDG and DGDG (Figure 26). This is an interesting observation that would have to be confirmed with a stronger constitutive promoter, as this could be explained by an increase in thylakoid generation: lipids are first synthesized in the saturated form.

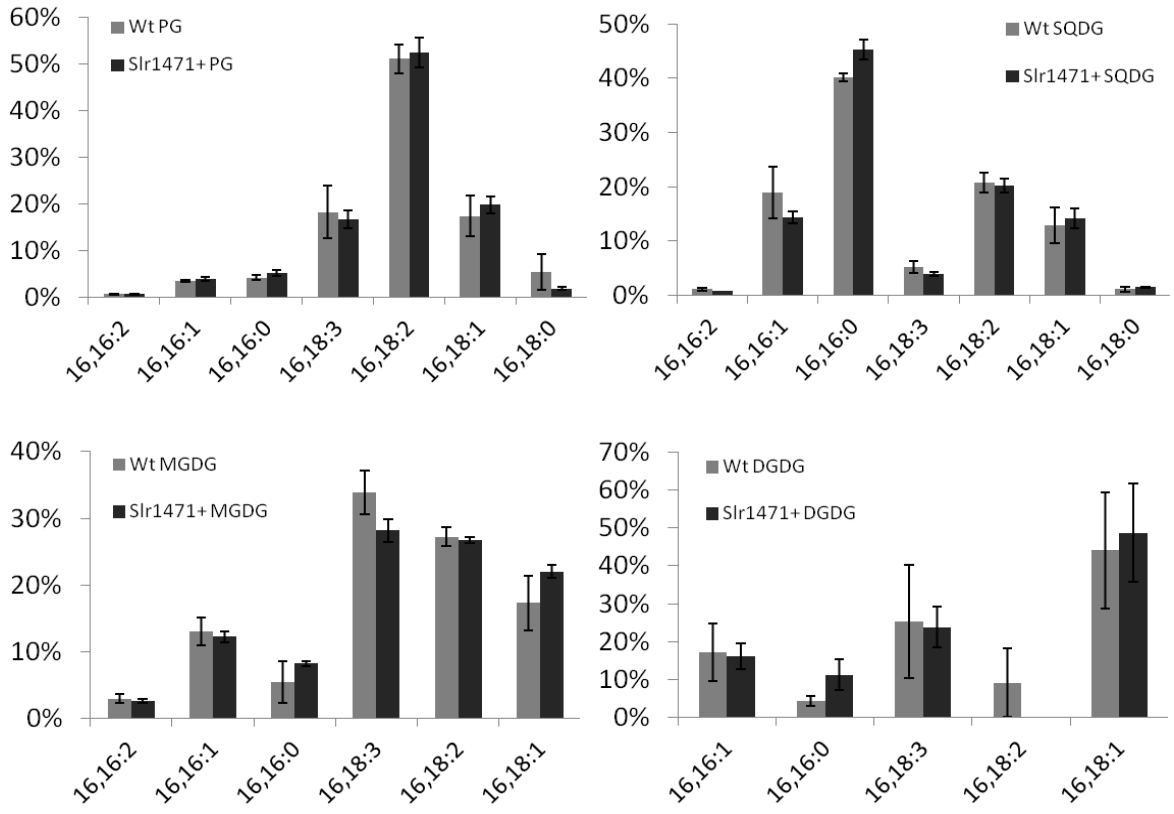

Figure 26. Comparison of wild-type and Slr1471+ lipid profiles. Composition of diglycerides (membrane lipids) with different chain lengths of the contributing fatty acids and total number of unsaturated bonds for each of the four different diglyceride classes (PG, top left; SQDG, top right; MGDG, bottom left; and DGDG, bottom right) extracted from wild type (light gray bars) and Slr1471+ (dark grey bars) (n=3).

Chapter 4

INCREASING PRODUCT RECOVERY

"Development of an *in situ* two-phase liquid-liquid extraction method of carbon-based molecules secreted by engineered *Synechocystis* sp PCC 6803 cultures"

Summary

A main challenge for emerging microbial biofuel technologies is the extraction and recovery of products from growth media. Here, we aimed to develop a liquid-liquid extraction method as an alternative to solid-phase extraction for molecules secreted by *Synechocystis* cultures. Initially, we evaluate a solid-phase approach (ion exchange and hydrophobic resins) and confirm that resins are effective in fatty acid harvesting from cyanobacterial cultures. To develop a two-phase liquid-liquid extraction approach, hydrophobic solvents were screened and long-chain alkanes were found to be biocompatible; fatty acid extraction was achieved at pH 4, a pH where *Synechocystis* does not grow. Addition of surfactants increased extraction efficiency and maintained biocompatibility, but the efficiency was not comparable to that of the solid-phase approach. Isoprene extracted well into alkanes, as long as the culture was grown in a sealed container. Two-phase liquid-liquid extraction is not yet suitable for applications at this point, since it requires special conditions that are impractical at larger scale, such as gas-sealed bioreactors for isoprene partitioning or frequent pH adjustments for fatty acid extraction.

Introduction

There is a need for a fast and efficient recovery of metabolites from industrial microalgae cultures when scaling-up to commercial scale. Solid-phase extraction is a commonly used method to extract molecules from fermentation cultures (Srivastava et al., 1992); however, the cost of elution of products from the resin is high. Two-phase liquid extraction is a promising alternative for large-scale harvesting, since it could overcome such high costs.

Solid-phase extraction is based on contacting a liquid or gaseous sample with a solid matrix (usually flowing the sample through a column or cartridge) that retains the compounds of interest, either by adsorption or by penetration of the pores in the matrix (Fontanals et al., 2010). The use of solid-phase extractants (resins) with various modes of action (hydrophobic, ionic interaction and a combination of both) have been evaluated for fatty acid removal from aqueous solutions and all resins tested showed great efficiency (Yuan et al., 2013). Continuous removal of fatty acids from cyanobacterial cultures by resin beads in a column has been analyzed previously (Wang, 2012) with positive results.

Once the compounds of interest are recovered from the liquid, the compound must be eluted by a solvent that can overcome the interaction with the matrix without degrading it. Elution from resins often has a high economic cost: large volumes of solvent are used, concentration/purification will require further energy and chemical inputs, etc.

Two-phase liquid extractions are based on the concentration equilibrium established between two immiscible liquids, one of them serving as extractant phase. They show potential to overcome high costs in comparison to a solid-phase extraction approach, as the use of expensive resins and large volumes of elution solvents can be

avoided. Aqueous two-phase extractions are based on the use of polymers that at a certain concentration form a second aqueous layer and they are good at extracting labile molecules such as enzymes. This strategy has shown promise for recovery of *Synechocystis* pigments (Chavez-Santoscoy et al. , 2010). Organic-aqueous two-phase extraction is the most common two-phase liquid approach and it is based on the immiscibility of polar and non-polar solvents. Attempts at *in situ* extraction of hydrocarbons using organic solvents were made in the cultures of the microalga *Botryococcus braunii* (Sim et al., 2001).

Long-chain fatty acids have been extracted into an organic phase from a fermentation medium after a pH adjustment (Lalman & Bagley, 2004), in order to protonate the fatty acid and ease its transfer through the interface. Volatile molecules are likely to partition to the air phase due to their high vapor pressure, but could accumulate efficiently in an organic phase if their LogP value (partition coefficient of a molecule between octanol and water) is high enough. Isoprene has a vapor pressure of 73.33 kPa (at 25 °C) and a logP of 2.42 (OECD, 2005). The high vapor pressure of isoprene allows us to accumulate isoprene in the headspace of sealed vials, while its logP suggests that it can be captured in an organic phase (likely in a proportion close to 2.42). Likely, the distribution between the organic and the air phase in a sealed vial would not be an issue, since volatile molecules such as isoprene concentrate in the organic phase in a manner analogous to the headspace microextraction method (HSME) (Bicchi et al., 2008). Unfortunately, to our knowledge, no Henry's constant values for isoprene in alkanes have been reported.

In order to develop a liquid-liquid extraction methodology one must choose an extractant phase that meets certain requirements (low toxicity, low photoreactivity, does not attack plastics or rubber components, compatible with downstream processing, etc.).

Aliphatic alkanes and fatty alcohols are commonly used extractant phases that are compatible with biofuel production processes that use fatty acids (such as fatty acid decarboxylation by palladium catalysts (Immer et al., 2010)). Alkanes have also been used to capture volatile isoprenoids, such as amorphadiene, from *E. coli* cultures (Newman et al., 2006). Isoparaffinic fluids (mixtures of saturated, aliphatic and branched hydrocarbons of various chain lengths) have potential since they have the previously mentioned characteristics, although they usually are obtained from petroleum feedstocks (Cheremisinoff & Archer, 2003). Similarly, alkylamines may be used to extract organic products from aqueous solutions (Matsumoto et al., 2003). In theory, a microbe could even produce its own extractant phase (e.g., aliphatic alkanes).

The most common structure affected by organic solvents is the cytoplasmic membrane, which gets inflated, solubilized and eventually disrupted when solvents partition into it (Sikkema et al., 1994). The more solvent goes into membranes, the more toxic the solvent will be (Sardessai & Bhosle, 2002). Hence, a parameter frequently used to predict solvent biocompatibility of bacterial cultures is the LogP value (Laane et al., 1987). A good correlation between LogP and partitioning of hydrocarbons into membranes was determined experimentally in *E. coli* liposomes (Sikkema et al., 1994). Even though LogP is a good predicting parameter, solvent biocompatibility must be studied on a case-by-case basis. For example, many bacteria may also possess efflux pumps or other adaptation mechanisms (Kieboom, 1998; Sardessai & Bhosle, 2002). Also, even though very non-polar solvents have high affinity for membranes, their solubility in water is so low that such solvents will never reach a high enough concentration in the membrane to cause cell death. In addition, cell surface might play a role in solvent tolerance, as Gram-positive bacteria are generally more sensitive than Gram-negative bacteria (Inoue & Horikoshi, 1991).

The biocompatibility of some organic solvents has been tested previously in photosynthetic microorganisms (León et al., 2001), but little biocompatibility information is available for *Synechocystis*. Here, we analyzed the toxicity of a wide array of organic solvents against *Synechocystis,* with the purpose of selecting an organic phase for liquid-liquid extraction. The organic solvent chosen was compared to a solid-liquid extraction approach for the extraction of fatty acids and isoprene from *Synechocystis* cultures.

Materials and Methods

Chemicals. Unless stated otherwise, chemicals and resins were obtained from Sigma Aldrich and Acros Organics. Isoprene standard was obtained from SPEX Certiprep and propylene glycol esters of fatty acids were a gift from Abitec Corp.

Organism and growth conditions. The background cyanobacterium used was wild-type *Synechocystis*. For *in situ* fatty acid recovery experiments, the mutant strain TE/Δ*slr1609* was used, which lacked the acyl-ACP synthethase gene *slr1609* and carried a thioesterase gene from *Umbellularia californica*. For isoprene recovery, the IspS+ strain was used, which expresses a synthetic isoprene synthase (see Chapter 3 for details). All strains were grown in BG-11 medium (Rippka et al., 1979) supplemented with 5 mM glucose or 10 mM bicarbonate, in a rotary shaker set at 130 rpm, 30 °C and at a light intensity of 50 μmol photons m^{-2} s^{-1} (hereafter normal conditions for this study).

Biocompatibility analysis of chemicals with *Synechocystis*. A wide range of solvents were tested to observe their effect on *Synechocystis*. Culture aliquots were grown in sealed autosampler vials under normal conditions in the presence of known concentrations of the soluble chemicals tested. For non-miscible solvents, 1 ml solvent was added to 10 ml culture aliquots (in 20 ml culture tubes), so that there was an

obvious organic layer. Growth was measured as an increase in culture optical density at 730 nm using a Shimadzu UV-VIS double beam spectrophotometer and biocompatibility was determined by growth comparison against a no-solvent control (n=3).

***In situ* recovery.** For solid-phase extraction of fatty acids 350 ml TE/Δ*slr1609* cultures were grown with known amounts of resin beads mixed in the culture (2 g and 20 g each L-493 (hydrophobic) and IRA-900 (mixed mode)), bubbled with ambient air and illuminated at a light intensity of 150 μmol photons m^{-2} s^{-1}. Supernatant samples were taken periodically for fatty acid analysis and resin bead samples for scanning electron microscopy (SEM).

For liquid-liquid extraction, 1 ml of compatible alkane solvents were added to 10 ml TE/Δ*slr1609* culture aliquots (in 20 ml culture tubes), and the fatty acid content was measured in the organic and aqueous phases. For laurate partitioning in the absence of cells, the culture was replaced with a 100 ml solution of lauric acid at known concentration. The pH of the solution was adjusted under continuous stirring and the 10 ml aliquots/1 ml solvent samples were prepared as described previously. Samples were allowed to equilibrate for two hours at room temperature in a rotary shaker and both phases were tested for fatty acids.

For isoprene accumulation, a 1 ml culture (approx. OD_{730}= 0.5) aliquot was placed in an autosampler vial, supplemented with 10 mM bicarbonate and if indicated, a 200 μl dodecane layer for isoprene accumulation in the organic phase, and sealed. The sample was incubated for 12-24 h at normal conditions and shaken briefly 2-3 times throughout the incubation period to keep the cells suspended. One μl of the dodecane (upper) layer was injected into the gas-chromatograph-MS.

Isoprene quantification. 1 ml culture aliquots (approx. OD_{730}= 0.5) were placed in 2 ml clear autosampler vials and supplemented with 10 mM bicarbonate. Vials were incubated at a light intensity of 50 μmol photons/m^2/s for 12-16 h and subsequently 5 μl from the headspace, or 1 μl of the dodecane layer, was injected into a HP 5890 GC connected to a MDN-5S column with He used as carrier gas. The injector temperature was set at 260 °C, the oven started at 40 °C for the first 5 min, ramped to 250 °C (at a rate of 50 °C/min) and held for 2 min at 250 °C. The GC was interfaced to an HP 5972 Quadrupole MS Detector set at 200 °C and SIM acquisition mode (m/z 53, 67 and 68). Isoprene yields were obtained by comparison to a curve of known isoprene concentrations.

Fatty acid quantification. Fatty acids in the organic phase were analyzed by direct infusion into the ESI-MS of a Bruker MicrOTOF-Q mass spectrometer, similar to the method described by Han and Gross (2005). To analyze the aqueous phase, a 490 μl aliquot was mixed with 10 μl 0.5 M EDTA; then 20 μl of the sample was mixed with an equal volume of 20 μM heptadecanoic acid standard (not detected at significant amounts in *Synechocystis*) dissolved in methanol containing 20 mM NH_4OH. 5 μl of the sample with the internal standard were injected into a Dionex Ultimate 3000 HPLC using a Zorbax Extend C-18 column using a linear gradient of 50-87% methanol in 26 min with 10 mM NH_4OH at a flow rate of 150 μl/min. Fatty acids were detected by a Bruker Micro-TOF-Q mass spectrometer detector in the negative ion mode. Fatty acids were identified by comparison with standards and concentrations were determined as a function of the relative monoisotopic peaks compared to the heptadecanoic acid internal standard.

Scanning electron microscopy. Resins beads were harvested by pipetting out of the cultures, spun down to remove the supernatant and air dried at room temperature. Once the beads were dry they were mounted in aluminum stubs and coated with gold-

palladium in a Hummer Sputter Coater (Technics) until about 10-15 nm thickness. Samples were visualized in a JEOL JSM6300 Scanning Electron Microscope at 15 kV and working distance of 39 mm and images were obtained by an IXRF digital processing system.

Results

Solid-phase cyanobacterial laurate extraction. Initially, for comparison purposes we used resin beads (L493 and IRA900) at different mass/volume proportions (2 g/L and 20 g/L each) free-floating in *Synechocystis* TE/Δ*slr1609* cultures. Both L493 and IRA900 were biocompatible in the amounts tested (Figure 27 A) since *Synechocystis* grew in both at the same rate as the control. IRA900 at 2 g/L did not remove all laurate produced, whereas L493 was efficient at doing so at the same proportion of resin. (Figure 27 B). Resin beads analyzed by SEM did not show any issues with fouling, as the most of the surface of the resin bead was free of cells, permitting adherence of fatty acids (Figure 28). When comparing both resins, L493 had less cells adhered to its surface.

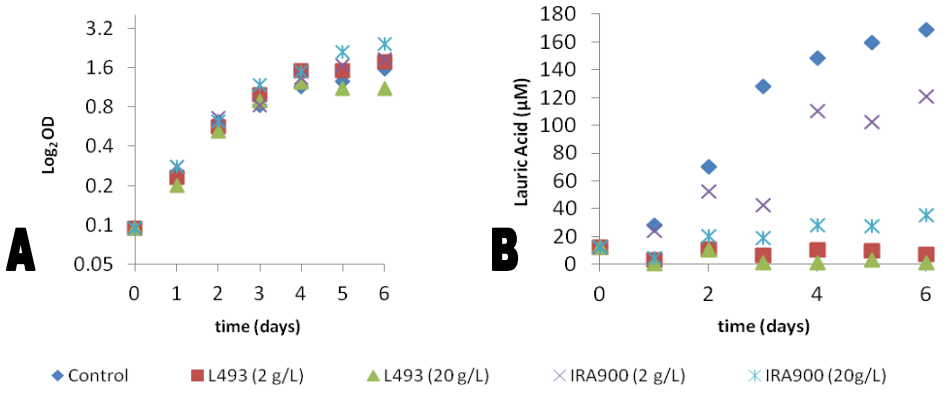

Figure 27. Effect of resin beads free-floating in *Synechocystis* cultures. A) Semi-log plot of culture growth and B) residual laurate in the culture compared to a TE/Δ*slr1609* resin-less control. Resin types and amounts are indicated at the bottom of the figure.

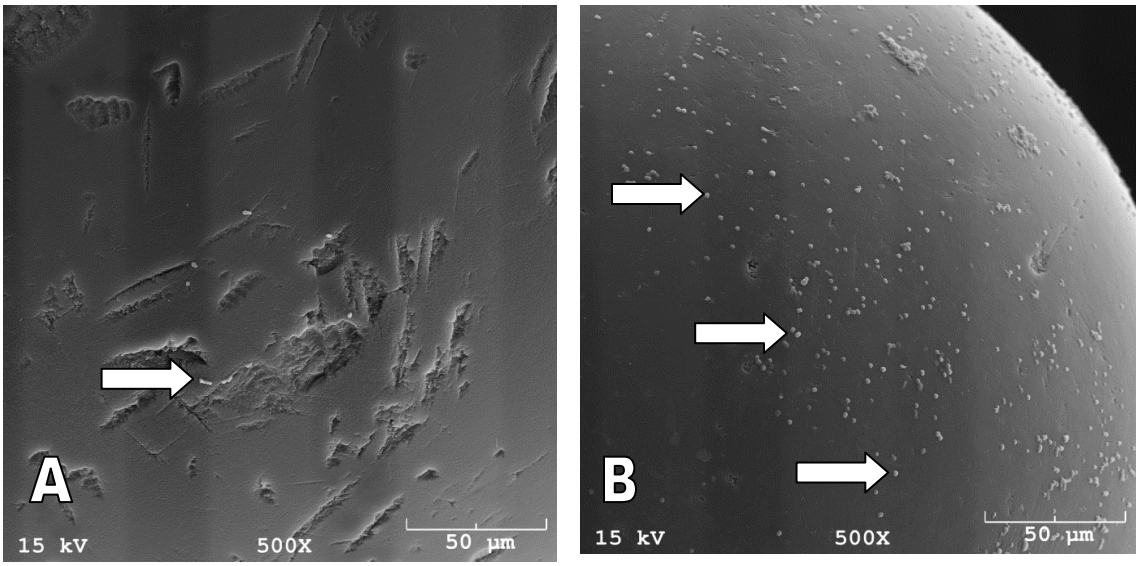

Figure 28. SEM of resin beads. A) L493 and B) IRA900 after a 5-day contact with cultures. Arrows show cells (bright spots) attached to the resin beads.

Selection of hydrophobic extractant phase. We tested the tolerance of *Synechocystis* to a wide array of hydrophobic organic solvents (99% purity from manufacturer; used without further purification) based on culture growth. We analyzed long-chain aliphatic alkanes, alcohols and trialkylamines, which spanned a range of LogP values from 2.9 to 16.9. Long-chain alcohols and trialkylamines were determined to be toxic for *Synechocystis*. In the case of the alkanes, the bacterial cultures grew at rates similar to that of the solvent-less control when in contact with alkanes of 10 carbons and longer, with a short lag time before the bacteria began growing. No differences in solvent tolerance were observed between wild type and the fatty acid-producing strain TE/Δ*slr1609*. The growth curves for TE/Δ*slr1609* in the presence and absence of solvents (10% volume relative to that of the culture) is shown in Figure 29.

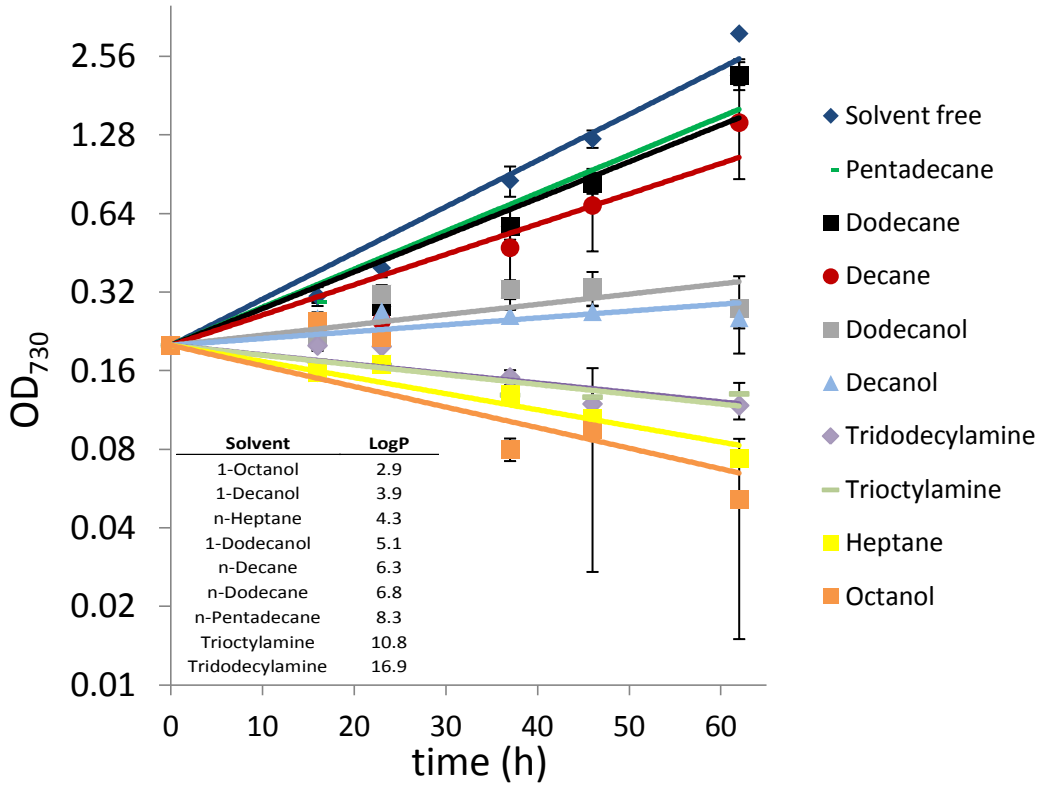

Figure 29. Biocompatibility of *Synechocystis* with hydrophobic organic solvents. Semi-log plot of TE/Δ*slr1609* growth in the presence of an upper layer of organic solvent. Insert: LogP values of the solvents tested obtained from Sangster (1989) and Chemspider.com. (n=3).

Liquid-liquid extraction. Aliquots of 350 µM laurate in BG-11 were extracted with dodecane at a 1:10 v/v ratio of alkane to BG-11. Concentrations in both organic and aqueous phases were determined by comparison to an internal standard by LC-MS. The results are shown in Figure 30. Maximum laurate extraction (~43%) into the organic phase occurred at pH 4, but at pH >8 (pH permissive for *Synechocystis* growth) extractions were highly inefficient. Even though some laurate is removed from the aqueous solution, the mass balance of laurate in aqueous plus organic phases cannot account for the total initial laurate. Such unaccounted mass can likely be found as

precipitate or in the interface (Figure 30). An unexpected effect due to pH adjustment on the total laurate concentrations occurred at pH 4 and pH 12. At acid pH, precipitation of the lauric acid occurs and it is difficult to maintain the homogeneity of the solution by mixing. At basic pH, the apparent increase in total laurate concentration is likely due to a pH effect on the internal standard.

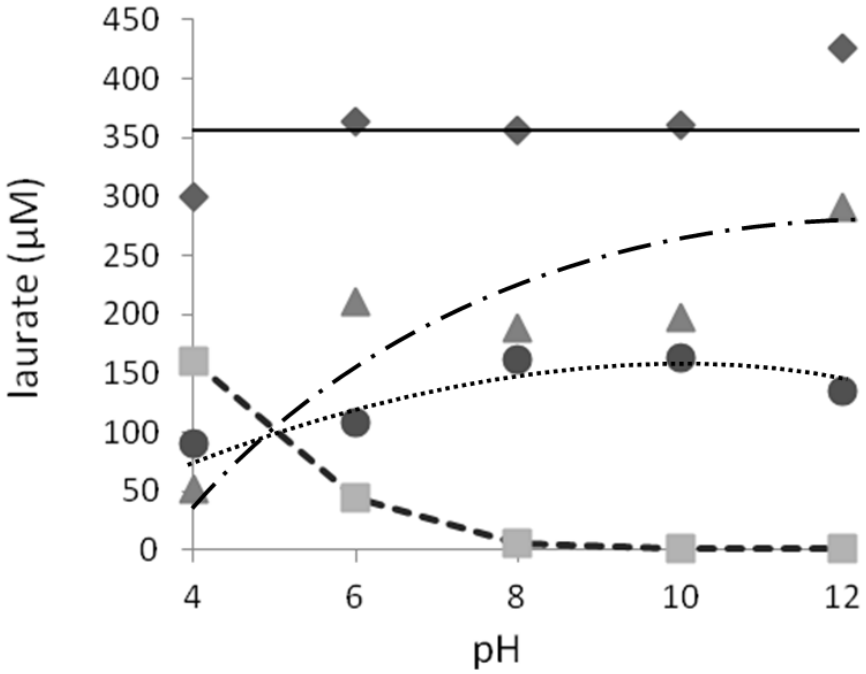

Figure 30. Cell-free extraction of laurate from BG-11 by dodecane. Diamonds and solid line: starting laurate concentration; triangles and point/dash line: laurate in BG-11; circles and stippled line: laurate that is unaccounted for; squares and dashed line: laurate extracted to dodecane (n=2).

In situ continuous extraction of laurate by an upper dodecane phase in growing TE/Δ*slr1609* cultures was attempted, but it was terminated due to large amounts of emulsion due to culture bubbling. It is feasible that emulsion formation can be used to

extract laurate from cultures; however, breaking the emulsions (e.g., by acidification) is a labor-intensive process that may not be feasible for large-scale extraction.

Next, batch extractions were performed from growing cultures that had already accumulated laurate. The pH of the culture was at 9.3, and in accordance to the data shown in Fig. 27, negligible extraction was achieved (Table 13).

Table 13

In Situ Laurate Extraction from 10-ml Cultures of Synechocystis TE/Δslr1609

	Laurate in BG-11 (µg)	**Extracted to Alkane (µg)**	**Final culture pH**
Control	184	N/A	9.3
Dodecane	131	0.3	9.3
Pentadecane	155	0.4	9.2

Since pure alkanes were not able to extract laurate at physiological pH, the extractant phase needed to be optimized. In order to do so, two surfactants of the series of propylene glycol esters of fatty acids (PGEs) were used as co-solvents with dodecane: PGE-caprylic acid (PGE-C8) and PGE-lauric acid (PGE-C12). Surfactants have both polar and non-polar components that locate them at in the interface of an organic/aqueous system. They may work by decreasing the surface tension in the interface, or by stabilizing laurate-containing micelles, and allowing them to cross the interface. PGEs could potentially have high biocompatibility due to the length of the fatty acid component, may be produced biologically (lipases), and could be further modified by swapping the acyl-chain.

Cell-free extraction using the PGE-C8/dodecane mixture (tested up to 25% PGE-C8 in dodecane) increased the amount of laurate going into the organic phase and decreased the laurate concentration in the aqueous phase; however, after mass balance analysis we concluded that most laurate was unaccounted for (precipitated or located at the interface) (Figure 31). Unfortunately, even 5% PGE-C8 in dodecane was toxic to cell cultures. The increased length of the acyl-chain in PGE-C12 allowed *Synechocystis* growth below 10% PGE-C12 in dodecane; however, growth patterns were irreproducible: cultures had lag phases of different lengths and when the resumed growth, they doubled at slower rates than the control.

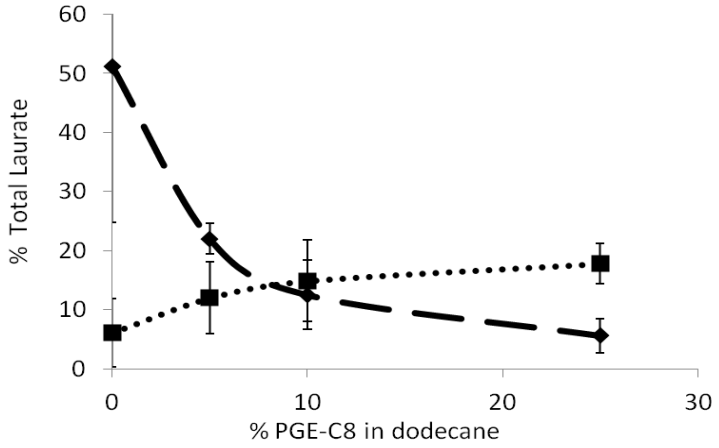

Figure 31. Laurate extraction from BG-11 medium by different percentages of PGE-C8 in dodecane. Diamonds and dashed line: % laurate remaining in BG-11; squares and dotted line: % laurate extracted to the organic phase (n=2).

The only concentration of PGE-C12 that had no effect on *Synechocystis* growth was 2.5% PGE-C12 in dodecane and so this proportion was used for *in situ* extraction. Extremely high amounts of laurate were observed in the organic extracts, likely due to degradation of PGE-C12. To avoid this issue, a minor product produced by TE/Δ*slr1609* culture was analyzed: myristate (~6% of total fatty acids produced), since it can be easily

distinguished by its two extra carbon atoms. The results are shown the percentages of myristate in each phase, considering 0% PGE-C12 in dodecane as 100% (Table 14). The total production of a culture cannot be obtained due to the unknown quantity of fatty acid being lost to precipitation or to the interface.

Table 14

Percentage of Synechocystis-secreted Myristate Extracted In Situ by Dodecane and PGE-C12. Data presented as a percentage of the total in the control without PGE-C12.

	Myristate in the organic phase	Myristate in the aqueous phase	Total
0% PGE-C12 in dodecane	4%	96%	**100%**
2.5% PGE-C12 in dodecane	10%	23%	33%
5% PGE-C12 in dodecane	24%	1%	25%

As expected, when no surfactant is added the amount of myristate accumulating in the aqueous phase is larger than the amount that is extracted into dodecane when no surfactant is added. Although the use of 5% PGE-C12 in dodecane greatly decreased the myristate in the aqueous phase and increased the amount in the interface, based on the data from Fig. 31 it is likely that this effect is due to accumulation at the interface.

The use of PGEs generated more issues than it solved: PGEs were prone to hydrolysis, which would require continuous supply of the surfactant to the culture (increasing material cost) and increased the loss of laurate by either precipitation or interface accumulation. In some cases, even fungal growth was observed in the dodecane layer. In addition, cultures died after a few days, possibly due to toxic effects of the co-solvent (for example, excessive accumulation of lauric acid in the aqueous phase due to degradation of PGE-C12).

In situ cyanobacterial isoprene extraction. Dodecane was tested to determine its efficiency to retain isoprene produced by the isoprene-evolving IspS+ *Synechocystis* mutant, avoiding isoprene partitioning to air. 1 ml cultures in sealed autosampler vials were compared to a similar setup with a 200 µl dodecane layer on top of the culture. In these sealed vials, the organic phase did not affect the production of isoprene in the 1 ml cultures significantly and furthermore concentrated it nearly 5 times in the solvent compared to in the headspace, which provides an advantage for further downstream processing. The results are shown in Table 15.

Table 15

*Harvesting of Cyanobacterial Isoprene in Sealed Vials***.**

	Isoprene in dodecane (ng/ml)	**Isoprene in headspace (ng/ml)**	**Total produced (ng per (ml culture)$^{-1}$ day^{-1})**
IspS+ (no solvent)	--	149.6 ± 16.4	134.6 ± 14.8
IspS+/Dodecane	462.4 ± 190	6.7 ± 7.5	97.2 ± 38

To analyze the versatility of this harvesting method, isoprene was collected for 1 day from 50 ml cultures of IspS+ in 150 ml Erlenmeyer flasks, covered with a cotton plug, grown in a rotary shaker at normal light and temperature conditions and with a 10 ml dodecane layer on top. Under these conditions where isoprene can partition into air, we captured isoprene in the dodecane phase equivalent to a production rate of 54 ng per (ml culture)$^{-1}$ day^{-1}. In sealed vials, the isoprene production rate was 97.2 ng per ml culture^{-1} day^{-1}; therefore about 55% of the isoprene was retained in the dodecane phase after 1 day.

Discussion

Our goal was to develop a liquid-liquid extraction method to recover laurate from TE/Δ*slr1609* cultures and isoprene from IspS+ cultures. The current strategy for laurate recovery is based on flow-through resin columns with hydrophobic and ion exchange properties. These often result in high costs due to the quantities of resin and eluting solvents used. Two-phase liquid extraction is a promising alternative for large-scale harvesting, since it could overcome the high costs in comparison to solid-phase extraction.

To gain insight regarding solvent toxicity, especially to select for potential extractant phases, a suitable method to probe biocompatibility is required. Oxygen evolution has been used previously to determine toxicity of compounds in photosynthetic organisms (León et al., 2001). However, oxygen evolution is a short-term assay whereas solvent effects may be longer-term. When monitoring growth, long-term effects of the spiked chemical can be observed (e.g., continued growth due to the degradation of the spiked chemical or synthesis of efflux pumps, etc.). For the selection of an extraction solvent, we compared the growth of *Synechocystis* in contact with three types of hydrophobic chemicals with various LogP values: long-chain alcohols, trialkylamines and aliphatic alkanes. Toxic effects were observed for long-chain alcohols, which was expected since these molecules have low logP values and many alcohols are considered microbicides (McDonnell & Russell, 1999). Surprisingly, the trialkylamines, which have high partition coefficient values, were also toxic to *Synechocystis*. Therefore, LogP comparisons are a good way of estimating toxicity but are not always perfect. Previous studies on trialkylamine toxicity showed that toxicity is dependent on the microbe tested, and that trialkylamines have been successful at removing compounds

from fermentation broths as a co-solvent in low-percentage mixtures (Keshav et al., 2012).

Aliphatic alkanes with chain lengths of 12 carbons and longer were found to be biocompatible in the case of *Synechocystis*. This is in line with other studies (Leon et al., 2001). It was noted that even decane could be compatible depending on mixing/stirring speeds of the culture being extracted (lower speed leads to higher biocompatibility). Comparison of biocompatibility values are shown in Table 16. Dodecane was chosen as primary extractant phase for our study; however, optimization by acidification or surfactant addition did not result in extraction efficiencies that were close to the ones obtained with resin beads.

Table 16

Comparison of the Biocompatibility of Alkanes for Different Microbes

Microbe	Alkane	Bicompatibility parameter (%)*	Reference
Dunaliella salina	Decane	111[1]	(León et al., 2003)
Anabaena	Heptane	99[1]	(León et al., 2001)
Chlamydomonas	Undecane	90[1]	(León et al., 2001)
Synechocystis sp PCC 6803	Dodecane	66[2]	(this study)
E. coli JA300	Heptane	100[3]	(Tsukagoshi & Aono, 2000)

* Comparison vs. solvent-less control of: [1] % of photosynthetic efficiency, [2] growth curve and [3] plating/colonies formed

There are methods that may be used to improve efficiency of liquid-liquid extraction (León et al., 1998): A) cell immobilization would allow the use of a more toxic solvent by protecting the cell or slowing the diffusion of the solvent into it (e.g.,

immobilized *Synechocystis* in polyvinyl alcohol (Avramescu et al., 1999)), but such method would be impractical at large scale since generally cells do not stay viable for long periods of time and diffusion of molecules out of the cell is also slowed down; B) reverse micelles are a liquid-liquid extraction method commonly used for proteins, in which an amphiphilic molecule forms a polar core (containing the molecule being extracted) in non-polar liquids. There is little literature about fatty acid extraction using reverse micelles; however, they have been used to dissolve myristoylated proteins as a preparative step for NMR (Valentine et al., 2010). Reverse micelles and coacervate (small lipid droplet) formation have shown potential to extract organic molecules from aqueous solutions (Ruiz et al., 2007). Feasibility of large-scale extraction by micelles is unlikely, since micelles are only formed under a narrow range of conditions specific for each component of the micelle (pH, mixing, surfactant proportion, etc.); C) reactive extraction, which is based on the formation of esters (fatty acid with an alcohol) in the presence of a lipase and an organic layer (Kiss & Bildea, 2012). This method shows promise for several reasons: (a) an alcohol ester of fatty acid can partition easier into the organic layer, (b) *Synechocystis* produces several lipases of unknown characteristics and (c) alcohol esters could be used as fuel. Even though the results shown here are not promising for *in situ* fatty acid harvesting by organic solvents, genetic engineering of *Synechocystis* to increase tolerance to acid pH or to evaluate the lipases found in the *Synechocystis* genome could allow the implementation of a liquid-liquid extraction approach in the future.

Extraction of isoprene is a different challenge. Since isoprene is a volatile compound, it is commonly removed by air stripping. Removal of *Synechocystis*-produced isoprene from the headspace of sealed bioreactors has been shown (Bentley & Melis, 2011). Due to the nature of the isoprene molecule, it was expected to be able to

cross the organic-aqueous interface without problem but because of its high vapor pressure it was possible that it could escape to the gas phase. When cultures were sealed in autosampler vials, isoprene efficiently accumulated in the organic phase. On the other hand, during growth of unsealed cultures, the equilibrium between the aqueous, organic and air phase is never established and evaporative loss of isoprene can occur; hence only a portion of the produced isoprene is retained in dodecane. The needs of downstream processing of isoprene/dodecane must be carefully assessed since the solubility of oxygen, which can react with isoprene, in dodecane is several-fold higher than that in water (Battino et al., 1983), and with proper agitation dodecane has been shown to be a good oxygen vector for *Aspergillus* (Wang, 2000). Nevertheless, in a closed (air-tight) growth system/harvest condition, dodecane is a good option for *in situ* harvesting and concentration of cyanobacterial isoprene.

Chapter 5

PERSPECTIVE

Synechocystis is a platform suitable for manipulation towards production of renewable chemicals, comparable to current biotechnological approaches using *E. coli* or yeast. Even though all are easily transformable and have a wide knowledge base for researchers, the photosynthetic capacity of cyanobacteria sets these organisms apart as a potential top driving force against climate change. For a detailed list of uses and produced chemicals from cyanobacteria, see Ruffing (2011). Taking recently granted patents as indicators, companies that are currently and visibly pursuing cyanobacteria as biofuel production platforms are: Joule Unlimited Inc (Cambridge, MA) for the production of alkanes (Reppas & Ridley, 2010), Algenol Biofuels (Bonita Springs, FL) for the production of ethanol (Fu & Dexter, 2011), Proterro (Ewing, NJ) for the production of fermentable sugars (Aikens & Turner, 2009) and Matrix Genetics LLC (Seattle, WA) for the production of triglycerides (Roberts et al., 2013). Most of these companies are still in a pilot stage; some of the companies using cyanobacteria have reached commercial stage by producing high-value chemicals with potential markets in the cosmetic, pharmaceutical and nutrition industries (such as astaxanthin production by Cyanotech Corp. in Kalaoa, HI or various DNA technologies by Synthetic Genomics in La Jolla, CA). Others have failed to reach scale due to high production cost or due to laws and regulations (Borowitzka, 2013). Companies that produce ethanol, like Algenol, are helped by mandates such as the Renewable Fuel Standard that state that gasoline must be blended with a certain percentage of ethanol (~10%), but since most of the ethanol comes from corn (which is also a food source) and cellulosic ethanol cannot meet the demand, there has been a push by oil companies towards decreasing blending of ethanol

into gasoline. There are also worries about the fate of genetically modified organisms in the environment (Snow & Smith, 2012).

The Southwest USA, and especially Arizona, has ideal conditions for large-scale microalgae production facilities. Arizona has abundant unused land, plenty of sunlight days and brackish water that can be used. Algae grown in Arizona yield high biomass amounts (Yang et al., 2011). However, as it is a desert region, it can reach extreme temperatures (record high: 52.8 °C and record low -40 °C, in different areas of Arizona) (Hendricks, 1985). Culture temperature would likely be higher (as dark objects absorb more incident radiation from the sun), and a tight control of temperature at a commercial scale is not viable. That is why solutions at the microbe level are sought, including screening and selection of temperature tolerant strains and/or genetic engineering of strains to confer thermotolerance.

In Chapter 2 we applied genetic engineering of heat shock proteins to increase cell survival after heat stress in *Synechocystis*. If one assumes that the low and high daily temperatures for a hypothetical growth site in Arizona are 30 °C at 6 AM and 45 °C at 4 PM (~July in Yuma, AZ), the temperature increase rate would only be 1.5 °C/h, which is a rate that allows cellular response to heat stress. However, we must consider that the culture would be above ambient temperature, since a dense dark-green culture will absorb a large percentage of the incident light that will dissipate as heat. Sheng et al. (2011) showed how temperature shifts after biomass generation in a photobioreactor even with long ramp-up rates. Temperature-change rates could further increase depending on the bioreactor design. For example, novel biofilm photobioreactors, such as those described by Tian et al. (2010), would lose/gain temperature at faster rates due to their smaller water volume and thereby smaller thermal capacity. By overexpressing ClpB1+ we allowed the cell to respond to very rapid temperature changes (1 °C/s from 30

°C to 50 °C), without affecting the health of the culture. ClpB1+ complementation with overexpression of DnaK2 resulted in a further increase in heat tolerance, which shows that mimicking the heat response artificially by successive chaperone overexpression is a good strategy to increase thermotolerance in *Synechocystis*. Other candidates for overexpression to increase thermotolerance are the co-chaperones DnaJ and GrpE, which act together with ClpB1 and DnaK2, chaperones GroESL, as shown for *Anabaena* (Chaurasia & Apte, 2009), or the production of membrane stabilizing chemicals such as isoprene, as many plants do during heat stress (Sharkey et al., 2008).

Chapter 3 was dedicated to *Synechocystis* genetic engineering to increase yields of biofuel precursors. In the first segment of the chapter, we sought to increase isoprene production by the IspS+ mutant. As previously mentioned, isoprene protects heat-stressed cells. However, in this case our interest was focused on the industrial use of the isoprene molecule, which is used as precursor for synthetic rubber and tires (Leber, 2001). Poor production rates from cyanobacterial mutants have not helped in gaining interest from industry. Few companies like DuPont/Goodyear (Wilmington, DE) and Amyris/Michelin (Emeryville, CA) have pursued patents for isoprene production by other microbes (McAuliffe & Paramonov, 2012; McPhee, 2012) but are still in the process of developing a pilot system. Although the basis for microbial isoprene production would be the same for bacteria like *E. coli* and *Synechocystis* (fixed carbon going towards DMAPP through an isoprenoid-precursor pathway and concentrating process by air-stripping or two-phase extraction), the important difference is the fixed carbon source: *Synechocystis* isoprene comes directly from CO_2 and sunlight.

In order to commercialize isoprene from cyanobacteria, it is necessary to increase isoprene yields. Overexpression of the MEP pathway in plants has resulted in mutants with increased carotenoid content (Hasunuma et al., 2008), so we assumed that MEP

overexpression would result in higher isoprene production, but only a slight increase was observed.

DMAPP is a metabolite in the MEP pathway and is the direct precursor of isoprene. The DMAPP concentration in the chloroplast has been estimated at 0.13 to 3.0 mM (Rosenstiel et al., 2002). We were not able to detect any accumulation of DMAPP or the isomer IPP even in overexpression strains. The approximate detection limit for DMAPP under our LC-MS experimental conditions was ~1 μM in the extract. Spiking the original 2-ml cell extract in methanol (originating from 50 ml of culture) with 60 μM DMAPP, we observed a final concentration of 115 μM DMAPP in the 50-μl final extract that was used for LC-MS. The remainder of the DMAPP precipitated and/or broke down. Therefore, the minimum DMAPP concentration that needs to be present in the original extract (2 ml) in order for DMAPP to be detected is about 0.5 μM. In order to be able to detect 0.5 μM in a 50-μl extract from a 200 ml culture (OD_{730}=0.5) aliquot, the concentration inside the cells would have needed to be 25 μM DMAPP (assuming 10^8 cells/ml of OD_{730}=1 and a volume of 2 fl/cell). Since the Km of IspS-poplar was shown to be ~3.7 mM and the DMAPP level in *Synechocystis* is at least an order of magnitude less, it can be understood why the IspS+ strain does not produce isoprene in large amounts. The production by 1-ml culture aliquot (OD_{730}=1) in 24 h would be equivalent to ~4 nmole used for isoprene production, compared to <5 pmole found at any given time in the total cell volume (2 fl per cell; 10^8 cells per ml per OD_{730}=1). Therefore, about 1,000 DMAPP pool turnovers per day satisfy all isoprene production requirements. Such usage rate of DMAPP does not seem to have provoked limitation for other molecules formed by precursors from the MEP pathway. Alternatives for improvement could be: (a) find the right combination of MEP enzyme overexpression, (b) sequester MEP enzymes plus the isoprene synthase in an artificial bacterial microcompartment (Frank et al., 2013) to

increase DMAPP in an area where the isoprene synthase is located, (c) downregulate the GGPP synthethase to favor the use of DMAPP by the IspS, or (d) use protein engineering to increase the affinity of the isoprene synthase for DMAPP.

Other experiments shown in Chapter 3 were not followed up on, since they did not yield results relevant for improving biofuel strains. The results obtained for the Slr1471+ strain were difficult to evaluate since there was little overexpression. This shows the importance of selecting appropriate promoters based on the growth condition they will be used at. Based on the results obtained, the *ftsQ* promoter turned out to not be a good candidate for overexpression analysis under normal growth conditions and a future direction would be to swap the *ftsQ* promoter with a known strong promoter, such as *psbA2*.

In Chapter 4 we analyzed extraction methodologies to recover secreted products from *Synechocystis* cultures. Extraction is a relevant process because most of the time metabolites of interest need to be separated from biomass or culture in order to be processed. In addition, extraction can aid in controlling contamination of cultures, since at large scale the presence of heterotrophs (scavengers or grazers that will diminish yields) is unavoidable. In the case of *Synechocystis* secreting fatty acids, recovering of the product as fast and as efficiently as possible may leave less fatty acid available for microbes to use as carbon source.

Resin extraction is commonly used in industrial settings, since it is very efficient, although costly. The alternative liquid-liquid extraction is generally restricted to fermentative processes, and as we observed in Chapter 4, a main reason for this is the need for biocompatible solvents. Generally, good extractant solvents are toxic to the bacteria, most likely because of the facile penetration of cell membranes. A strategy moving forward would be to enhance solvent tolerance; proteomic studies in

Synechocystis have already shown which proteins are overexpressed and downregulated in response to hexane (Liu et al., 2012). The expression of such proteins can be modified to increase solvent tolerance.

Regarding the control of bacterial scavengers, a strategy is to adapt the growth conditions to be non-permissive for the problematic scavengers (e.g., increasing salinity (Das et al., 2011) or adding antibiotics); however, chances are that a microbe of some type will be able/evolve to grow in what was considered non-permissive at some point. Another alternative could be to modify the intercellular communication mechanisms, although this strategy will affect a smaller spectrum of cell types, due to the species-specificity of such communication mechanisms.

Some bacterial cells produce cell-to-cell communication molecules such as acyl-homoserine lactones (AHL) (Miller & Bassler, 2001) that regulate cellular processes dependent on population size, such as biofilm formation, virulence, etc. Some cyanobacteria, like *Gloeothece* PCC 6909 produce *N*-octanoyl homoserine lactone (C8-AHL), and upon treatment with C8-AHL, changes in protein expression were identified (Sharif et al., 2008). On the other hand, some cyanobacteria, like *Anabaena*, produce an enzyme (AiiC) that efficiently degrades AHL (Romero et al., 2008). In *Synechocystis,* there are no reports of either quorum sensing or quorum quenching. We supplemented *Synechocystis* cultures with 10 μM of C8-AHL, and observed no effects on cell growth (Figure 32 A). Furthermore, supernatants from AHL-supplemented cultures accumulated homoserine (Figure 32 B), which could be due to an acylase activity or by degradation due to alkaline pH. An acylase, encoded by *slr0378*, has been suggested to be a good candidate for an AiiC-homolog in *Synechocystis* (Romero et al., 2008).

The identification and manipulation of AHL signals may be helpful for large-scale biofuel production. It is possible that by either allowing accumulation of AHL (by a

deletion of AiiC) the contaminant cells form biofilms that are less active at scavenging, or by overproducing an AiiC in *Synechocystis*, it is possible that the scavenger cells are not able to communicate between one another, and the effect on their metabolic pathways could allow them to be controlled more easily.

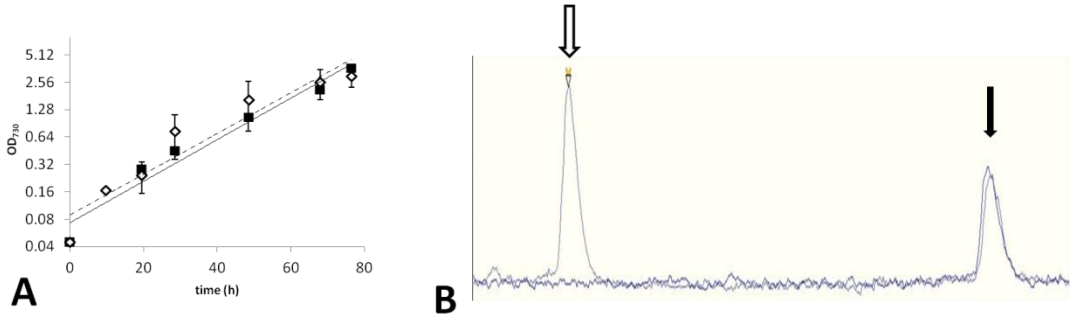

Figure 32. Acyl homoserine lactone effects in *Synechocystis* cultures. A) Semi-log plot of *Synechocystis* growth in the presence (white diamonds, dashed line) and absence (black squares, black line) of 10 μM C8-AHL. B) LC-MS chromatogram showing the degradation of C8-AHL in a TE/Δ*slr1609* culture (white arrow: homoserine peak, black arrow: laurate peak).

Understanding the mechanisms of quorum sensing in *Synechocystis* could allow us to manipulate promoters based on population numbers (e.g., to induce flocculation of cyanobacterial biomass when a certain amount of culture density is reached, etc.).

In conclusion, *Synechocystis* is a versatile platform for biofuel production. It can be easily manipulated to meet the specifications of a production process and with a continued research effort *Synechocystis*-based biofuel production can be brought closer to commercial feasibility.

REFERENCES

Adam, P., Hecht, S., Eisenreich, W., Kaiser, J., Grawert, T., Arigoni, D., Bacher, A., Rohdich, F. (2002). Biosynthesis of terpenes: studies on 1-hydroxy-2-methyl-2-(E)-butenyl 4-diphosphate reductase. *Proceedings of the National Academy of Sciences of the United States of America*, *99*, 12108–12113.

Aikens, J., Turner, R. J. (2009). Transgenic photosynthetic microorganisms and photobioreactor. Patent US 8367379 B2.

Anderson, S. L., McIntosh, L. (1991). Light-activated heterotrophic growth of the cyanobacterium *Synechocystis* sp. strain PCC 6803: a blue-light-requiring process. *Journal of Bacteriology, 173*, 2761–2767.

Antal, T. K., Lindblad, P. (2005). Production of H_2 by sulphur-deprived cells of the unicellular cyanobacteria *Gloeocapsa alpicola* and *Synechocystis* sp. PCC 6803 during dark incubation with methane or at various extracellular pH. *Journal of Applied Microbiology*, *98*, 114–120.

Arrhenius, S. (1896). On the influence of carbonic acid in the air upon the temperature of the ground. *Philosophical Magazine and Journal of Science*, *41*, 237–276.

Avramescu, A., Rouillon, R., Carpentier, R. (1999). Potential for use of a cyanobacterium *Synechocystis* sp. immobilized in poly(vinylalcohol): Application to the detection of pollutants. *Biotechnology Techniques*, *13*, 559–562.

Banerjee, A., Wu, Y., Banerjee, R., Li, Y., Yan, H., Sharkey, T. D. (2013). Feedback inhibition of deoxy-D-xylulose-5-phosphate synthase regulates the methylerythritol 4-phosphate pathway. *Journal of Biological Chemistry*, *288*, 16926–16936.

Barkley, S. J., Desai, S. B., Poulter, C. D. (2004). Type II isopentenyl diphosphate isomerase from *Synechocystis* sp. strain PCC 6803. *Journal of Bacteriology*, *186*, 8156–8158.

Battino, R., Rettich, T. R., Tominaga, T. (1983). The solubility of oxygen and ozone in liquids. *Journal of Physical and Chemical Reference Data*, *12*, 163.

Bentley, F. K., Melis, A. (2011). Diffusion-based process for carbon dioxide uptake and isoprene emission in gaseous/aqueous two-phase photobioreactors by photosynthetic microorganisms. *Biotechnology and Bioengineering*, *109*, 100-109.

Berthelot, K., Estevez, Y., Deffieux, A., Peruch, F. (2012). Isopentenyl diphosphate isomerase: A checkpoint to isoprenoid biosynthesis. *Biochimie*, *94*, 1621–1634.

Bicchi, C., Cordero, C., Liberto, E., Sgorbini, B., Rubiolo, P. (2008). Headspace sampling of the volatile fraction of vegetable matrices. *Journal of Chromatography. A*, *1184*, 220–233.

Borowitzka, M. A. (1999). Commercial production of microalgae: ponds, tanks, tubes and fermenters. *Journal of Biotechnology*, *70*, 313–321.

Borowitzka, M. A. (2013). High-value products from microalgae—their development and commercialisation. *Journal of Applied Phycology*, *25*, 743–756.

Botella-Pavía, P., Besumbes, O., Phillips, M. A., Carretero-Paulet, L., Boronat, A., Rodríguez-Concepción, M. (2004). Regulation of carotenoid biosynthesis in plants: evidence for a key role of hydroxymethylbutenyl diphosphate reductase in controlling the supply of plastidial isoprenoid precursors. *Plant Journal*, *40*, 188–199.

Carretero-Paulet, L., Cairó, A., Botella-Pavía, P., Besumbes, O., Campos, N., Boronat, A., Rodríguez-Concepción, M. (2006). Enhanced flux through the methylerythritol 4-phosphate pathway in *Arabidopsis* plants overexpressing deoxyxylulose 5-phosphate reductoisomerase. *Plant Molecular Biology*, *62*, 683–695.

Carson, M. J., Barondess, J., Beckwith, J. (1991). The FtsQ protein of *Escherichia coli*: membrane topology, abundance, and cell division phenotypes due to overproduction and insertion mutations. *Journal of Bacteriology*, *173*, 2187–2195.

Celerin, M., Gilpin, A. A., Schisler, N. J., Ivanov, A. G., Miskiewicz, E., Krol, M., Laudenbach, D. E. (1998). ClpB in a cyanobacterium: predicted structure, phylogenetic relationships, and regulation by light and temperature. *Journal of Bacteriology*, *180*, 5173–5182.

Chaurasia, A. K., Apte, S. K. (2009). Overexpression of the *groESL* operon enhances the heat and salinity stress tolerance of the nitrogen-fixing cyanobacterium *Anabaena* sp. strain PCC 7120. *Applied and Environmental Microbiology*, *75*, 6008–6012.

Chavez-Santoscoy, A., Benavides, J., Vermaas, W., Rito-Palomares, M. (2010). Application of aqueous two-phase systems for the potential extractive fermentation of cyanobacterial products. *Chemical Engineering & Technology*, *33*, 177–182.

Cheremisinoff, N. P., Archer, W. L. (2003). *Industrial solvents handbook*. New York: Marcel Dekker Inc.

Chisti, Y. (2007). Biodiesel from microalgae. *Biotechnology Advances*, *25*, 294–306.

Chisti, Y. (2008). Biodiesel from microalgae beats bioethanol. *Trends in Biotechnology*, *26*, 126–131.

Chow, I. T., Baneyx, F. (2005). Coordinated synthesis of the two ClpB isoforms improves the ability of *Escherichia coli* to survive thermal stress. *FEBS Letters*, *579*, 4235–4241.

Clarke, A. K. (1996). Variations on a theme: Combined molecular chaperone and proteolysis functions in Clp/HSP100 proteins. *Journal of Biosciences*, *21*, 161–177.

Clarke, A. K., Eriksson, M. J. (2000). The truncated form of the bacterial heat shock protein ClpB/HSP100 contributes to development of thermotolerance in the cyanobacterium *Synechococcus* sp. strain PCC 7942. *Journal of Bacteriology*, *182*, 7092–7096.

Collier, J. L., Grossman, A. R. (1994). A small polypeptide triggers complete degradation of light-harvesting phycobiliproteins in nutrient-deprived cyanobacteria. *EMBO Journal*, *13*, 1039–1047.

Cordoba, E., Salmi, M., León, P. (2009). Unravelling the regulatory mechanisms that modulate the MEP pathway in higher plants. *Journal of Experimental Botany*, *60*, 2933–2943.

Cunningham, F .X., Lafond, T. P., Gantt, E. (2000). Evidence of a role for LytB in the nonmevalonate pathway of isoprenoid biosynthesis. *Journal of Bacteriology*, *182*, 5841–5848.

Dalbey, R. E., Chen, M. (2004). Sec-translocase mediated membrane protein biogenesis. *Biochimica et Biophysica Acta*, *1694*, 37–53.

Das, P., Aziz, S. S., Obbard, J. P. (2011). Two phase microalgae growth in the open system for enhanced lipid productivity. *Renewable Energy*, *36*, 2524–2528.

Deng, R., Chow, T. J. (2010). Hypolipidemic, antioxidant, and antiinflammatory activities of microalgae *Spirulina*. *Cardiovascular Therapeutics*, *28*, e33–e45.

Dexter, J., Fu, P. (2009). Metabolic engineering of cyanobacteria for ethanol production. *Energy & Environmental Science*, *2*, 857.

Doornbosch, R., Steenblik, R. (2008). Biofuels: Is the cure worse than the disease? *Revista Virtual REDESMA*, 63–100.

Drocourt, D., Calmels, T., Reynes, J. P., Baron, M., Tiraby, G. (1990). Cassettes of the *Streptoalloteichus hindustanus ble* gene for transformation of lower and higher eukaryotes to phleomycin resistance. *Nucleic Acids Research*, *18*, 4009.

Eriksson, M. J., Clarke, A. K. (1996). The heat shock protein ClpB mediates the development of thermotolerance in the cyanobacterium *Synechococcus* sp. strain PCC 7942. *Journal of Bacteriology*, *178*, 4839–4846.

Eriksson, M. J., Schelin, J., Miskiewicz, E., Clarke, A. K. (2001). Novel form of ClpB/HSP100 protein in the cyanobacterium *Synechococcus*. *Journal of Bacteriology*, *183*, 7392–7396.

Ershov, Y. V., Gantt, R. R., Cunningham, F. X., Gantt, E. (2002). Isoprenoid biosynthesis in *Synechocystis* sp. strain PCC 6803 is stimulated by compounds of the pentose phosphate cycle but not by pyruvate or deoxyxylulose-5-phosphate. *Journal of Bacteriology*, *184*, 5045–5051.

Estévez, J. M., Cantero, A., Reindl, A., Reichler, S., León, P. (2001). 1-deoxy-D-xylulose-5-phosphate synthase, a limiting enzyme for plastidic isoprenoid biosynthesis in plants. *Journal of Biological Chemistry*, *276*, 22901–22909.

Flores-Pérez, U., Pérez-Gil, J., Rodríguez-Villalón, A., Gil, M. J., Vera, P., Rodríguez-Concepción, M. (2008). Contribution of hydroxymethylbutenyl diphosphate synthase to carotenoid biosynthesis in bacteria and plants. *Biochemical and Biophysical Research Communications*, *371*, 510–514.

Folch, J., Less, M., Sloane Stanley, G. H. (1957). A simple method for the isolation and purification of total lipids from animal tissues. *Journal of Biological Chemistry*, *226*, 497–509.

Fontanals, N., Marcé, R. M., Borrull, F., Cormack, P. A. G. (2010). Mixed-mode ion-exchange polymeric sorbents: dual-phase materials that improve selectivity and capacity. *Trends in Analytical Chemistry*, *29*, 765–779.

Frank, S., Lawrence, A. D., Prentice, M. B., Warren, M. J. (2013). Bacterial microcompartments moving into a synthetic biological world. *Journal of Biotechnology*, *163*, 273–279.

Fu, P. P., Dexter, J. P. (2011). Methods and compositions for ethanol producing cyanobacteria. Patent EP 1979481 B1.

Fulgosi, H., Gerdes, L., Westphal, S., Glockmann, C., Soll, J. (2002). Cell and chloroplast division requires ARTEMIS. *Proceedings of the National Academy of Sciences of the United States of America*, *99*, 11501–11506.

Gathmann, S., Rupprecht, E., Kahmann, U., Schneider, D. (2008). A conserved structure and function of the YidC homologous protein Slr1471 from *Synechocystis* sp. PCC 6803. *Journal of Microbiology and Biotechnology*, *1*, 1090–1094.

Giese, K. C., Vierling, E. (2002). Changes in oligomerization are essential for the chaperone activity of a small heat shock protein *in vivo* and in *vitro*. *Journal of Biological Chemistry*, *277*, 46310–46318.

Göhre, V., Ossenbühl, F., Crèvecoeur, M., Eichacker, L. A., Rochaix, J.-D. (2006). One of two alb3 proteins is essential for the assembly of the photosystems and for cell survival in *Chlamydomonas*. *Plant Cell*, *18*, 1454–1466.

Griffiths, M. J., Harrison, S. T. L. (2009). Lipid productivity as a key characteristic for choosing algal species for biodiesel production. *Journal of Applied Phycology*, *21*, 493–507.

Hamad, S. W. (2008). *Aspects of thylakoid membrane biogenesis in the cyanobacterium Synechocystis sp. PCC 6803: Role of Vipp1 and chlorophyll availability*. Arizona State University.

Han, X., Gross, R. W. (2005). Shotgun lipidomics: electrospray ionization mass spectrometric analysis and quantitation of cellular lipidomes directly from crude extracts of biological samples. *Mass Spectrometry Reviews*, *24*, 367–412.

Hanaichi, T., Sato, T., Iwamoto, T., Malavasi-Yamashiro, J., Hoshino, M., Mizuno, N. (1986). A stable lead by modification of Sato's method. *Journal of Electron Microscopy*, *35*, 304–306.

Hansen, J., Sato, M., Kharecha, P., Beerling, D., Berner, R., Masson-Delmotte, V., Pagani, M., Raymo, M., Royer, D. L., Zachos, J. C. (2008). Target atmospheric CO_2: Where should humanity aim? *Open Atmospheric Science Journal*, *2*, 217–231.

Hasunuma, T., Takeno, S., Hayashi, S., Sendai, M., Bamba, T., Yoshimura, S., Tomizawa, K.I, Fukusaki, E., Miyake, C. (2008). Overexpression of 1-deoxy-D-xylulose-5-phosphate reductoisomerase gene in chloroplast contributes to increment of isoprenoid production. *Journal of Bioscience and Bioengineering*, *105*, 518–526.

Hejazi, M. A., Wijffels, R. H. (2004). Milking of microalgae. *Trends in Biotechnology*, *22*, 189–194.

Hendricks, D. M. (1985). *Arizona Soils*. Tucson , AZ: College of Agriculture, University of Arizona.

Hill, J., Nelson, E., Tilman, D., Polasky, S., Tiffany, D. (2006). Environmental, economic, and energetic costs and benefits of biodiesel and ethanol biofuels. *Proceedings of the National Academy of Sciences of the United States of America*, *103*, 11206–11210.

Hong, S. Y., Zurbriggen, A. S., Melis, A. (2012). Isoprene hydrocarbons production upon heterologous transformation of *Saccharomyces cerevisiae*. *Journal of Applied Microbiology*, *113*, 52–65.

Howarth, R. W., Santoro, R., Ingraffea, A. (2011). Methane and the greenhouse-gas footprint of natural gas from shale formations. *Climatic Change*, *106*, 679–690.

Immer, J. G., Kelly, M. J., Lamb, H. H. (2010). Catalytic reaction pathways in liquid-phase deoxygenation of C18 free fatty acids. *Applied Catalysis A: General*, *375*, 134–139.

Inoue, A., Horikoshi, K. (1991). Estimation of solvent-tolerance of bacteria by the solvent parameter log P. *Journal of Fermentation and Bioengineering*, *71*, 194–196.

Inoue, N. (2001). Acclimation to the growth temperature and the high-temperature effects on photosystem II and plasma membranes in a mesophilic cyanobacterium, *Synechocystis* sp. PCC 6803. *Plant and Cell Physiology*, *42*, 1140–1148.

IPCC. (2007). *Climate Change 2007: The Physical Science Basis. Contribution of Working Group I to the Fourth Assessment Report of the Intergovernmental Panel on Climate Change*. United Kingdom and New York, NY, USA: Cambridge University Press.

Jaeger, K. E., Eggert, T. (2002). Lipases for biotechnology. *Current Opinion in Biotechnology*, *13*, 390–397.

Kaneko, T., Sato, S., Kotani, H., Tanaka, A., Asamizu, E., Nakamura, Y., Miyajima, N., Hirosawa, M., Sugiura, M., Sasamoto, S., Kimura, T., Hosouchi, T., Matsuno, A., Muraki, A., Nakazaki, N., Naruo, K., Okumura, S., Shimpo, S., Takeuchi, C., Wada, T., Watanabe, A., Yamada, M., Yasuda, M., Tabata, S. (1996). Sequence analysis of the genome of the unicellular cyanobacterium *Synechocystis* sp. strain PCC 6803. II. Sequence determination of the entire genome and assignment of potential protein-coding regions. *DNA Research*, *3*, 109–136.

Karradt, A., Sobanski, J., Mattow, J., Lockau, W., Baier, K. (2008). NblA, a key protein of phycobilisome degradation, interacts with ClpC, a HSP100 chaperone partner of a cyanobacterial Clp protease. *Journal of Biological Chemistry*, *283*, 32394–32403.

Kedzierska, S., Matuszewska, E. (2001). The effect of co-overproduction of DnaK/DnaJ/GrpE and ClpB proteins on the removal of heat-aggregated proteins from *Escherichia coli ΔclpB* mutant cells: A new insight into the role of Hsp70 in a functional cooperation with Hsp100. *FEMS Microbiology Letters*, *204*, 355–360.

Keeling, C. D., Whorf, T. P., Wahlen, M., Van der Plichtt, J. (1995). Interannual extremes in the rate of rise of atmospheric carbon dioxide since 1980. *Nature*, *375*, 666–670.

Kerr, R. A. (2010). Energy. Natural gas from shale bursts onto the scene. *Science*, *328*, 1624–1626.

Keshav, A., Norge, P., Wasewar, K. L. (2012). Reactive extraction of citric acid using tri-n-octylamine in nontoxic natural diluents: Part 1--equilibrium studies from aqueous solutions. *Applied Biochemistry and Biotechnology*, *167*, 197–213.

Kieboom, J. (1998). Identification and molecular characterization of an efflux pump involved in *Pseudomonas putida* S12 solvent tolerance. *Journal of Biological Chemistry*, *273*, 85–91.

Kiss, A. A., Bildea, C. S. (2012). A review of biodiesel production by integrated reactive separation technologies. *Journal of Chemical Technology & Biotechnology*, *87*, 861–879.

Kjarstad, J., Johnson, F. (2009). Resources and future supply of oil. *Energy Policy*, *37*, 441–464.

Kuzma, J., Nemecek-Marshall, M., Pollock, W. H., Fall, R. (1995). Bacteria produce the volatile hydrocarbon isoprene. *Current Microbiology*, *30*, 97–103.

Laane, C., Boeren, S., Vos, K., Veeger, C. (1987). Rules for optimization of biocatalysis in organic solvents. *Biotechnology and Bioengineering*, *30*, 81–87.

Lagarde, D., Beuf, L., Vermaas, W. (2000). Increased production of zeaxanthin and other pigments by application of genetic engineering techniques to *Synechocystis* sp. strain PCC 6803. *Applied and Environental Microbiology, 66*, 64–72.

Lalman, J. A., Bagley, D. M. (2004). Extracting long-chain fatty acids from a fermentation medium. *Journal of the American Oil Chemists' Society*, *81*, 105–110.

Laskowska, E. (2004). Aggregation of heat-shock-denatured, endogenous proteins and distribution of the IbpA/B and Fda marker-proteins in *Escherichia coli* WT and grpE280 cells. *Microbiology*, *150*, 247–259.

Leber, A. P. (2001). Overview of isoprene monomer and polyisoprene production processes. *Chemico-Biological Interactions*, *135-136*, 169–173.

Lee, R. A., Lavoie, J.M. (2013). From first- to third-generation biofuels: Challenges of producing a commodity from a biomass of increasing complexity. *Animal Frontiers*, *3*, 6–11.

Lee, S., Sowa, M. E., Watanabe, Y., Sigler, P. B., Chiu, W., Yoshida, M., Tsai, F. T. . (2003). The structure of ClpB. *Cell*, *115*, 229–240.

León, R., Fernandes, P., Pinheiro, H. M.,Cabral, J. M. S. (1998). Whole-cell biocatalysis in organic media. *Enzyme and Microbial Technology*, *23*, 483–500.

León, R., Garbayo,I., Hernández, R., Vigara, J. Vilchez, C. (2001). Organic solvent toxicity in photoautotrophic unicellular microorganisms. *Enzyme and Microbial Technology*, *29*, 173–180.

León, R., Martín, M., Vigara, J., Vilchez, C., Vega, J. M. (2003). Microalgae mediated photoproduction of β-carotene in aqueous–organic two phase systems. *Biomolecular Engineering*, *20*, 177–182.

Li, Z., Sharkey, T. D. (2013). Metabolic profiling of the methylerythritol phosphate pathway reveals the source of post-illumination isoprene burst from leaves. *Plant, Cell & Environment*, *36*, 429–437.

Lichtenthaler, H. K. (1987). Chlorophylls and carotenoids: Pigments of photosynthetic biomembranes. *Methods in Enzymology*, *148*, 350–382.

Lindberg, P., Park, S., Melis, A. (2010). Engineering a platform for photosynthetic isoprene production in cyanobacteria, using *Synechocystis* as the model organism. *Metabolic Engineering*, *12*, 70–79.

Lindquist, S., Craig, E. A. (1988). The heat-shock proteins. *Annual Review of Genetics*, *22*, 631–677.

Liu, J., Chen, L., Wang, J., Qiao, J., Zhang, W. (2012). Proteomic analysis reveals resistance mechanism against biofuel hexane in *Synechocystis* sp. PCC 6803. *Biotechnology for Biofuels*, *5*, 68.

Livak, K. J., Schmittgen, T. D. (2001). Analysis of relative gene expression data using real-time quantitative PCR and the 2(-Delta Delta C(T)) method. *Methods*, *25*, 402–408.

Loreto, F., Mannozzi, M., Maris, C., Nascetti, P., Ferranti, F., Pasqualini, S. (2001). Ozone quenching properties of isoprene and its antioxidant role in leaves. *Plant Physiology*, *126*, 993–1000.

Los, D. A., Suzuki, I., Zinchenko, V. V., Murata, N. (2008). Stress responses in *Synechocystis*: Regulated genes and regulatory systems. Antonia Herrero & Enrique Flores (Eds.). In *The cyanobacteria: Molecular biology, genomics and evolution* (117-157). Norfolk, UK: Caister Academic Press.

Lu, W., Clasquin, M. F., Melamud, E., Amador-Noguez, D., Caudy, A. A., Rabinowitz, J. D. (2010). Metabolomic analysis via reversed-phase ion-pairing liquid chromatography coupled to a stand alone orbitrap mass spectrometer. *Analytical Chemistry*, *82*, 3212–3221.

Machado, I. M. P., Atsumi, S. (2012). Cyanobacterial biofuel production. *Journal of Biotechnology*, *162*, 50–56.

Maheswaran, M., Ziegler, K., Lockau, W., Hagemann, M., Forchhammer, K. (2006). PII-regulated arginine synthesis controls accumulation of cyanophycin in *Synechocystis* sp. strain PCC 6803. *Journal of Bacteriology*, *188*, 2730–2734.

Matsumoto, M., Takahashi, T., Fukushima, K. (2003). Synergistic extraction of lactic acid with alkylamine and tri-n-butylphosphate: effects of amines, diluents and temperature. *Separation and Purification Technology*, *33*, 89–93.

McAuliffe, J. C., Paramonov, S. E. (2012). Fuel compositions comprising isoprene derivatives. Patent US 8450549 B2.

McDonnell, G., Russell, A. D. (1999). Antiseptics and disinfectants: Activity, action, and resistance. *Clinical Microbiology Reviews*, *12*, 147–179.

McGrath, P. T., Iniesta, A. A., Ryan, K. R., Shapiro, L., McAdams, H. H. (2006). A dynamically localized protease complex and a polar specificity factor control a cell cycle master regulator. *Cell*, *124*, 535–547.

McPhee, D. (2012). Microbial derived isoprene and methods for making the same. Patent US 8324442 B2

Miller, M. B., Bassler, B. L. (2001). Quorum sensing in bacteria. *Annual Review of Microbiology*, *55*, 165–199.

Mogk, A., Deuerling, E., Vorderwülbecke, S., Vierling, E., Bukau, B. (2003). Small heat shock proteins, ClpB and the DnaK system form a functional triade in reversing protein aggregation. *Molecular Microbiology*, *50*, 585–595.

Mori, H., Ito, K. (2001). The Sec protein-translocation pathway. *Trends in Microbiology*, *9*, 494–500.

Myouga, F., Motohashi, R., Kuromori, T., Nagata, N., Shinozaki, K. (2006). An *Arabidopsis* chloroplast-targeted Hsp101 homologue, APG6, has an essential role in chloroplast development as well as heat-stress response. *Plant Journal*, *48*, 249–260.

Nakamura, Y., Gojobori, T., Ikemura, T. (2000). Codon usage tabulated from international DNA sequence databases: status for the year 2000. *Nucleic Acids Research*, *28*, 292.

Newman, J. D., Marshall, J., Chang, M., Nowroozi, F., Paradise, E., Pitera, D., Newman, K. L., Keasling, J. D. (2006). High-level production of amorpha-4,11-diene in a two-phase partitioning bioreactor of metabolically engineered *Escherichia coli*. *Biotechnology and Bioengineering*, *95*, 684–691.

OECD. (2005). Isoprene. *SIDS Initial Assessment Report for SIAM 20*. UNEP Publications.

Ossenbühl, F., Inaba-Sulpice, M., Meurer, J., Soll, J., Eichacker, L. A. (2006). The *Synechocystis* sp PCC 6803 Oxa1 homolog is essential for membrane integration of reaction center precursor protein pD1. *Plant Cell*, *18*, 2236–2246.

Pacala, S., Socolow, R. (2004). Stabilization wedges: solving the climate problem for the next 50 years with current technologies. *Science, 305*, 968–972.

Panda, B., Jain, P., Sharma, L., Mallick, N. (2006). Optimization of cultural and nutritional conditions for accumulation of poly-beta-hydroxybutyrate in *Synechocystis* sp. PCC 6803. *Bioresource Technology*, *97*, 1296–1301.

Poliquin, K., Ershov, Y. V., Cunningham, F. X., Woreta, T. T., Gantt, R. R., Gantt, E. (2004). Inactivation of *sll1556* in *Synechocystis* strain PCC 6803 impairs isoprenoid biosynthesis from pentose phosphate cycle substrates in vitro. *Journal of Bacteriology*, *186*, 4685–4693.

Poliquin, K., Cunningham, F. X., MacDonald, I., Gantt, R. R., Gantt, E. (2008). Impaired isoprenoid biosynthesis: A competitive disadvantage under light stress in *Synechocystis* PCC 6803. In *Photosynthesis. Energy from the Sun* (763-766). Springer: Netherlands.

Pulz, O., Gross, W. (2004). Valuable products from biotechnology of microalgae. *Applied Microbiology and Biotechnology*, *65*, 635–648.

Quintana, N., Van der Kooy, F., Van de Rhee, M. D., Voshol, G. P., Verpoorte, R. (2011). Renewable energy from cyanobacteria: Energy production optimization by metabolic pathway engineering. *Applied Microbiology and Biotechnology*, *91*, 471–490.

Radakovits, R., Jinkerson, R. E., Darzins, A., Posewitz, M. C. (2010). Genetic engineering of algae for enhanced biofuel production. *Eukaryotic Cell*, *9*, 486–501.

Reddy, C. S., Ghai, R., Kalia, V. (2003). Polyhydroxyalkanoates: an overview. *Bioresource Technology*, *87*, 137–146.

Reppas, N. B., Ridley, C. P. (2010) Methods and compositions for the recombinant biosynthesis of n-alkanes. Patent US 7794969 B1.

Rippka, R., Deruelles, J.,Waterbury, J.B., Herdman, M., Stanier, R. (1979). Generic assignments, strain histories and properties of pure cultures of cyanobacteria. *Journal of General Microbiology*, *111*, 1–61.

Rivasseau, C., Seemann, M., Boisson, A.-M., Streb, P., Gout, E., Douce, R., Rohmer, M., Bligny, R. (2009). Accumulation of 2-C-methyl-D-erythritol 2,4-cyclodiphosphate in illuminated plant leaves at supraoptimal temperatures reveals a bottleneck of the prokaryotic methylerythritol 4-phosphate pathway of isoprenoid biosynthesis. *Plant, Cell & Environment*, *32*, 82–92.

Roberts, J., Cross, F., Warrener, P., Munoz, E. J., Lee, M. H., Romari, K, Kotovic, K. M., Hickman, J. W. (2013). Modified photosynthetic microorganisms for producing triglycerides. Patent US 8394614 B2.

Rohdich, F., Hecht, S., Gärtner, K., Adam, P., Krieger, C., Amslinger, S., Arigoni, D., Bacher, A., Eisenreich, W. (2002). Studies on the nonmevalonate terpene biosynthetic pathway: metabolic role of IspH (LytB) protein. *Proceedings of the National Academy of Sciences of the United States of America*, *99*, 1158–1163.

Rokney, A., Shagan, M., Kessel, M., Smith, Y., Rosenshine, I., Oppenheim, A. B. (2009). *E. coli* transports aggregated proteins to the poles by a specific and energy-dependent process. *Journal of Molecular Biology*, *392*, 589–601.

Romero, M., Diggle, S. P., Heeb, S., Cámara, M., Otero, A. (2008). Quorum quenching activity in *Anabaena* sp. PCC 7120: identification of AiiC, a novel AHL-acylase. *FEMS Microbiology Letters*, *280*, 73–80.

Rosenberg, J. N., Oyler, G. A., Wilkinson, L., Betenbaugh, M. J. (2008). A green light for engineered algae: redirecting metabolism to fuel a biotechnology revolution. *Current Opinion in Biotechnology*, *19*, 430–436.

Rosenstiel, T. N., Fisher, A. J., Fall, R., Monson, R. K. (2002). Differential accumulation of dimethylallyl diphosphate in leaves and needles of isoprene- and methylbutenol-emitting and nonemitting species. *Plant Physiology*, *129*, 1276–1284.

Rosenzweig, R., Moradi, S., Zarrine-Afsar, A., Glover, J. R., Kay, L. E. (2013). Unraveling the mechanism of protein disaggregation through a ClpB-DnaK interaction. *Science, 339*, 1080-1083.

Rowland, J. G., Pang, X., Suzuki, I., Murata, N., Simon, W. J., Slabas, A. R. (2010). Identification of components associated with thermal acclimation of photosystem II in *Synechocystis* sp. PCC 6803. *PloS One*, *5*, e10511.

Ruffing, A. M. (2011). Engineered cyanobacteria: Teaching an old bug new tricks. *Bioengineered Bugs*, *2*, 136–149.

Ruffing, A. M., Jones, H. D. T. (2012). Physiological effects of free fatty acid production in genetically engineered *Synechococcus elongatus* PCC 7942. *Biotechnology and Bioengineering*, *109*, 2190–2199.

Ruiz, F.J., Rubio, S., Pérez-Bendito, D. (2007). Water-induced coacervation of alkyl carboxylic acid reverse micelles: phenomenon description and potential for the extraction of organic compounds. *Analytical Chemistry*, *79*, 7473–7484.

Rupprecht, E., Gathmann, S., Fuhrmann, E., Schneider, D. (2007). Three different DnaK proteins are functionally expressed in the cyanobacterium *Synechocystis* sp. PCC 6803. *Microbiology*, *153*, 1828–1841.

Samuelson, J. C., Chen, M., Jiang, F., Möller, I., Wiedmann, M., Kuhn, A., Phillips, G. J., Dalbey, R. E. (2000). YidC mediates membrane protein insertion in bacteria. *Nature*, *406*, 637–641.

Sangster, J. (1989). Octanol-water partition coefficients of simple organic compounds. *Journal of Physical and Chemical Reference Data*, *18*, 1111.

Sardessai, Y., Bhosle, S. (2002). Tolerance of bacteria to organic solvents. *Research in Microbiology*, *153*, 263–268.

Schäfer, L., Vioque, A., Sandmann, G. (2005). Functional in situ evaluation of photosynthesis-protecting carotenoids in mutants of the cyanobacterium *Synechocystis* PCC 6803. *Journal of Photochemistry and Photobiology. B, Biology*, *78*, 195–201.

Schirmer, E. C., Glover, J. R., Singer, M. A., Lindquist, S. (1996). HSP100/Clp proteins: a common mechanism explains diverse functions. *Trends in Biochemical Sciences*, *21*, 289–296.

Schnitzler, J. P., Zimmer, I., Bachl, A., Arend, M., Fromm, J., Fischbach, R. J. (2005). Biochemical properties of isoprene synthase in poplar (*Populus x canescens*). *Planta*, *222*, 777–786.

Scott, S. A., Davey, M. P., Dennis, J. S., Horst, I., Howe, C. J., Lea-Smith, D. J., Smith, A. G. (2010). Biodiesel from algae: challenges and prospects. *Current Opinion in Biotechnology*, *21*, 277–286.

Serek, J., Bauer-Manz, G., Struhalla, G., Van den Berg, L., Kiefer, D., Dalbey, R., Kuhn, A. (2004). *Escherichia coli* YidC is a membrane insertase for Sec-independent proteins. *EMBO Journal*, *23*, 294–301.

Sharif, D. I., Gallon, J., Smith, C. J., Dudley, E. (2008). Quorum sensing in cyanobacteria: N-octanoyl-homoserine lactone release and response, by the epilithic colonial cyanobacterium *Gloeothece* PCC 6909. *ISME Journal*, *2*, 1171–1182.

Sharkey, T. D., Yeh, S., Wiberley, A. E., Falbel, T. G., Gong, D., Fernandez, D. E. (2005). Evolution of the isoprene biosynthetic pathway in kudzu. *Plant Physiology*, *137*, 700–712.

Sharkey, T. D., Wiberley, A. E., Donohue, A. R. (2008). Isoprene emission from plants: why and how. *Annals of Botany*, *101*, 5–18.

Sheng, J., Kim, H. W., Badalamenti, J. P., Zhou, C., Sridharakrishnan, S., Krajmalnik-Brown, R., Rittmann, B. E., Vannela, R. (2011). Effects of temperature shifts on growth rate and lipid characteristics of *Synechocystis* sp. PCC 6803 in a bench-top photobioreactor. *Bioresource Technology*, *102*, 11218–11225.

Sikkema, J., De Bont, J. A., Poolman, B. (1994). Interactions of cyclic hydrocarbons with biological membranes. *Journal of Biological Chemistry*, *269*, 8022–8028.

Sim, S. J., An, J. Y., Kim, B. W. (2001). Two-phase extraction culture of *Botryococcus braunii* producing long-chain unsaturated hydrocarbons. *Biotechnology Letters*, *23*, 201–205.

Simmons, L. A., Grossman, A. D., Walker, G. C. (2008). Clp and Lon proteases occupy distinct subcellular positions in *Bacillus subtilis*. *Journal of Bacteriology*, *190*, 6758–6768.

Snow, A. A., Smith, V. H. (2012). Genetically engineered algae for biofuels: A key role for ecologists. *BioScience*, *62*, 765–768.

Sommer, U., Herscovitz, H., Welty, F. K., Costello, C. E. (2006). LC-MS-based method for the qualitative and quantitative analysis of complex lipid mixtures. *Journal of Lipid Research*, *47*, 804–814.

Spence, E., Bailey, S., Nenninger, A., Møller, S. G., Robinson, C. (2004). A homolog of Albino3/OxaI is essential for thylakoid biogenesis in the cyanobacterium *Synechocystis* sp. PCC6803. *Journal of Biological Chemistry*, *279*, 55792–55800.

Squires, C. L., Pedersen, S., Ross, B. M., Squires, C. (1991). ClpB is the *Escherichia coli* heat shock protein F84.1. *Journal of Bacteriology*, *173*, 4254–4262.

Srivastava, A., Roychoudhury, P. K., Sahai, V. (1992). Extractive lactic acid fermentation using ion-exchange resin. *Biotechnology and Bioengineering*, *39*, 607–613.

Sticklen, M. B. (2008). Plant genetic engineering for biofuel production: towards affordable cellulosic ethanol. *Nature Reviews:Genetics*, *9*, 433–443.

Suzuki, I., Kanesaki, Y., Hayashi, H., Hall, J. J., Simon, W. J., Slabas, A. R., Murata, N. (2005). The histidine kinase Hik34 is involved in thermotolerance by regulating the expression of heat shock genes in *Synechocystis*. *Plant Physiology*, *138*, 1409–1421.

Suzuki, I., Simon, W. J., Slabas, A. R. (2006). The heat shock response of *Synechocystis* sp. PCC 6803 analysed by transcriptomics and proteomics. *Journal of Experimental Botany*, *57*, 1573–1578.

Tholl, D., Croteau, R., Gershenzon, J. (2001). Partial purification and characterization of the short-chain prenyltransferases, geranyl diphosphate synthase and farnesyl diphosphate synthase, from *Abies grandis* (Grand Fir). *Archives of Biochemistry and Biophysics*, *386*, 233–242.

Tian, X., Liao, Q., Zhu, X., Wang, Y., Zhang, P., Li, J., Wang, H. (2010). Characteristics of a biofilm photobioreactor as applied to photo-hydrogen production. *Bioresource Technology*, *101*, 977–983.

Tritsch, D., Hemmerlin, A., Bach, T. J., Rohmer, M. (2010). Plant isoprenoid biosynthesis via the MEP pathway: in vivo IPP/DMAPP ratio produced by (E)-4-hydroxy-3-methylbut-2-enyl diphosphate reductase in tobacco BY-2 cell cultures. *FEBS Letters*, *584*, 129–134.

Tsukagoshi, N., Aono, R. (2000). Entry into and release of solvents by *Escherichia coli* in an organic-aqueous two-liquid-phase system and substrate specificity of the AcrAB-TolC solvent-extruding pump. *Journal of Bacteriology*, *182*, 4803–4810.

Urbanus, M. L., Scotti, P. A., Froderberg, L., Saaf, A., De Gier, J. W., Brunner, J., Samuelson, J. C., Dalbey, R. E., Oudega, B., Luirink, J. (2001). Sec-dependent membrane protein insertion: sequential interaction of nascent FtsQ with SecY and YidC. *EMBO Reports*, *2*, 524–529.

Valentine, K. G., Peterson, R. W., Saad, J. S., Summers, M. F., Xu, X., Ames, J. B., Wand, A. J. (2010). Reverse micelle encapsulation of membrane-anchored proteins for solution NMR studies. *Structure*, *18*, 9–16.

Vermaas, W. F. J. (1996). Molecular genetics of the cyanobacterium *Synechocystis* sp. PCC 6803: Principles and possible biotechnology applications. *Journal of Applied Phycology*, *8*, 263–273.

Vermaas, W. F. J., Williams, J. G. K., Arntzen, C. J. (1987). Sequencing and modification of psbB, the gene encoding the CP-47 protein of Photosystem II, in the cyanobacterium *Synechocystis* 6803. *Plant Molecular Biology*, *8*, 317–326.

Wang, J. L. (2000). Enhancement of citric acid production by *Aspergillus niger* using n-dodecane as an oxygen-vector. *Process Biochemistry*, *35*, 1079–1083.

Wang, W., Liu, X., Lu, X. (2013). Engineering cyanobacteria to improve photosynthetic production of alka(e)nes. *Biotechnology for Biofuels*, *6*, 69.

Wang, Y. (2012). *Characterization of polymer resins and magnetic particles for biofuel recovery via solid phase extraction*. Arizona State University.

Work, V. H., D'Adamo, S., Radakovits, R., Jinkerson, R. E., Posewitz, M. C. (2012). Improving photosynthesis and metabolic networks for the competitive production of phototroph-derived biofuels. *Current Opinion in Biotechnology*, *23*, 290–297.

Xue, J., Ahring, B. K. (2011). Enhancing isoprene production by genetic modification of the 1-deoxy-d-xylulose-5-phosphate pathway in *Bacillus subtilis*. *Applied and Environmental Microbiology*, *77*, 2399–2405.

Yang, C. (2002). Metabolic flux analysis in *Synechocystis* using isotope distribution from ^{13}C-labeled glucose. *Metabolic Engineering*, *4*, 202–216.

Yang, J., Xu, M., Zhang, X., Hu, Q., Sommerfeld, M., Chen, Y. (2011). Life-cycle analysis on biodiesel production from microalgae: water footprint and nutrients balance. *Bioresource Technology*, *102*, 159–165.

Yang, J., Xian, M., Su, S., Zhao, G., Nie, Q., Jiang, X., Zheng, Y., Liu, W. (2012). Enhancing production of bio-isoprene using hybrid MVA pathway and isoprene synthase in *E. coli*. *PloS One*, *7*, e33509.

Yee, K. F., Tan, K. T., Abdullah, A. Z., Lee, K. T. (2009). Life cycle assessment of palm biodiesel: Revealing facts and benefits for sustainability. *Applied Energy*, *86*, S189–S196.

Yuan, J. P., Peng, J., Yin, K., Wang, J.-H. (2011). Potential health-promoting effects of astaxanthin: a high-value carotenoid mostly from microalgae. *Molecular Nutrition & Food Research*, *55*, 150–165.

Yuan, W., Wiehn, M., Wang, Y., Kim, H. W., Rittmann, B. E., Nielsen, D. R. (2013). Solid-phase extraction of long-chain fatty acids from aqueous solution. *Separation and Purification Technology*, *106*, 1–7.

Zhao, Y., Yang, J., Qin, B., Li, Y., Sun, Y., Su, S., Xian, M. (2011). Biosynthesis of isoprene in *Escherichia coli* via methylerythritol phosphate (MEP) pathway. *Applied Microbiology and Biotechnology*, *90*, 1915–1922.

Zingaro, K. A., Papoutsakis, E. T. (2012). Toward a semisynthetic stress response system to engineer microbial solvent tolerance. *mBio*, *3*, e00308-e00312.

Zurbriggen, A., Kirst, H., Melis, A. (2012). Isoprene production via the mevalonic acid pathway in *Escherichia coli* (Bacteria). *BioEnergy Research*, *5*, 814–828.

APPENDIX A

SEQUENCE OF THE SYNTHETIC ISOPRENE SYNTHASE GENE

ATGGCTTGCAGCGTTAGCACCGAAAACGTGACCTTTAGCGAAACCGAAACCGAAGCGCGC 60
CGCAGCGCGAACTATGAACCGAACAGCTGGGATTATGATTTTCTGCTGAGCAGCGATACC 120
GATGAAAGCATTGAAGTGTATAAAGATAAAGCGAAAAAACTGGAAGCGGAAGTGCGCCGC 180
GAAATTAACAACGAAAAAGCGGAATTTCTGACCCTGCTGGAACTGATTGATAACGTGCAG 240
CGCCTGGGCCTGGGCTATCGCTTTGAAAGCGATATTCGCCGCGCGCTGGATCGCTTTGTG 300
AGCAGCGGCGGCTTTGATGCGGTGACCAAAACCAGCCTGCACGCGACCGCGCTGAGCTTT 360
CGCCTGCTGCGCCAGCATGGCTTTGAAGTGAGCCAGGAAGCGTTTAGCGGCTTTAAAGAT 420
CAGAACGGCAACTTTAGCGAAAACCTGAAAGAAGATACCAAAGCGATTCTGAGCCTGTAT 480
GAAGCGAGCTTTCTGGCGCTGGAAGGCGAGAACATCCTGGATGAAGCGAAAGTGTTTGCG 540
ATTAGCCATCTGAAAGAACTGAGCGAAGAAAAAATTGGCAAAGAACTGGCGGAACAGGTG 600
AACCATGCGCTGGAACTGCCGCTGCATCGCCGCACCCAGCGCCTGGAAGCGGTGTGGAGC 660
ATTGAAGCGTATCGCAAAAAAGAAGATGCGGATCAGGTGCTGCTGGAACTGGCGATTCTG 720
GATTATAACACCATTCAGAGCGTGTATCAGCGCGATCTGCGCGAAACCAGCCGCTGGTGG 780
CGTCGCGTGGGCCTGGCGACCAAACTGCATTTTGCGCGCGATCGCCTGATTGAGAGTTTT 840
TATTGGGCGGTGGGCGTGGCGTTTGAACCGCAGTATAGCGATTGCCGCAACAGCGTGGCG 900
AAAATGTTTAGCTTTGTGACCATTATTGATGATATTTATGATGTGTATGGCACCCTGGAT 960
GAACTGGAACTGTTTACCGATGCGGTGGAACGCTGGGATGTGAACGCGATTGATGATCTG 1020
CCGGATTATATGAAACTGTGCTTTCTGGCGCTGTATAACACCATTAACGAAATTGCGTAT 1080
GATAACCTGAAAGAAAAAGGCGAGAACATTCTGCCGTATCTGACCAAAGCGTGGGCGGAT 1140
CTGTGCAACGCGTTTCTACAGGAAGCGAAATGGCTGTATAACAAAAGCACCCCGACCTTT 1200
GATGAATATTTTGGCAACGCGTGGAAAAGCAGCAGCGGCCCGCTACAGCTGATTTTTGCG 1260
TATTTTGCGGTGGTGCAGAACATTAAAAAAGAAGAAATTGATAACCTACAGAAATATCAT 1320
GATATTATTAGCCGCCCGAGCCATATTTTTCGCCTGTGCAACGATCTGGCGAGCGCGAGC 1380
GCGGAAATTGCGCGCGGCGAAACCGCGAACAGCGTGAGCTGCTATATGCGCACCAAAGGC 1440
ATTAGCGAAGAACTGGCGACCGAAAGCGTGATGAACCTGATTGATGAAACCTGGAAAAAA 1500
ATGAACAAAGAAAAACTGGGCGGCAGCCTGTTTGCGAAACCGTTTGTGGAAACCGCGATT 1560
AACCTGGCGCGCCAGAGCCATTGCACCTATCATAACGGCGATGCGCATACCAGTCCGGAT 1620
GAACTGACCCGCAAACGCGTGCTGAGCGTGATTACCGAGCCGATTCTGCCGTTCGAACGC 1680
TAA